PROTECTION OF THE MARBLE MONUMENT SURFACES BY USING BIODEGRADABLE POLYMERS

A Thesis Submitted to
the Graduate School of Engineering and Sciences of
İzmir Institute of Technology
in Partial Fulfillment of the Requirements for the Degree of

MASTER OF SCIENCE

in Environmental Engineering
(Emphasis on Environmental Pollution and Control)

by
Yılmaz OCAK

July 2007
İZMİR

We approve the thesis of **Yılmaz OCAK**

Date of Signature

..... **18 July 2007**
Asst. Prof. Dr. Aysun SOFUOĞLU
Supervisor
Department of Chemical Engineering
İzmir Institute of Technology

..... **18 July 2007**
Prof. Dr. Hasan BÖKE
Co-Supervisor
Department of Chemical Engineering
İzmir Institute of Technology

..... **18 July 2007**
Assoc. Prof. Dr. Funda TIHMINLIOĞLU
Co-Supervisor
Department of Chemical Engineering
İzmir Institute of Technology

..... **18 July 2007**
Asst. Prof. Dr. Sait SOFUOĞLU
Department of Chemical Engineering
İzmir Institute of Technology

..... **18 July 2007**
Asst. Prof. Dr. Erol ŞEKER
Department of Chemical Engineering
İzmir Institute of Technology

..... **18 July 2007**
Prof. Dr. Başak İPEKOĞLU
Department of Architectural Restoration
İzmir Institute of Technology

.....
Prof.Dr. M. Barış ÖZERDEM
Head of the Graduate School

ACKNOWLEDGEMENTS

I would like to acknowledge the people who have helped to make this work possible. I would like to thank to all my advisors Ass. Prof. Aysun SOFUOĞLU, Prof. Hasan BÖKE, Assoc. Prof. Funda TIHMINLIOĞLU for their recommendations, support, and thoughtful advise. I would also like to thank to my thesis jury members.

In this thesis the support of specialist for the analytical analysis from the Centers (MAM and Environmental R&D) of Iztech is also appreciated.

I would also like to acknowledge The Scientific and Technical Research Council of Türkiye (TUBİTAK) for financial support to 104M564 project.

Finally, I would like to express my heartfelt gratitude to my family İsmet OCAK, Cahide OCAK, Yeliz OCAK and Berna ÇOLAK for their patience, affection, encouragement and eternal love.

ABSTRACT

PROTECTION OF THE MARBLE MONUMENT SURFACES BY USING BIODEGRADABLE POLYMERS

The deterioration of historic buildings and monuments constructed by marble has been accelerated in the past century due to the effects of air pollution. The main pollutant Sulphur dioxide (SO_2) reacts with marble composed primarily of calcite ($CaCO_3$), the firs step of decay which called gypsum ($CaSO_4.2H_2O$) crust is formed and this process can be accelerated when the surfaces exposed to the rain.

In this study, the possibilities of slowing down the SO_2-marble reactions were investigated by coating the surface of marble with some bio-degradable polymers: zein, chitosan, polyhydroxybutyrate (PHB) and polylactic acid (PLA) as protective agents. Uncoated control marbles and biodegradable polymer coated marbles were exposed at nearly 8 ppm SO_2 concentration at 100 % relative humidity conditions in a reaction chamber for several days. The extent of reaction was determined by leaching sulphate from the marble surface into deionized water and measuring the total concentration of sulphate with ion chromatography (IC). Then, gypsum crust thickness, polymers % protection factor and average deposition velocity were calculated. Concurrently, the ratio and amount of calcium sulfite hemihydrate ($CaSO_3.½H_2O$) and gypsum ($CaSO_4.2H_2O$) were determined by FT-IR analysis. The surface morphology of SO_2 exposed marble to distinguished calcium sulfite hemihydrate and gypsum crystals were determined by Scanning Electron Microscope (SEM).

The results of the study showed that SO_2-calcite reaction increased in the use of zein, glycerol added zein and chitosan polymers on the surface of marble. While, PHB treated marble surfaces had 5 % increases in the protection factor. The low molecular weight PLA protection factor was 45 % after 85 days exposure. Similar results were observed when the high molecular weight of PLA used. The protection was extended to more than 90 days having 60 % protection factor.

ÖZET

MERMER ANIT YÜZEYLERİNİN BİO-BOZUNUR POLİMERLERLE KORUNMASI

Hava kirliliği son yüzyılda endüstriyel gelişmelere paralel olarak giderek artmıştır. Bu artış günümüzde sadece insan sağlığını etkilememekte, aynı zamanda tarihi anıtlarda kullanılan mermerler malzemenin bozulmasının artmasına da neden olmaktadır. En önemli hava kirliliği etmenlerinden sayılan kükürt dioksit gazı (SO_2), mermer yapısını oluşturan kalsit kristalleri ($CaCO_3$) ile reaksiyona girerek alçı taşını ($CaSO_4$. 2 H_2O) oluşturmaktadır. Alçı taşı kristalleri kalsit kristallerine göre suda daha kolay çözündüğü için yağmura açık bölgelerde mermer yüzeylerinde aşınmalar görülmektedir. Yağmurdan korunan bölgelerde ise mermer yüzeylerinde kabuklanmalar oluşmakta ve bu kabuklar dökülerek mermer yüzeyinde bozulmalara neden olmaktadır. Geçmişte mermerlerin korunmasına yönelik olarak gerek anıtlardan alınan mermerler üzerinde gerekse laboratuar ortamlarında kirli havaya tabi tutulan mermerler üzerinde birçok çalışma yapılmıştır. Mermerlerin polimerlerle kaplanarak yapılan araştırmalarda polimerlerin SO_2-kalsit reaksiyonunu azaltmak yerine daha da artırdığı tespit edilmiştir.

Bio-bozunur polimerler geri dönüşebilir ve başka müdahalelere olanak tanımayabilmektedirler aynı zamanda düşük gaz ve su buharı geçirgenlikleri vardır. Bu özellikleri göz önüne alarak, projede taş yüzeylerinin bio-bozunur polimerler ile kaplanarak hava kirliğinden korunması araştırılmıştır. Çalışma laboratuar koşullarında kurulan gaz odasında yürütülmüştür. Çalışmada mermer yüzeylerinde polylactide (PLA), polyhydroxybutyrate (PHB), zein ve chitosan gibi bio polimerler kullanılmıştır. Polimer kaplanmış ve kaplanmamış olarak düzgün kesilmiş mermer plakalar ve yüzey koruyucu olarak mermer yüzeylerinde kükürt dioksitin etkisi ile oluşan ürünlerin mineralojik yapıları FTIR kullanarak belirlenmiştir. Mermer yüzeylerinde oluşan ürünlerin miktarları FTIR ve iyon kromotografisi kullanılarak belirlenmiştir. Yüzey morfolojilerindeki değişimler ve oluşan ürünler ise taramalı elektron mikroskop (SEM) kullanılarak belirlenmiştir. Çalışmanın sonucunda, PLA ve PHB polimerlerinin mermer yüzeylerinde alçı taşı oluşumunu azalttıkları ve bu özellikleri ile korumada kullanılabilecekleri görülmüştür.

TABLE OF CONTENTS

LIST OF FIGURES

LIST OF TABLES

CHAPTER 1

INTRODUCTION

Historical monuments have to exist during the cultures to pass cultural information to the next generation. Most of the historical monuments and buildings were made of natural stones which are subject to degradation due to environmental conditions. Thus, the cause of decay on the marble surfaces on the sheltered building in industrial countries was found as a result of sulphur dioxide (SO_2) deposition to the surfaces in the past century (Gauri et al. 1989). The main pollutant which affects the marble structure is primarily SO_2. SO_2 reacts with marble composed primarily of calcite ($CaCO_3$) and converts it into calcium sulphite hemihydrate ($CaSO_3$. $½H_2O$) (Böke et al. 1999, Gauri and Bandyopadhyay 1999). In the presence of water, calcium sulphite hemihydrate is not a stable product and rapidly converted to gypsum ($CaSO_4$. $2H_2O$). Gypsum is moderately soluble and occupies more volume than calcite. As a result, the marble surfaces are eroded in rain-washed areas and disintegrated in sheltered places.

The formed crusts eventually exfoliate reducing sculptures or building surfaces to hunks of rock if the surface is unprotected. Therefore, it is reported that acid rain has a scouring action and causes accelerated erosion on the historical building and sculptures (Gauri et al. 1989). Due to this effect, the inscriptions upon such surfaces become faint and the details of relief highly reduced over time.

In order to prevent this kind of decay, researchers started using some methods. The first one was converting the formed gypsum back to calcite by the use of carbonate solution; yet it was not as effective as expected due to poor adherence of formed calcite crystals (Skoulikidis and Belayannis 1984).

Another method was the coating application by isolating marble from atmospheric sulphure dioxide (SO_2) and had been mostly used methods to protect statues. Such coatings, particularly when applied upon rain protected surfaces, have often been found more harmful than if the marble was left untreated. Inhibition of gypsum formation by coating of stone surfaces with synthetic polymers also conducted (Gauri et al. 1973, Elfving and Johanson 1994, Gauri and Bandyopadhyay 1999, Thompson et al. 2003). Hence, most of the coated marble surfaces were more

deteriorated than those of the uncoated ones due to high absorbing of SO_2 and the entrapment of water vapor by polymers (Gauri and Bandyopadhyay 1999).

Furthermore, researchers have studied the possible ways of slowing down the SO_2-calcite reaction by producing less reactive substrate on the marble surface by using some water soluble organic and inorganic compounds such as oleate, oxalate and phosphate ions (Böke et al. 2002, Böke and Gauri 2003, Thompson et al. 2003). It is reported that oxalate and oleate anions produce less reactive calcium oxalate and calcium oleate substrate and provide significant protection to marble exposed only in sheltered places (Böke and Gauri 2003).

All of these methods had some disadvantages. For example, the application of synthetic polymers resulted in peeling problems after a short time period of the treatment (Böke and Gauri 2003). Therefore the use of appropriate protective agent is important. The protective agent should not require peeling for the reapplication when its life-time was completed. In other words, the protective agent should be degradable therefore no need peeling and reapplicable without having thick coating surfaces. Biodegradable polymers seem to have the potential to comply these properties. Some of the biodegradable polymers have good moisture barrier and degradability which make application possible.

In this study, the protection extend of some bio-degradable polymers on marble-SO_2 reaction were investigated. The biodegradability of these kinds of polymers allows new treatment of the material surfaces to be protected. Although many synthetic polymers were tested and used to protect the marble surfaces from air pollution, bio-degradable polymers have not yet been tested for this purpose.

Specifically, biopolymer coated marble slabs were exposed at nearly 8 ppm. SO_2 concentration at 100 % relative humidity conditions together with uncoated ones in a reaction chamber for extended time duration.

To determine the extent of reaction

To determine sulphate content

To estimate the extent of reaction

To determine the efficiency of polymer treatments by comparing the gypsum crust thickness of the treated and uncoated marble slabs.

CHAPTER 2

LITERATURE REVIEW

2.1. Air Pollutants in Urban Atmosphere

Air pollutants can be expressed as any kind of atmospheric substances that are present in the atmosphere at concentrations higher than their normal background levels for a duration which creates a harmful effect on living organisms and materials. Air is composed of particles, aerosols and gases. Larger particles settle near the source, but smaller particles can be transported by winds over some significant distance. Aerosols are liquid or solid particles of small size that remain suspended in the air and can be transported over long distances (Torfs and Grieken 1997). Gases, of course, mix thoroughly with the air. Gaseous air pollutants can be counted as oxides of sulphur and nitrogen, ozone, hydrocarbons and, to a lesser extent, hydrogen sulphide and other inorganic and organic substances.

The air pollutants can be described into two classes as primary and secondary air pollutants. Primary pollutants are emitted directly from some identifiable sources. These are oxides of sulphure, nitrogen, carbon and particulate matters are the examples of primary pollutants. The secondary pollutants are formed by the interaction of primary pollutants with normal atmospheric constituents, such as sulphuric acid, nitric acid, etc (WEB_1).

One of the primary pollutant sulphur dioxide is the main atmospheric pollutant and can be found the atmosphere in the form of SO_2, SO_3^- and H_2S. State Institute of Statistics of Turkey (WEB_2) reported that, the average of SO_2 was increased year by year. Annual average of SO_2 concentrations of the cities of Turkey are represented in Table 2.1.

Table 2.1. Annual High SO_2 Concentrations of the Cities of Turkey.
(Source: WEB_2)

Sulphur Dioxide (SO_2) µg/m^3	
Kütahya	146
Erzurum	132
Çanakkale (City Center)	107
Çorum	101
Bingöl	98
Bursa	95
Tekirdağ	95
Elazığ	84
Kayseri	84
Gaziantep	82

Eventhough, there is a decrease in usage of sulphur contained fossil fuels, the problem related to SO_2 in the urban areas continues due to long range transport of this pollutant from the countries use sulphur contained fossil fuel as energy sources. The known effects of these pollutants are precursors of acid rain in a humid environment. Aas et al. measured air concentration and wet deposition of major inorganic ions at five non-urban sites in China from 2001-2003 they concluded that the air concentration including SO_2 (annual average range 0.5-40 µm/m^3) was very high and would have a large impact on the air quality. They mentioned that this high concentration was a result of long-range transport of air pollutants to rural areas, similarly for the acid rain research (Aas et al. 2007).

The global sulphur emissions have fallen at an average rate of 2.7 % per annum since 1990, if this trend continued the effect on acid rain and deposition and global warming still have been keeping the importance (Stern 2005).

Other significant primary pollutants are particulate matters (PM) and nitrogen gases which can be found in forms of nitrous oxide (N_2O), nitric oxide (NO) and nitrogen dioxide (NO_2) in the atmosphere. Nitrous oxide is produced from soil and water by microbiological processes. Other processes are agricultural activities like the usage of nitrogen fertilizer, combustion processes and photochemical reactions in the

stratosphere. Combustion engines, lightening and soils produce nitric oxide (NO) (Fassina 1986). Particulate matters or aerosols small size liquid or solid particles and can be transported over long distance by winds. Particulate matters often contain soot from incomplete combustion, tarry material, traces of metals like iron and vanadium as well as adsorbed sulphur dioxide and water. Particles can also arise from asphalt roads, vehicle tires, and breaks (Rosvall et al. 1986).

2.2. Effects of SO_2 on Deterioration of Marble

Most of the historical buildings were made of limestone and marble and the buildings for this century were made of concrete. The impact of acid deposition on stone monuments made of marble and lime stone and building materials containing large amount of carbonate has been recognized for over the century. High buildings made of concrete in urban areas were also studied to characterize the damage due to cloud water with high acidity for a long time exposure. When considering the acidity of precipitation in relation to marble is the relative proportion of CO_2, SO_2 and NO_2 in the atmosphere. In the 1950s and earlier, when the precipitation had started to become significantly acidic, CO_2 was the main cause for marble. Then SO_2 became responsible as the main source of acidity due to industrial development. When the acidity contribution of CO_2 was compared with the acidity of SO_2, even very small amounts of SO_2 contributed strong acidity due to their acidity structure. Presently due to increase in NO_2 concentrations of H_2SO_4 and HNO_3 were 65-70% and 30-35% respectively (Gauri and Gwinn 1982).

SO_x not only react with marble either in the gaseous phase as SO_2 and SO_3 in the presence of water vapor in the atmosphere , but also in solution as H_2SO_3 or H_2SO_4. The gaseous reactions which are called dry deposition occur at all times whereas acid reactions which are called wet deposition are confined to episodes of rainfall (Gauri and Gwinn 1982).

Nord and Holenyi pointed out that SO_2 and SO_3 in the air were a significant source to accelerate sulphation of calcite and deterioration of limestone. In addition the presence of iron and soot particles were catalyzed these reactions. The study showed that, there were positive correlation between traffic intensity and damage, between car

traffic and soiling of the buildings, and sulphur contents at the stone surface (Nord and Holenyi 1997).

The effects of SO_2 on wildlife and the others like visibility reduction, enhancement corrosion in materials. Xie et al. studied the effect of acid rain in the cement concrete to obtain the damage. The results showed that H^+ in acid rain dissolved $Ca(OH)_2$ in the hardened cement paste and that SO_4^{2-} also corroded it (Xie et al. 2004).

Acidic gases attack mechanisms on stone materials are not completely known. The common idea is that, the sulphuric acid content of rain water is responsible for formation of gypsum crust on limestone and marble, but there are also other studies indicating that gypsum formed elsewhere can be transported by the air and adhere to stone surfaces through action of organic dirt (Rosval et al. 1986).

The formation of gypsum crusts and the loss of material due to solubilization are the main effects of SO_2 on limestone and cause 30-35 % of material lost. The stone surface where the crust is detached usually presents desegregation higher porosity and higher surface area than the original stone, being then weaker to further weathering processes (Bernal and Bello 2003).

There are two way of gypsum formation; In the first way, calcium sulfite is formed with reaction of calcite and sulfur dioxide, then it reacts with oxygen and water the formation of gypsum can be schematized as

$$CaCO_3 + SO_2 + H_2O \rightarrow CaSO_3 \cdot {}^1/_2H_2O \quad (2.1)$$

$$CaSO_3 \cdot {}^1/_2H_2O + O_2 + H_2O \rightarrow CaSO_4 \cdot 2H_2O \quad (2.2)$$

Another definite formation is the adsorption of sulfur dioxide in rain water, liquid atmospheric aerosols, or moist film supported on a stone surface where it is oxidized to form a sulfuric acid solution that dissolves the calcium carbonate by gypsum formation (Bernal and Bello 2003):

$$SO_2 + O_2 + H_2O \rightarrow H_2SO_4 \quad (2.3)$$

$$CaCO_3 + H_2SO_4 + H_2O \rightarrow CaSO_4 \cdot 2H_2O \quad (2.4)$$

2.3. Deposition of Pollutants on Calcareous Stones

Sulphur dioxide is the most significant pollutant which causes the deformation of calcareous stone. In the same way gypsum is the most abundant pollution product of calcareous stones. Gypsum is formed on the calcareous stones when sulphur dioxide or its oxidizing product reaches the stone surface by two mechanisms. The first of these is "dry" deposition where the pollutant in gaseous form interacts with the surface by winds and turbulence, and the second is wet deposition, where the pollutant, as an oxidized or derived species dissolved in atmospheric moisture, is presented to the stone surface during precipitation as acid rain (Garland 1978).

In the following section dry and wet deposition process of pollutants on the stone surfaces are summarized.

2.3.1. Dry Deposition of the Sulphur Dioxide on Calcareous Stones

Dry deposition is one of the removal pathways of pollutants from atmosphere. The removal of SO_2 from the atmosphere by surfaces such as soil, water, vegetation or stone is known as dry deposition of sulphur dioxide. In dry areas or in dry weather conditions the most of acid deposition can occur through dry deposition process. The variable that are necessary for estimating cumulative deposition flux at a certain time period is the time averaged dry deposition rate or velocity (in $cm.s^{-1}$) V_d, which is related to the time-averaged flux per unit area and to its concentration. Dry deposition rate depends on the type of surface, and meteorological conditions of atmosphere such as wind speed and atmospheric stability. The difficulty of atmospheric concentration of SO_2 was mentioned due to too much variability of the concentration. The estimation of SO_2 deposition in the ambient air was measured by using sulphation plates made with PBO_2 or CaO paste as a surrogate surface. They found out that due to local SO_2 emission variation, there were seasonal variation with the maxima in winter and minima in summer. The SO_2 deposition velocity varied from 0.09-9.72 $cm.s^{-2}$ in 11 cities in China (Ta et al. 2005).

Grossi and Murray searched characteristics of carbonate building stones that influence the dry deposition of gases. They found out porosity, pore distribution and specific surface area were important for water sorption. On the other hand, dry

deposition was important for the accumulation of dissolving salts as well as gypsum. They mentioned that these salts could increase dry deposition by increasing the water content of the stones which allows more acidic gases absorption until they washed away with rain, otherwise they stayed there indefinitely (Grossi and Murray 1999).

The comparison of the sulphur dioxide absorption rate on unweathered calcium carbonate stones such as limestone, marble and travertine was also studied in literature. The limestone samples had the largest absorption rate due to their large porosity and effective surface area (Johansson et al. 1988).

In a dry atmosphere SO_2 and calcite do not react with each other. In this reaction, the main increasing factor that affects the reaction rate is humidity. Calcium sulphate hemihydrate ($CaSO_3.½\ H_2O$) is always the initial reaction product that transforms partially to gypsum ($CaSO_4.\ 2H_2O$) crust in increased humidity. Gauri et al. showed the effect of the humidity on gypsum formation. In this study the $CaSO_3$ formation rate was determined and the reaction curves were similar in form at all levels of humidity (low humidity, normal humidity and high humidity), although formed products quantity varied at each humidity level. At the same time, the $CaSO_3$ formation rate was increased with a direct proportion of the relative humidity (Gauri et al. 1982).

Spiker et al. researched the effective parameters of SO_2 deposition on the stones. The study resulted increase in absorbed water, porosity, surface finish and roughness increased SO_2 deposition. Spiker et al. also measured the SO_2 deposition velocity on Salem limestone and Shelbourne marble by using computerized well controlled environmental chamber. Deposition was monitored by an ultraviolet (UV) fluorescence analyzer. They observed that deposition velocity of sulphur dioxide on limestone was about twenty six times greater than that of marble. They concluded that this difference was due to the high porosity and water absorption characteristic of Salem limestone (Spiker et al. 1992).

The deposition velocity measurement of SO_2 on marble and dolomite surfaces method was conducted in a gas chamber by indirectly using a continuous flame photometric detector and directly by quantitative analyses of formed gypsum and epsomite using atomic absorption spectrophotometer and turbidimetry (Coburn et al. 1993). The measured deposition velocities varied between 0.02 and 0.10 cm s^{-1} for dolomite and 0.02-0.23 cm s^{-1} for marble. For both type of stones, the deposition velocity increased significantly when condensed moisture was observed on the stone surface. Yet, one should note that the indirect measurements may cause significant

experimental errors because of the deposition of sulphur dioxide on the walls of the gas chambers due to condensation. Therefore the measurement of dry deposition velocity needed longer exposure periods and/or higher SO_2 concentrations in order to obtain significant amount of SO_2 deposits on the stone materials (Gauri et al. 1989, Kulshreshtha et al. 1989).

2.3.2. Wet Deposition of the Sulphur Dioxide on Calcareous Stones

Water can affect the stone surfaces in a different way. Water can be formed by condensation on a surface of stone may create problem due to gases, aerosols dust or dirt particles. Water aerosol in the form of mist or fog can concentrate pollutants over long transportation stretches and finally discharge them on the surfaces of buildings. Another effect that can lead to increased water content in porous building materials is capillary rise. This problem can be still more pronounced if soluble salts are present. Due to the composition of atmospheric aerosols, the salts can be found in the form of sulphate of sodium, potassium, magnesium and calcium which result in severe damage (Torfs and Grieken 1997). Atmospheric water can be in different form like liquid water reaching to the surfaces in the form of rain. If it is combined with wind which can contribute to the decay of the building materials through erosion is caused by transported particles. At the same time, if the rain water dissolves salts such as SO_2, NO_x on its way, the decay rate will be higher on the surface (Torfs and Grieken 1997). This kind of rain is known as “acid rain”. In the 20^{th} century acid rain was defined as a problem.

The first phase occurring in the acid rain is the increase in the acidity of rainwater together with an increase of the sulfate and nitrate concentrations. Wet deposition generally includes all forms of precipitation, but mostly rainfall can be considered as the dominant pathway for the wet deposition of pollutants on stone surfaces. The acidity of rainfall may lead to direct attack on mineral compounds of a stone material.

The role of rain in the weathering of stones is very complex and it strongly depends on the interaction of many parameters such as chemical composition of precipitation, concentration of gaseous and particulate pollutants, the properties of the stone material, kind of exposure etc.

Pope et al. reported that while dry deposition of SO_2 was the chief weathering agent on vertical marble tombstone faces, horizontal stone tablets at a ground level records actual acid precipitation and calcite dissolution eventough lower recession rates were determined than those due to SO_2. Acid precipitation varies over a broader gradient, while SO_2-gypsum weathering was confined to local areas (Pope et al. 2002).

In the study of Kim et al. some materials were exposed to wet deposition under the sheltered and unsheltered outdoor conditions. The corrosion rates of the test material in the outdoor conditions were found to be at highest in carbon steel following with marble. These rates 2.28-6.24 times were larger than those under the sheltered conditions. They also found that the rate of corrosion were higher in the heavily polluted areas (Kim et al. 2004).

It is also obtained that corrosivity due to wet deposition of sulphur dioxide on calcareous stone in urban atmosphere is higher than the rural atmosphere due to emission of SO_2 rates.

2.4. Homogeneous Gas-Phase Oxidation of Sulphur Dioxide

Now we will look at how SO_2 will be converted to acid rain. Fassina separated the atmospheric SO_2 homogeneous gas-phase into three different mechanisms (Fassina 1986):

In the first mechanism, the absorption of UV solar radiation produced direct-photo oxidation which includes the reactions of excited SO_2 molecules. This reaction takes place with low efficiency under atmospheric conditions.

SO_2 oxidation by reactive species produced such as hydrocarbons in thermal reaction is the second mechanism. In the presence of propone (>50 ppb) and ozone, the SO2 oxidation rate is greater than 0.1 % h^{-1}. This mechanism is only important in the atmosphere because of high olefin concentrations.

Last mechanism is SO_2 oxidation by reactive intermediates such as atoms, free radicals and excited molecular species which are generated photochemically. In the atmosphere where photochemical smog present the atmospheric oxidation of hydrocarbons and related substances can occurs and proceeds as a chain- reaction with the help of free radicals.

When SO_2 reacted with O_2, SO_3 is formed then part of the sulphate in the droplets can be present as sulphuric acid which is known as very aggressive on limestone is formed. Main stages in the process of the homogeneous sulphur dioxide oxidation in the atmosphere may be outlined as follows:

$$SO_2 \text{ (gas)} \rightarrow SO_3 \text{ (aerosol)} \rightarrow H_2SO_4 \text{ (Droplets)} \rightarrow CaSO_4.2H_2O \qquad (2.5)$$

Most effective homogeneous gas-phase reaction is the reaction of OH radicals with SO_2 which represented as follow:

$$SO_2 + OH\cdot \rightarrow HSO_3\cdot \rightarrow SO_3 + HO_2 \qquad (2.6)$$

2.5. Heterogeneous Oxidation of Sulphur Dioxide in the Aqueous Phase

SO_2 oxidation in aqueous systems involves a number of mechanisms concurrently in a real atmosphere. Dissolution of gaseous SO_2 in aqueous system which is the water droplets may present in clouds, fog etc. and then liquid-phase SO_2 oxidation occurs by oxygen, ozone and hydrogen peroxide in the absence or in the presence of catalyst (Fassina 1986).

Hydrogen peroxide, ozone and ammonia are known as strong oxidizing agents. The oxidation of sulphur dioxide by ozone may dominate over the oxygen reaction in clouds having a pH around 5. The rate of reaction of sulphur dioxide with ozone (50 ppb) is thousand times faster than its rate with oxygen. The reaction order with respect to sulphite ions and ozone at pH 4.6 is found to be first order (Larson et al. 1978, Penkett et al. 1979).

Sulphur species is also very rapidly oxidized in the presence of H_2O_2. The rate of oxidation is first order up to pH = 8. If the pH is higher than the 8, the rate would be second order (Larson et al. 1978).

The oxidation of sulphite ions increase with the acidity of the water but do not take place at pH values smaller than two, since the solubility of sulphur dioxide becomes very small. Basic substances such as ammonia increase the pH of the water,

increasing the dissolution of sulphur dioxide so ammonia may not play a catalytic role in sulphur dioxide oxidation but rather increase the absorption of sulphur dioxide.

2.5.1. Absorption and Dissolution of SO_2 in Aqueous Solution

The SO_2 absorption by aqueous solutions plays a principal significant removal in the atmosphere. The absorption is a complex mechanism, and includes the transport of the gas to the air – water interface and lets the absorption of gaseous SO_2 in the water. Absorption and dissociation of SO_2 in aqueous solutions are influenced by some factors such as acidity, ionic strength and temperature of the solution which will be discussed in the following paragraphs successively.

In the literature, the absorption of sulphur dioxide in aqueous solutions can be defined by the following equilibriums (McKay 1971).

$$SO_{2\,(g)} + H_2O_{(l)} \Leftrightarrow (SO_2 \,.\, H_2O)_l \qquad K_H = \frac{[SO_2 \,.\, H_2O]}{P_{SO_2}} \tag{2.7}$$

$$(SO_2 \,.\, H_2O)_l + H_2O \Leftrightarrow HSO_3^- + H_3O^+ \qquad K_1 = \frac{[HSO_3^-]\,[H_3O^+]}{[SO_2 \,.\, H_2O]} \tag{2.8}$$

$$HSO^-_3 + H_2O \Leftrightarrow SO_3^{=} + H_3O^+ \qquad K_2 = \frac{[SO_3^{=}]\,[H_3O^+]}{[HSO_3^-]} \tag{2.9}$$

The absorption rate of sulphur dioxide in water which called as two-film theory can be expressed in general by the following formula (Sevilla et al. 1993).

$$N_A = k_G\,(P_A - P_{AI}) = E\,k_L\,(C_{AI} - C_{A0}) \tag{2.10}$$

Where;

N_A = Flux of SO_2, k mole/m^2.s,

k_G = Mass transfer coefficient in the gas phase,

P_A , P_{AI} = partial pressure of SO_2 in the bulk of the gas and at the interface, bar,

E = Enhancement factor for absorption, caused by chemical reaction,

k_L = Mass transfer coefficient in the liquid phase, m/s,

C_{AI} = Interfacial molecular concentration of SO_2 in equilibrium with P_{AI}, kmole/m^3

C_{A0} = molecular concentration of SO_2 in the bulk of the liquid, kmole/m^3

Supposing that the dissociation equilibrium (2.7) occurs instantaneously at the interface,

$$N_A = \frac{P_A - \left(\frac{C_{A0}}{H_C}\right)}{\left(\frac{1}{k_G}\right) + \left(\frac{1}{E.H_C.k_L}\right)} \qquad (2.11)$$

Where H_C is the apparent equilibrium solubility constant, based on concentrations. In the equation (2.9), the numerator represents the global driving force, and the denominator is the sum of the mass transfer resistances of each phase. If the absorption is physical (E = 1) and the resistances of the gas phase negligible (H_C . k_L << k_G) therefore, the system resistance can be explained by liquid film resistant coefficient k_L. While if the absorption is accompanied by a chemical reaction and the value of E is large, the resistance of the liquid phase may be very small (E . H_C . k_L << k_G) and the system allows determination of the coefficient k_G.

In strongly acid solutions, the hydrolysis of SO_2 is strongly inhibited. Under that condition, using the aqueous solutions of the H_2SO_4, k_L can be calculated. In alkaline solution equilibrium (2.8) and (2.9) are favored and the absorption occurs by instantaneous chemical reactions. Then by using the alkaline solutions such as sodium hydroxide, it is possible to calculate the k_G in the gas phase.

In the dissolution of gaseous SO_2 in aqueous system, $SO_{2\,(g)}$ in the air is in equilibrium with SO_2 dissolved in distilled water in a heterogeneous system in accord with following chemical equilibrium (Fassina 1986):

Dissolution of gaseous SO_2 in aqueous system occurs by equilibrium of SO_2 in air with SO_2 dissolved in distilled water in a heterogeneous system following with chemical reactions as follows:

Across the gas-liquid interface:

$$SO_{2\,(gas)} + H_2O_{\,(liquid)} \Leftrightarrow SO_2 \,.\, H_2O \qquad (2.12)$$

In the liquid phase:

$$SO_2 \,.\, H_2O \Leftrightarrow H^+ + HSO_3^- \qquad (2.13)$$

In Figure 2.1 the distribution of dissolved Sulphur dioxide species at various pH values in aqueous media can be seen (Fassina 1986). Around pH 4, HSO_3^- ion is the most abundant S (IV) species whereas above pH 10, SO_3^{2-} ion seems to dominate.

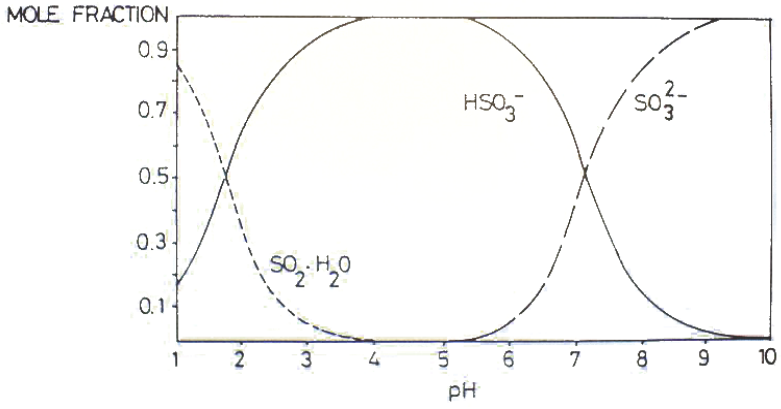

Figure 2.1. Distribution of Dissolved Sulphur Dioxide Species Versus pH at 25 °C. (Source: Fassina 1986)

The ionic strength of the aqueous solutions also affects the absorption of the sulphur dioxide in the aqueous solutions. Chang and Rochelle measured the absorption rate of SO_2 in NaCl solutions at 25 °C in a continuously stirred vessel without breaking gas-liquid interface. The SO_2 concentration in the gas phase was 1250 ppm and the NaCl concentrations was varying from 0.1 to 1 molar. Due to relatively high concentration of NaCl which affect the activity coefficient hydrogen ion diffuses faster. The presence of NaCl also increases the value of effective equilibrium constant. This resulted in 20 % increase in the SO_2 absorption rate. Due to high concentration of NaCl, hydrogen ion diffused faster which affects the activity coefficient (Chang and Rochelle 1981).

The presence of certain heavy metal ions in water also increases the absorption of sulphur dioxide. They have tried to observe this effect using low concentration of sulphur dioxide (10-1000 ppb) and low concentration of iron and manganese (10^{-5} M). They found out the time to reach equilibrium was about five minutes in the pure distilled water which was too low to observe any SO_2 removal. However, when they used manganese or iron in the water, absorption and oxidation rate was speeded up to such an extent that SO_2 was absorbed even after 5 min (Barrie et al. 1976).

Temperature is also an important factor affecting the absorption of sulphur dioxide. Hales et al. measured the solubility of the SO_2 gas in water using low concentration of sulphur dioxide (0.00178 – 0.1075 μmole L^{-1}) by a flow technique at different temperatures. They concluded that the solubility of the sulphur dioxide decreases with increasing temperature (Hales et al. 1973).

The effect of temperature on the absorption rate of sulphur dioxide has also been conducted in the literature. The experiments was carried out by using a wetted wall column with precautions to prevent rippling of the falling film. The exposure time of the liquid to the gas was varied from 0.049 to 0.97 second by changing the liquid flow rate and the film height. The experiments were run at atmospheric pressure and at 15°, 25°, 35°, and 45°C temperatures. In the gas phase they used SO_2 saturated with water vapor at the temperature of the experiments. Their results were reported in terms of the average SO_2 absorption flux. They stated that the solubility of sulphur dioxide in water decreases with increasing temperature and increases as the potential pressure of SO_2 over the solution increases (Hikita et al. 1978).

Dissociation of Sulphur Dioxide: Dissociation in chemistry and biochemistry is a general process in which ionic compounds (complexes, molecules or salts) separate or split into smaller molecules, ions or radicals, usually in a reversible manner. SO_2 exist in water as physically dissolved ($SO_2.H_2O$) and in dissociated form as bisulphate (HSO_3^-) and sulphite (SO_3^{2-}) as expressed in equations (2.7), (2.8) and (2.9). In these equations, the Henry's law constant K_H, the first and second dissociation constants K_1 and K_2 are temperature dependent (Howards 1982, Koziol et al. 1993). These constant values decrease with increasing temperature as described in equations (2.14), (2.15) and (2.16). There is a relation between temperature and Henry's law constant K_H in the equation as follows:

$$\log K_H \left[\frac{mol.SO_2}{atm.L.2H_2O} \right] = \frac{1376.1}{T} - 4.5210 \qquad (2.14)$$

There is a limitation in the use of equation. The temperature range is 0-50 C and partial pressure of $SO_2^{2-} = 2 \times 10^{-4}$ to 1.3 atm. at 25 °C

Due to differences in the experimental conditions, the first dissociation constant K_1 of the SO_2 showed differences in the literature. Therefore researchers obtained the correlation given in (2.11). Similarly K_2 (Second dissociation constant) were also reported by researchers and given in equation (2.12) (Howards 1982, Koziol et al. 1993).

$$\log K_1 = \frac{853.0}{T} - 4.740 \qquad \text{At 25 °C } K_1 = 0.0132 \text{ M} \qquad (2.15)$$

$$\log K_2 = \frac{621.9}{T} - 9.278 \qquad \text{At 25 °C } K_2 = 0.38 \times 10^{-8} \text{ M} \qquad (2.16)$$

CHAPTER 3

PROTECTION OF THE MARBLE SURFACE

Polymer coatings are used for protection of historical monuments to reduce calcite from acid attack. The detrimental effects of weathering on historical monuments and facades range from distortions in aesthetic appearance to alterations in the physical and chemical characteristics of the stone. The formation of gypsum is effected by many factors which are porosity of stone, relative humidity, SO_2 and NO_x gases, temperature and collected organic and inorganic matters on the surface. Stones which have high porosity increase the SO_2-stone reaction because of the wide surface area which reacted with SO_2 (Johansson 1988). In addition to this, previous studies showed that, high relative humidity and SO_2 concentrations increased the SO_2-calcite reaction and cause stone deformation (Gauri and Gwinn, 1982; 1983). Protection and air pollution effects on the historical stones were studied in many studies which were realized under artificial or natural atmospheric conditions (Cheng et al. 1987, Johansson 1988, Gauri 1989, Ausset et al. 1996, Böke et al. 1999, Gauri and Bandyopadhyay 1999). Therefore protection of the marble surfaces gained importance to increase life-time of statues and historical monuments. The protection studies can be divided into four groups.

In the first study the formation of gypsum was tried to converted back by using water soluble $CaCO_3$. Unfortunately, the formed $CaCO_3$ on the surface stayed in the form of powder and deformation of stone was not inhibited (Skoulikidis and Beloyannis 1984). The reaction can be expressed as follows;

$$CaSO_4 . 2H_2O + CO_3^{2-} \rightarrow CaCO_3 + SO_4^{2-} \qquad (3.1)$$

In the second group studies, polymer coating materials such as polyacrylonitrile (PAN) and polyacrylic acid (PAA) were used to decrease stone degradation on the surfaces (Gauri 1973, Atlas 1988, Elfving 1994, Thompson et al. 2002, Striegel 2003, Thompson 2003). These polymers decreased the SO_2-calcite reaction in the short term. However, in the long term this effect was disappeared and stone degradation by the mean SO_2-calcite reaction was increased exponentially. In addition to this event, lots of polymers lost their recoverable properties in the course of time and coated stones need

mechanic methods, which were unfavorable for historical stones, to send away polymer coating on the stone surface.

In the third group studies, solubility of the calcium carbonate was tried to decrease by using surfactants which were used on the gypsum. Under the laboratory conditions, gypsum formation was reduced in proportion of 10% (Böke et al. 2002).

Calcium carbonate surface was coated to oppose a resistance to the acidic conditions by using anionic certain surfactants such as phosphate, oxalate ($C_2O_4^{-2}$), oleate ($C_{17}H_{33}COO^-$) (Böke and Gauri 2003, Thompson 2003). When these solutions were used on the calcium carbonate surfaces, calcium oxalate, calcium oleate or calcium phosphate layer would be formed on the surface (3.2-3.6). The formed compounds on the surface reduced the SO_2- calcite reaction approximately 15 % (Böke and Gauri 2003). Related reactions are as follows:

$$CaCO_3 \quad Ca^{2+} + CO_3^{2-} \tag{3.2}$$

$$Ca^{2+} + C_2O_4^{2-} \quad CaC_2O_4.\,H_2O \tag{3.3}$$

$$Ca^{2+} + HPO_4^{2-} \quad Ca\,HPO_4.2\,H_2O \tag{3.4}$$

$$Ca^{2+} + 2\,F^- \quad Ca\,F_2 \tag{3.5}$$

$$Ca^{2+} + 2\,C_{17}H_{33}COO^- \quad Ca\,(C_{17}H_{33}COO)_2 \tag{3.6}$$

3.1. Biobased Polymers

The synthetic polymers mostly are the petroleum-derived polymers called products and degrability of these polymers take long time. Therefore they are called nondegradable polymers which are used in a wide range application today. The increased consumption of nondegradable polymers causes too much of solid waste, and the negative effects of these type of waste on the environment increase day by day (Dorgan et al. 2001). The amount of waste originated from polymer use can be decreased by either recycling if polymer is recyclable or incineration. Due to difficulty in biodegradability of synthetic polymers alternative polymer types gained an attention

by researchers. Especially in the packaging industry, biobased packaging polymers have attracted significant research (Weber et al. 2000).

Biodegradable polymers or biobased polymers can be divided into 3 main categories. These categories are called as Category 1, 2 and 3 respectively (Table 3.1).

In the Category 1, the polymers directly extracted/removed from biomass. The examples are polysaccharides such as starch and cellulose proteins.

In the Category 2, the polymers are produced by classical chemical synthesis using renewable biobased monomers. A good example is polylactic acid (PLA), which is a biopolyester polymerized from lactic acid monomers. The monomers themselves may be produced via fermentation of carbohydrate feedstock.

In the Category 3, polymers produced by microorganisms or genetically modified bacteria. Up to date, this group of biobased polymers consists of mainly polyhydroxyalkonoates, but developments with bacterial cellulose are in progress. Description of the polymers presented in Table 3.1 (Weber et al. 2000).

Table 3.1. Schematic Presentation of Biobased Polymers Based on Their Origin and Method of Production. (Source: Adopted by Weber et al. 2000).

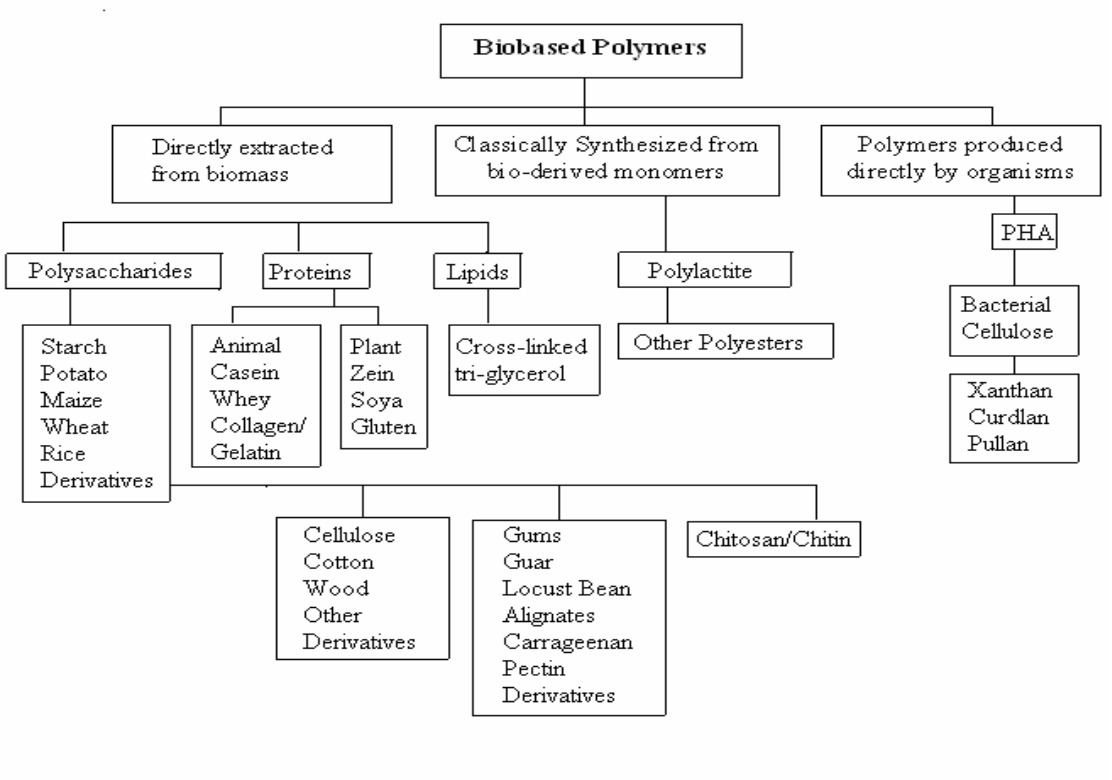

In general, compared to conventional plastics derived from mineral oil, biobased polymers have more diverse chemistry and architecture of the side chains giving the material scientist unique possibilities to tailor the properties of the final package.

In these polymers categories, the biodegradable polymers used in this study will given in details.

3.1.1. Zein

Zein is composed of a group of alcohol soluble proteins (prolamines) found in corn endosperm. Zein is mainly used in food and pharmaceutical coating and it is the water insoluble prolamine from corn gluten, manufactured initially as a concentrated powder. Zein is preferred for its coating properties such as odorless, tasteless, clear, hard and having invisible properties in the coating (Weber et al. 2000). The excellence of zein that makes it a prolamine, i.e. it's insolubility in anhydrous alcohol, and solubility in a mixture of the two, is considered on account of the preponderance of hydrophobic acids, leucine, proline and alanine. Zein`s insolubility in water is also due to the high proportion of hydrocarbon group side chains, and the high percentage of amide groups present with a relatively low amount of free carboxylic acid groups. In the study of Shukla and Cheryan, the solubility behavior of zein obtained in the form of phase diagram. According to their diagram, the solubility of the zein is increases in the certain range of solvent etc (Shukla and Cheryan 2001).

Zein has some potential advantages as a raw material for film, coatings and plastic applications. It is biodegdable and it is annually renewable due to its resource. The annual surpluses of corn provide a substantial raw material resource. However, there are also some problems with the use of as a plastically material. Zein is a biological material and, it is affected by water like most biological materials. This, couple with the fact that water is a plasticizer for zein, means that zein's properties are subject to change with humidity (Lawton 2002). Zein has good gas barrier properties when it compared other biopolymers. They provide a good barrier to O_2 and CO_2, but not to water (Tharanathan 2003).

3.1.2. Chitosan

Chitosan has most abundant natural polymer and it is obtained from the shells of crab, shrimp and krill. Chitosan is a de-N-acetylated form of chitin and it consists mainly of b(1-4)-2-amino-2-deoxy-D-glucose units. Chitosan is non-toxic, biodegradable and also has superior film forming properties, which find applications in various fields. The molecular weight of chitosan has a profound influence on the thermal, mechanical, and permeability properties of the films. Chitosan films can be modified by adding plasticizers, gelatin, cellulose and PVP to improve the strength and barrier properties (Srinivasa et al. 2007). Biodegradable chitosan films can reduce environmental problems associated with synthetic packaging. Biodegradable films still need a cost reduction to be economically beneficial. For instance, the use of chitosan which is a by-product obtained from wastes of the fishing industry would be a good alternative (Pinotti et al. 2007). Chemical structure of chitosan is shown in Figure 3.1 (Tharanathan 2003).

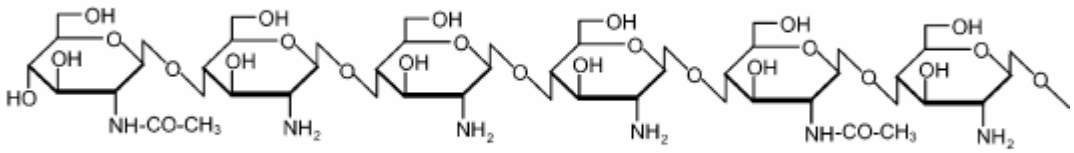

Figure 3.1. Chemical Structure of Chitosan.
(Source: Tharanathan 2003)

Chitosan has been widely used for the edible coatings. It produces materials with very high gas barrier properties and also readily forms films. Accountancy, chitosan may be used as coatings for other biobased polymers lacking gas barrier properties. However, as with other polysaccharide-based polymers, care must be taken for moist conditions (Weber et al. 2000).

3.1.3. Polylactic Acid (PLA)

Polylactic acid is the polyesters which are usually hard and brittle and it is based on a monomer produced in the fermentation of corn. The PLA have numerous

advantages which are ability to recycle back to lactic acid (non-toxic) and reduction of landfill volumes. Lactic acid can be produced by microorganisms, plants or animals. Lactic acid can be derived from intermediates with an origin in renewable materials such as acetaldehyde and ethanol, or from chemicals derived from coal like acetylene, or oil like ethylene. Lactic acid (2-hydroxypropanoic acid) is one of the smallest optically active molecules, which can be either of L (+) or D (-) stereoisomer. General structure of polylactide are shown in Figure 3.2 (Södengard and Stolt 2002).

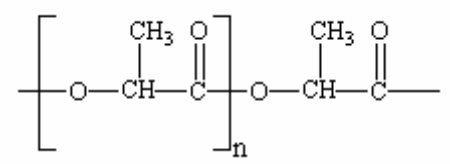

Figure 3.2. General Structure of Polylactide

The L-lactide acid has a great industrial interest due to the fact that, it is available from fermentation (Dorgan et al. 2001). Polylactic acid (PLA) has highest potential for a commercial major-scale production of renewable packaging materials. The PLA materials have a good water vapor barrier and have also relatively low gas transmittance. The raw materials used in the PLA production can be obtained from agricultural resources such as corn, wheat, or alternatively agricultural waste products, such as whey, or green juice, (Weber et al. 2002).

PLA was used as packaging materials for milk and cheese because of their high moisture barrier property compared to the conventional HDPE bottles and PE-laminates (Weber et al. 2000).

3.1.4. Polyhydroxybutyrate (PHB)

Polyhydroxybutyrate (PHB) is the member of polyhydroxyalkanoates (PHA) biopolymer group that has attracted much attention recently, due to their full biodegradability, biocompatibility and natural origin (Figure 3.3). PHB is a microbially produced thermoplastic, has similar material properties to polypropylene. It is highly crystalline. However, PHB is not widely used because of its both high and poor mechanical properties compared to synthetic plastics (Innocentini et al. 2003).

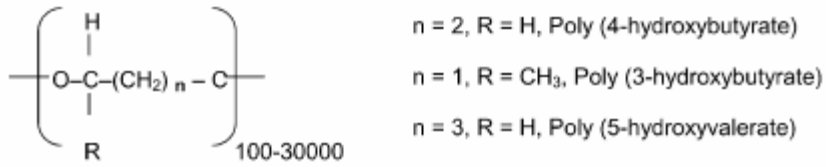

Figure 3.3. General Structures of Polyhydroxyalkanates.
(Source: Tharanathan 2003)

In contrast, PHAs are used for a wide range of applications due to their strange features. Initially, PHA was used in packaging films chiefly in bags, containers and paper coatings. Conventional commodity plastics include the disposable items, such as razors, utensils, diapers, feminine hygiene products, cosmetic containers, shampoo bottles and cups. In addition to its potential as a plastic material, PHA are also useful as stereo regular compounds which can serve as choral precursors for the chemical synthesis of optically active compounds (Reddy et al. 2003). The PHA material shows good water vapor barriers properties, which makes them interesting for a long range of food applications (Weber et al. 2002).

3.2. Material Properties

3.2.1. Gas Barrier Properties

Biobased polymers are particularly used for food packaging due to their good gas barrier properties. The packaging materials require having certain gas barrier properties to provide a constant gas composition inside the package. Carbon dioxide, oxygen and nitrogen or their combinations are mostly found inside the package. For this reason, gas barrier researches of the biobased polymers are focused on these gases. Biobased polymers show good gas barrier properties as much as mineral-oil-based polymers. In the Figure 3.4, oxygen permeability of biobased materials are compared to conventional mineral-oil-based polymer materials.

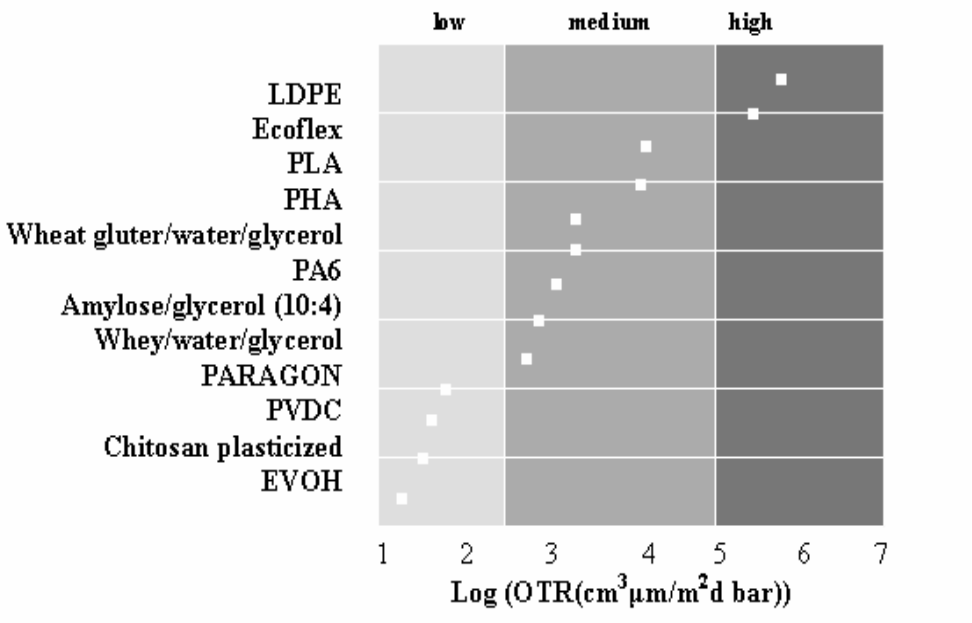

Figure 3.4. Comparison of Oxygen Permeability of Biobased Materials Compared to Conventional Mineral-Oil-Based Materials. (23 ºC, 50% RH), (Source: Adopted by Weber et al. 2000).

Biobased polymer materials are hydrophilic and their gas barrier properties are very much depending upon the humidity conditions for the measurements. The gas permeability of hydrophilic biobased materials may increase manifold when humidity increases. Especially, this is a phenomenon also seen with conventional polymers. Nylon and ethylvinyl alcohol which are high gas barrier materials are affected by increasing. Gas barriers based on PLA and PHA is not expected to be dependent on humidity (Weber et al. 2000).

3.2.2. Water Vapor Transmittance

Food applications require materials which hinder the moist condition due to the nature hydrophilic behavior of many biobased polymers. Figure 3.5 shows the corporation of the water vapor transmittance of various biobased materials based on mineral oil. Water vapor transmittance rates of biobased polymers are higher than some conventional mineral-oil-based plastics. Very few biobased materials show high water vapor barrier properties such as PLA and PHA. Especially, the researchers are concentrated on the development of water vapor barrier and future biobased materials

must also be able to mimic the water vapor barriers of the conventional materials known today (Weber et al. 2000).

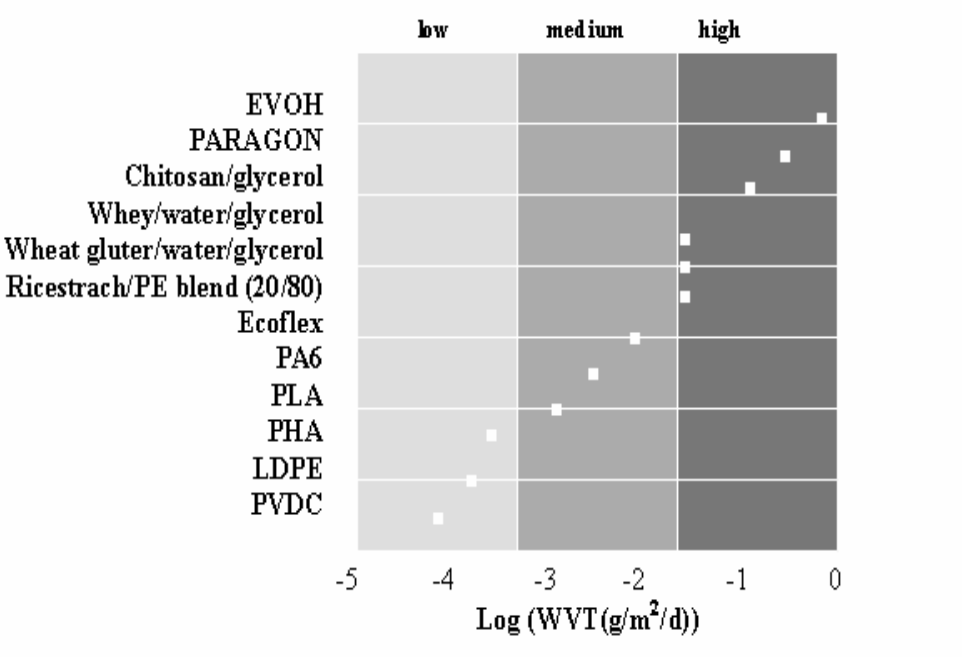

Figure 3.5. Water Vapor Transmittance of Biobased Materials Compared to Conventional Packaging Materials Based on Mineral Oil. (23 ºC, 50% RH), (Source: Adopted by Weber et al. 2000).

Most of the biobased polymers used in food industry packaging are the result of having good moisture and gas barrier properties. Haugaard et al. pointed out that some biobased packaging materials and edible films / coatings and their critical functions of packaging. Chitosan and corn zein are used for edible coatings due to having oxygen and carbon dioxide barrier properties, Polyhydroxybutyrate film, polylactic acid are used for biobased packaging due to having moisture, oxygen and carbon dioxide barrier (Haugaard et al. 2001).

CHAPTER 4

EXPERIMENTAL METHOD

4.1. Preparation of Marble Slabs

Rectangular slabs cut from large blocks of Marmara marble and polished with 400-grit silicon carbide powder. The samples were cleaned ultrasonically in deinozed water to remove fine particulates and dried at 105 ºC, and cooled in a desiccator till to reach a constant weight. The weights were then recorded to compare if any water adsorption were occurred during this preparation.

4.2. Preparation of Biobased Polymers

In this study, four different type biopolymers were used. Glycerol plasticizer added zein, zein, chitosan, polyhydroxybutyrate (PHB), low and high molecular weight Polylactic acid (PLA) were prepared for protection of the surfaces.

For the zein (Sigma-Aldrich), ethly alcohol (99.5%) was mixed with water to have 70% ethyl alcohol as solvent. Then, 7.5 gr. corn-zein was dissolved in this 50 ml. ethanol (70%) at room temperature to a concentration of 15% (w/v). This solution was stirred with magnetic stirrer for 6 hours to have a homogeneous film. Zein was also prepared with glycerol (Sigma) (M_w = 92 g/mol) due to brittle structure of zein. Similarly, this solution was stirred for 6 hours to have homogeneous solution. 15% zein with glycerol plasticizer was obtained. These solutions were used to coat marble slabs surfaces by using dip-coating apparatus.

Chitosan (Aldrich) was prepared using 0.5 gr chitosan in 25 ml. (2% (v/v)) acetic acid solution. The mixture was stirred to obtain a homogen 2% (w/v) chitosan solution as dip-coating solution.

The other biodegradable polymer PHB was prepared by using 1.25 gr of Poly[(R)-3-hydroxybutyric acid] (Fluka). The solvent for PHB was chloroform (Merck). 25 ml of chloroform (99-99.4%) was used to dissolve 1.25 of PHB and the mixture was heated at 50-55 C and stirred 1 day. 5% PHB solution was obtained for coating technique.

Low molecular weight L-lactide PLA (Purac) and high molecular weight L-lactide PLA (Boehringer) were prepared as other coating materials. Firstly, 1.20 gr. low molecular weight PLA was dissolved in 24 ml. chloroform (99-99.4%). Then solution was mixed with magnetic stirrer approximately 8 hours at the room temperature. 5% PLA solution was used for dip coating of marble slabs. The high molecular weight PLA was also prepared by same procedure.

4.3. Coating of the Marbles with Biopolymers

Cut, cleaned and dried marble slabs were coated with dip-coating machine apparatus supported NIMA software program. Thicknesses of the films on the marble surfaces were determined by adjusting NIMA dipper mechanism apparatus up and down speed. Marble slabs were immersed into the biopolymer solution with a constant speed at 100 mm/min by the dipper mechanism, and then marble slabs were left 30 second in the biopolymer solution. The slabs were removed from the solution with 150 mm/min up speed.

The parameters that used to conduct the experiment were summarized in the Table 4.1. ın this table, the polymer solution concentration, how many samples prepared for each biodegradable polymer can be seen.

Table 4.1. Experimental Conditions for Marmara Marble Slabs (C= coated, B= blank).

Polymer type	Zein	Zein+Gly	Chitosan	PHB	L.PLA	H.PLA
Polymer Conc.	15 %	15 %	2 %	5 %	5 %	5 %
Solvent	Ethly alcohol	Ethly alcohol	Acetic acid	Chloro-form	Chloro-form	Chloro-Form
Sampling number	9C+3B	15C+5B	15C+5B	18C+6B	18C+6 B	15C+5 B
Exposure Duration (day^{th})	10, 25 and 35	3, 7, 14, 21 and 35	3, 13, 21, 35 and 50	3, 13, 21, 35, 50 and 85	3, 13, 21, 35, 50 and 85	7, 21, 35, 65 and 85

4.4. Sulphation Reaction Experiment

The effects on the biodegradable polymer treated surfaces exposed to SO_2 with nearly 8 ppm and 100% relative humidity were determined.

Six set of samples were exposed in an atmosphere at nearly 100% relative humidity in a reactor, which was a modified 10 L desiccator, showed in Figure 4.1 (Böke and Gauri 2003). In the reactor, water was placed at the bottom of the reaction chamber. The dry air was passed over SO_2 permeation tubes (VICI Metronics), at the rate of 215 $cc.min^{-1}$. The SO_2-air stream was injected in the reactor beneath the water table to saturate the SO_2-air stream with water. After the water reached equilibrium with the above concentration of SO_2 and water reached constant pH, the samples were exposed. Several days experimental were required for the water to reach the equilibrium with SO_2 in the atmosphere.

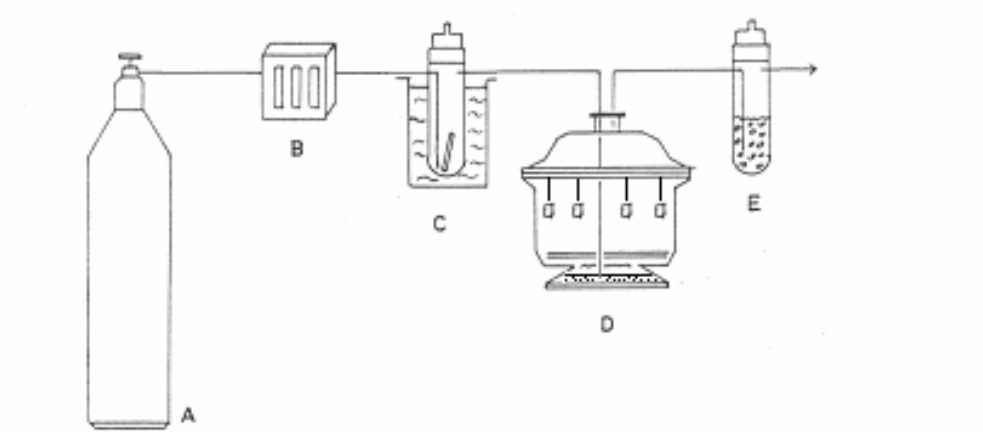

Figure 4.1. Schematic Presentation of Experimental Sulphation Reaction. Components of the Experiment are; A: Dry Air Cylinder, B: Mass Flow Controller, C: Permeation Tube in 30°C, D: Reaction Chamber, E: Washing Bottles.

The samples were tied to a glass stand by nylon threads so that they hang freely above the water table in the reactor (Figure 4.1). A maximum of eight samples were exposed at a time in order to maintain a constant concentration of the gas in the reactor. The concentration of SO_2 in the reactor was determined from the permeation rate obtained from the weights loss of the permeation tube over time.

In this study, formation of gypsum was monitored. By the time, the monitoring of gypsum thicknesses correlated with the total sulphate concentrations which were determined by using Ion Chromatography (IC).

Gauri et al. determined the crust formation on marble at relative humidity between 40-99 % in the experimental atmosphere and reported the equation given above previously (2.1 and 2.2) (Gauri et al. 1982; 1983). The first formed calcium sulfite hemihydrate oxidizes to gypsum if condensation of moisture is allowed to occur upon sample surfaces. The amount of total SO_4 which formed on the coated and blank samples as a result of sulphation were determined with IC technique. The reaction ratios between calcium sulfite hemihydrate ($CaSO_3.½H_2O$) and gypsum ($CaSO_4.2H_2O$) were determined by FT-IR analysis. The surface structure of calcium sulfite hemihydrate and gypsum crystals formation and degradation of the polymer films were determined by Scanning Electron Microscope (SEM).

4.5. Use of Sulphur Dioxide Permeation Tube for Low SO_2 Concentrations

Low concentration of SO_2 and air mixture was prepared by passing of the dry air over the sulphur dioxide permeation tube (Dynacal Standard type with a size 10 cm.). The air flow rate was adjusted with a mass flow controller at 216 ml/min. This air flow rate resulted in the permeation rate as 4580 ng/min/10cm at 30 °C which was obtained by following weight loss in the permeation tube at certain time intervals. Then, this SO_2 weight loss was plotted versus time. The slope of the graph gave the permeation rate for the constant known SO_2 concentration (Figure 4.2). 8.1 ppm SO_2 concentration in air was obtained. The calculation is shown below;

$$C = \frac{P\,K_m}{F_T} \qquad (4.1)$$

Where,

C: Concentration of SO_2 in air gas mixture (ppm)

P: Permeation rate ng/min/10 cm

K_m: Molar constant for sulphur dioxide (0.382)

F_T: Total flow of air gas mixture (ml/min)

Molar constant for sulphur dioxide obtained from permeation tube catalog and the measure value and calculated experimental concentration is given as an example.

SO_2 (gr /h) = Slope/24 = 0.0066 / 24 = 2.75×10^{-4}
SO_2 (gr /min) = 2.75×10^{-4} / 60 = 4.58×10^{-6}
SO_2 (ng /min) = 4580

$$C(SO_2) = \frac{4580\,(\text{ng/min}) \text{ x } 0.382}{216\,\text{ml/min (flow rate)}} = 8.1\,ppm$$

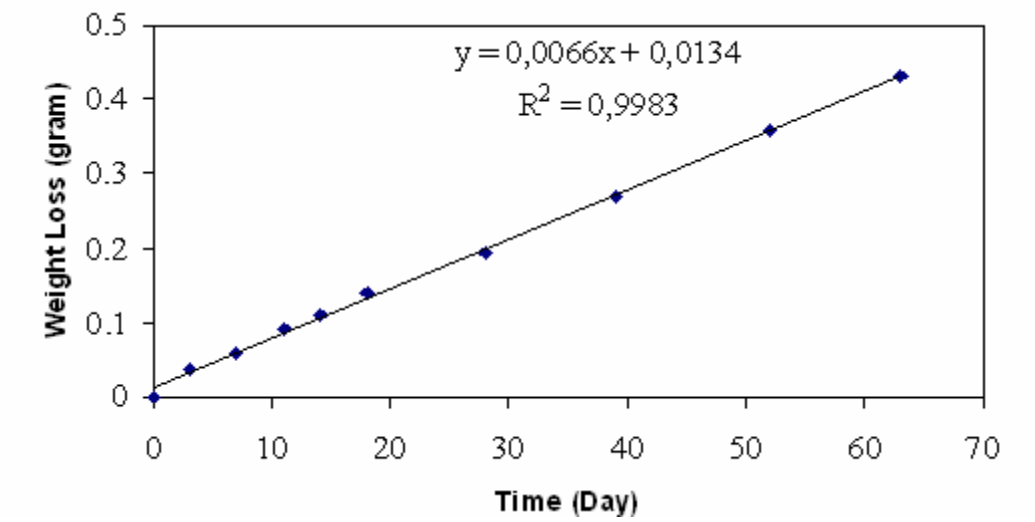

Figure 4.2. Weight Loss of SO_2 Permeation Tube at 30 C Temperature.

4.6. Methods Used in Quantitative and Qualitative Determination of Sulphation Products

Samples which were exposed to SO_2 and air mixtures under certain conditions were removed from the reaction chambers at definite time intervals. They were analyzed quantitatively and qualitatively by the use of IR spectrometry, scanning electron microscope and IC.

4.6.1. Quantitative Analyses of Sulphation Reaction Products by FTIR

The method developed by Böke et al. was used here to determine the sulphation reaction products: $CaSO_3.½H_2O$ and $CaSO_4.2H_2O$ quantitatively. In this method, the FTIR spectrum of pure calcium carbonate appeared as a strong band centered around 1453 cm^{-1}, characteristics of the C-O stretching mode of carbonate together with a narrow band around 873 cm^{-1} of the bending mode (Figure 4.3a). The observed bands around 980 cm^{-1} and 652 cm^{-1} were characteristics of those reported in the literature for sulphite ion, (Martin et al. 1987). The broad absorption at 980 cm^{-1} was assigned to the symmetric and asymmetric bending mode (Figure 4.3b). The strong band centered around 1140 cm^{-1} which splits into two components at around 1146 cm^{-1} and 1116 cm^{-1} and the small peaks at 669 and 602 cm^{-1} were assigned to the stretching and bending modes of sulphate as seen in the pure gypsum spectrum (Figure 4.3c). In this approach, among those bands described, the strong absorption band of carbonate at 1453 cm^{-1}, the band of sulphate centered around 1146 cm^{-1} and the characteristic band of sulphite at 980 cm^{-1} were used as analyze peaks for the analysis of the related components. It is reported that, the FTIR spectrum of the mixture of these components showed that there was no significant interference to any of the analyze peak of a component from the other two components present in the matrix, thus the, analyze peaks chosen could be safely used for the analysis of the individual components in their mixture (Böke et al. 1999).

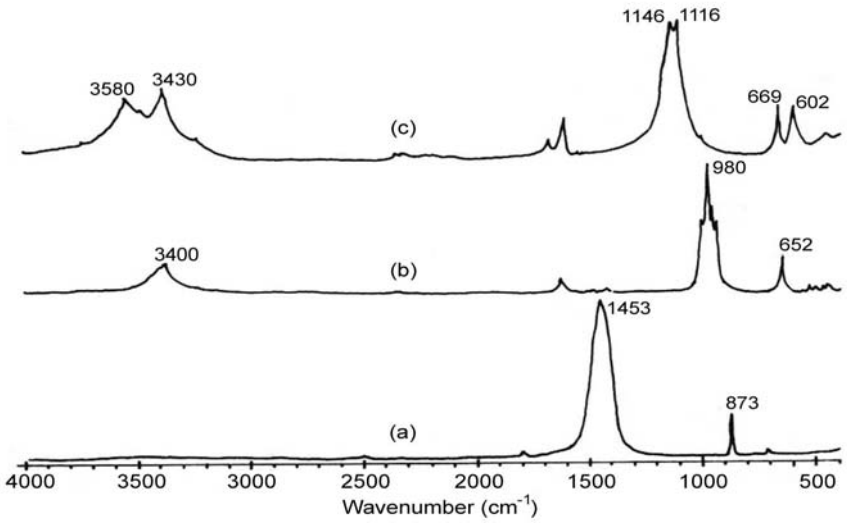

Figure 4.3. FTIR Spectra of Pure Calcium Carbonate (a), Pure Calcium Sulphite Hemihydrate (b) and Pure Gypsum (c) (Source: Böke et al. 1999).

Böke et al. determined the absorbance ratio of the sulphation products versus to their molar ratio (Figure 4.4). This figure was used to determine molar quantities of $CaSO_3.½H_2O$ and $CaSO_4.2H_2O$. Absorbance peaks of $CaSO_3.½H_2O$ and $CaSO_4.2H_2O$ were determined from FT-IR figures and molar ratio calculated from Figure 4.4 (Böke et al. 1999).

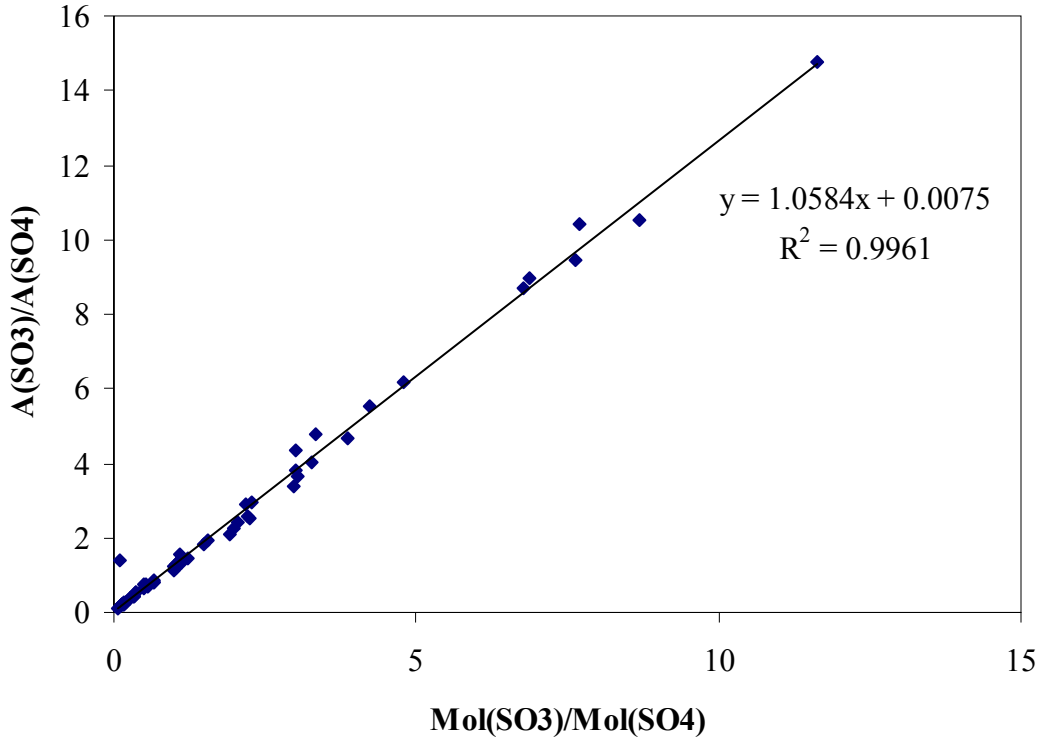

Figure 4.4. Absorbance Ratio Versus Molar Concentration Ratio Curve for Calcium Sulphite Hemihydrate and Gypsum.

SO_2 exposed marble slabs surface were shaved with lancet and taken 0.3- 0.5 mg from shaved powder for the FTIR analysis. This powder mixed with 80 mg pure KBr and pressed with 10 tones/cm^2 to obtain pellet. Then pressed pellets were analyzed with Perkin Elmer Spectrum BX II model IR with a range of 400 – 4000 cm^{-1}.

4.6.2. Determination of the Total Sulphate by Using Ion Chromatography

Calcium sulphite hemihydrate does not dissolved in water but it can be easily transformed to gypsum which dissolves in water. To find total sulphate concentration the $CaSO_3.½H_2O$ products which formed on the surface of marble after the exposure to artificial atmosphere in the reactor should be converted or transformed to gypsum to dissolve in water. Therefore exposed and unexposed marble slabs were put into 25 mL. of ultra-pure water which contains 2% H_2O_2 for 72 hours for the conversion of all sulphation products to gypsum. Then the dissolved sulphate of water analyzed as total sulphate with IC (Dionex with GP50 Gradient Pump and ED50 detector).

For calibration of ion chromatography, from the stock solution 2.3, 4.7, 7.4, 9.8, 12.5 and 15.4 ppm levels of sulphate standard solutions were prepared. 6 levels of calibration were conducted and curve was given in Figure 4.5.

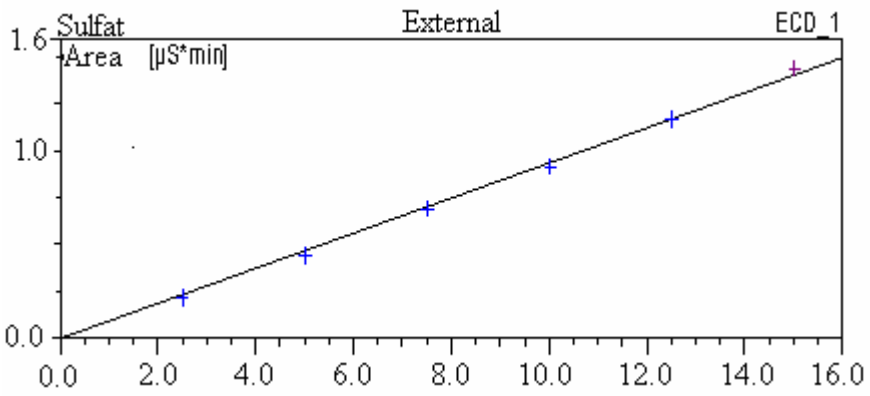

Figure 4.5. Calibration Curve of the Standard Sulphate Solution (R^2=1)

4.6.3. Determination of Microstructures and morphologies by Using Scanning Electron Microscopy (SEM)

Scanning electron microscope analysis have been carried out to determine the characterization of the microstructures and morphologies of coated and uncoated marble samples before and after exposure to SO_2 were examined by using a Philips XL-30-SFEG model scanning electron microscope (SEM) equipped with an Energy Dispersive

X-ray (EDX) analyser. Gold coated samples were used in the determinations. Magnifications varying from 2000 to 200 were used in investigations.

4.7. Calculations of the Gypsum Crust Thickness and Other Parameters

4.7.1. Thickness of Gypsum Crust on Marble Surface

In this thesis, the thickness of gypsum after each period of SO_2 exposure was determined by the following equations (Gauri and Bandyopadhyay 1999, Böke and Gauri 2003). In these equation;

$$Wp = \frac{M_p}{M_A} \cdot W_A \tag{4.2}$$

$$\delta_p = \frac{W_p}{A \cdot \rho_c} \cdot \frac{M_p \cdot \rho_c}{M_c \cdot \rho_p} \tag{4.3}$$

M_p = Molecular weight of gypsum ($CaSO_4.2H_2O$ = 172.17)

M_A = Molecular weight of sulphate ion ($SO_4^{=}$ = 96,056)

M_c = Molecular weight of calcite ($CaCO_3$ = 100.09)

W_A = Sulphate weight which formed on the marble surface (g).

δ_p = Crust thickness (cm),

$_c$ = Density of calcite

W_p = Weight of the product, gypsum (g)

$_p$ = Density of gypsum, (2.32 g/cm^3)

A = Surface area of the sample, (cm^2)

W_p , the weight of the gypsum, was determined by using the mass balance from the weight of SO_4^{2-} ions (W_A), obtained by leaching these in known volume (L) of water from the exposed sample and measuring their concentration (ppm) by IC (ion chromatography).

Sample calculations of the gypsum crust thicknesses which formed on the polymer coated and uncoated marble surfaces were shown in Appendix B.

4.7.2. Average Deposition Velocity

The results which obtained from experiments were used for calculation of the marble – SO_2 average deposition velocity. Calculations were used following equation which was developed by (Gauri and Bandyopadhyay 1999, Böke and Gauri 2003).

$$V_d = \frac{\rho_p}{M_p \cdot C_s} \cdot \frac{d\delta_p}{dt} \tag{4.4}$$

Where;

V_d = SO_2 – marble average deposition rate (cm/s);

$_p$ = Gypsum crust thickness (cm);

M_p = Molecular weight of gypsum (mol/g);

$_p$ = Density of gypsum (g/cm^3),

C_s = Concentration of SO_2

Sample calculation of the SO_2 - Marble average deposition velocity on the polymer coated and uncoated marble surfaces are represented in Appendix B.

4.7.3. Determination of the Quantity of Calcium Sulphite Hemihydrate and Gypsum

Formations and quantifications of calcium sulphite hemihydrate and gypsum which resulted from the SO_2–marble reaction were determined by the FTIR spectroscopy technique throughout the experiment study. SO_2 exposed coated and uncoated marble surfaces were shaved with knife carefully.

Formation of sulphation products ($CaSO_3.½H_2O$ and $CaSO_4.2H_2O$) which were observed throughout the experiment showed homogeneous dispersion and formed a thin layer on the marble surfaces. Shaved sulphation products were analyzed with FTIR spectrocopy and quantitities of calcium sulphite hemihydrate and gypsum were determined by using peak areas on the FTIR figures. Pursued following equations;

$$W_{Total\ (SO4)} = W_{SO3\ \ SO4} + W_{SO4} \tag{4.5}$$

Where;

$W_{Total\ (SO4)}$ = Weight of total SO_4 (obtained SO_4 concentration From IC, mg)

$W_{\ SO3\ \ SO4}$ = Weight of SO_3 which were transformed to SO_4

$W_{\ SO4}$ = Weight of SO_4

$$\text{mmol}_{\ \text{Total}\ \ (SO4)} = \frac{W_{Total(SO_4)}}{MW_{(SO_4)}} \tag{4.6}$$

Where;

$\text{mmol}_{\ \text{Total}\ \ (SO4)}$ = Total molar quantity of SO_4 (mmol)

$W_{Total\ (SO4)}$ = Weight of total SO_4 (obtained SO_4 concentration From IC, mg)

$MW_{\ (SO4)}$ = Molecular weight of SO_4

$$\frac{A_{SO_3}}{A_{SO_4}} = 1.0584 \cdot \frac{mmol_{(SO_3)}}{mmol_{(SO_4)}} - 0.0075 \tag{4.7}$$

Where;

$A_{(SO_3)}$ = SO_3 absorption value from IR

$A_{(SO_4)}$ = SO_4 absorption value from IR

$CaSO_4.2H_2O$ (mg) = $\text{mmol}_{\ (CaSO4.2H2O\ )}$ x M.W ($CaSO_4.2H_2O$)

$CaSO_3.0.5\ H_2O$ (mg) = $\text{mmol}_{\ (CaSO3.0.5\ H2O\ )}$ x M.W ($CaSO_3.0.5H_2O$)

Sample calculations of the quantity of calcium suphite hemihydrate and gypsum are shown in Appendix B.

4.7.4. Determination of Polymers Percentage Protection Factor

Polymers percentage protection factors were determined by comparing uncoated marbles and polymer coated marbles gypsum crust thicknesses. Uncoated marble gypsum crust thicknesses were consented as 100% and all calculations were done by

this assumption. Sample calculations of polymer % protection factors were showed in Appendix B.

$$\%PF = 100 - \frac{(U\delta_p).100}{(C\delta_p)} \tag{4.7}$$

U p = Gypsum crust thickness of uncoated marble surface

C p = Gypsum crust thickness biopolymer coated marble surface

CHAPTER 5

RESULTS AND DISCUSSION

5.1. Gypsum Crust Thickness and Average Deposition Velocity

As mentioned before, marble slabs were coated with either water barrier or gas barrier biopolymers. Among these biopolymers, zein and chitosan are known as good gas barrier polymers while PLA and PHB have good water barrier property.

In this part, gypsum crust formation, its thickness, and the average SO_2 deposition values for each biopolymer coated and uncoated control samples will be given.

Firstly the plasticized zein coated and uncoated marble slabs were put into reaction chamber. The exposed coated and uncoated slabs were taken out 3, 7, 14, 21 and 35^{th} days. Total sulphate amounts formed on the marble surfaces were determined by ion chromatography used to calculate gypsum crust thickness and average deposition velocity for each coated and uncoated marble sample.

Equations (4.2) and (4.3) were used to calculate gypsum crust thickness. The plasticized zein coated marble slabs showed higher crust thickness than uncoated marble slabs (Figure 5.1). The enhancement on the thickness could be the acceleration of the sulphation reaction. It may be resulted in low water vapor barrier properties of the zein biopolymer. As mentioned previously, water was one of the most significant components for the formation of gypsum crust thickness (Bernal and Bello 2003). Also, the enhancement of gypsum crust thickness might have been related to the porosity effect of glycerol similar to the literature survey. (Tapia-Blacido et al. 2005).

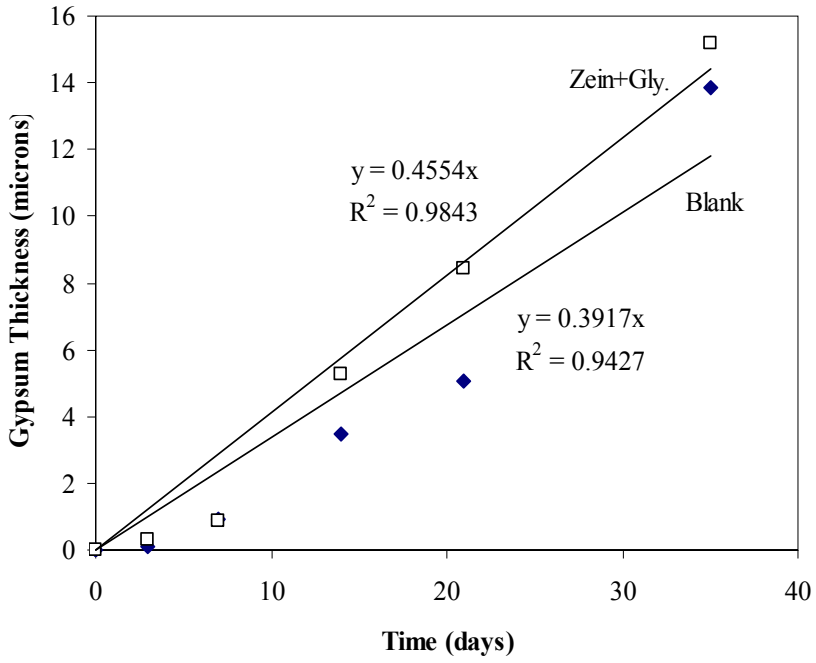

Figure 5.1. Gypsum Crust Thicknesses of Uncoated and Plasticized Zein Coated Marbles.

The equation (4.4) was used to calculate the average velocity of plasticized zein coated and uncoated marble slabs. Results were given in Table 5.1. The average deposition velocity of SO_2 on the plasticized zein coated marble slab surface also lead to the acceleration in SO_2-calcite reaction. Even though not much difference was observed in the average deposition velocity, high gypsum thickness showed that there would be water vapor and SO_2 gas absorption was highly possible by the film. Enhancement of SO_2-calcite reaction was reported previously in the study of Gauri in where synthetic polymer was used as a coating agent (Gauri 1973).

Table 5.1. The Average Deposition Velocity of the Plasticized Zein Coated and Uncoated Marbles on 35th Day.

Sample	Crust thickness (μm)	Average deposition velocity (cm/sec.)
Plasticized zein	15.18	0.021
Uncoated	13.84	0.018

In the second study, pure zein was prepared as coating agent, and the marble slabs were coated with zein itself to decrease the negative effects originated from the use of plasticizer. The exposed coated and uncoated slabs were taken out 10, 25 and 35th day to determine the gypsum crust thickness on the marble slab surfaces. Gypsum crust thicknesses of the pure zein coated marbles were also observed higher than uncoated marbles due to high water vapor permeability of the zein film (Figure 5.2). Pure zein is also brittle without plasticizer (Lawton 2004). Some cracks were observed on the zein coated surfaces. Directly exposure of the surface from these cracks, and movement of SO_2 gas and water vapor underneath of the film may be caused the high gypsum crust formation.

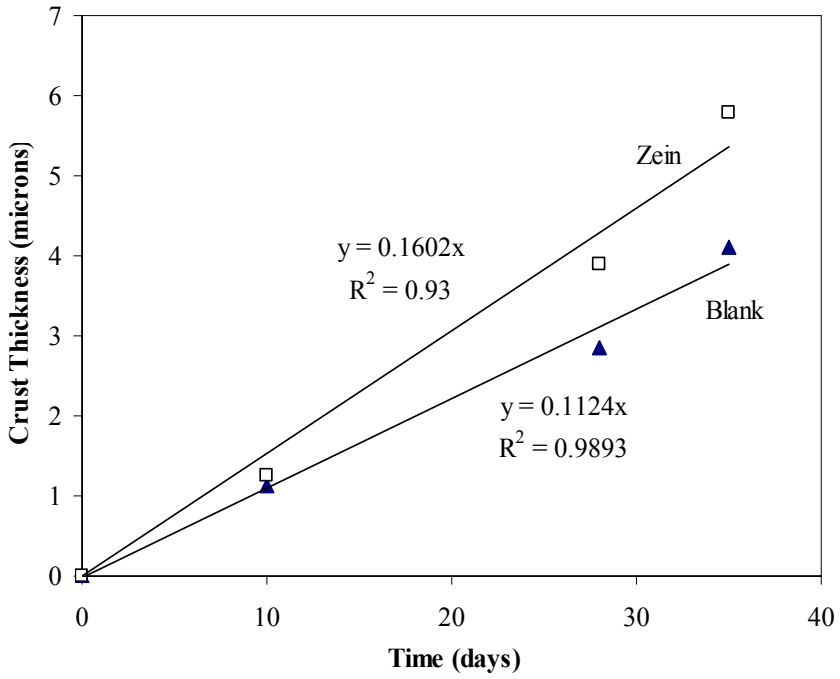

Figure 5.2. Gypsum Crust Thicknesses of Uncoated and Pure Zein Coated Marbles.

The average deposition velocity of the pure zein coated and uncoated marble slabs were calculated higher than control marble after 35 days exposure similar to the plasticized zein. The average velocity was one order of magnitude lower than the plasticized zein. As a result pure zein was found unsuitable for protection of the marble due to acceleration SO_2-marble reaction.

Table 5.2. The Average Deposition Velocity of the Pure Zein Coated and Uncoated Marble on 35th Day.

Sample	Crust thickness (μm)	Average deposition velocity (cm/sec.)
Zein	5.78	0.00728
Uncoated	4.10	0.00512

Another biopolymer used in this study was chitosan. Chitosan coated and uncoated marble slabs were exposed to 8.1 ppm. SO_2 and the samples were taken out from reactor on the day of 3, 13, 21, 35 and 50th to determine the gypsum crust thickness and average deposition velocities. Similarly, chitosan biopolymer also showed the similar behavior as zein and plasticized zein. The gypsum crust thickness on the surface of chitosan coated surface was higher than uncoated control samples (Figure 5.3). Chitosan is also referred as a good gas barrier polymer but it has low water vapor barrier property like zein (Weber 2000). Chitosan is also a hydrophilic material. Gas barrier properties in hydrophilic polymers are influenced by relative humidity. As a result gas permeability may increase manifold when humidity increases (Weber et al. 2002). The gypsum crust thickness of chitosan coating was worse than other biopolymers because of hydrophilicity and high water vapor permeability properties.

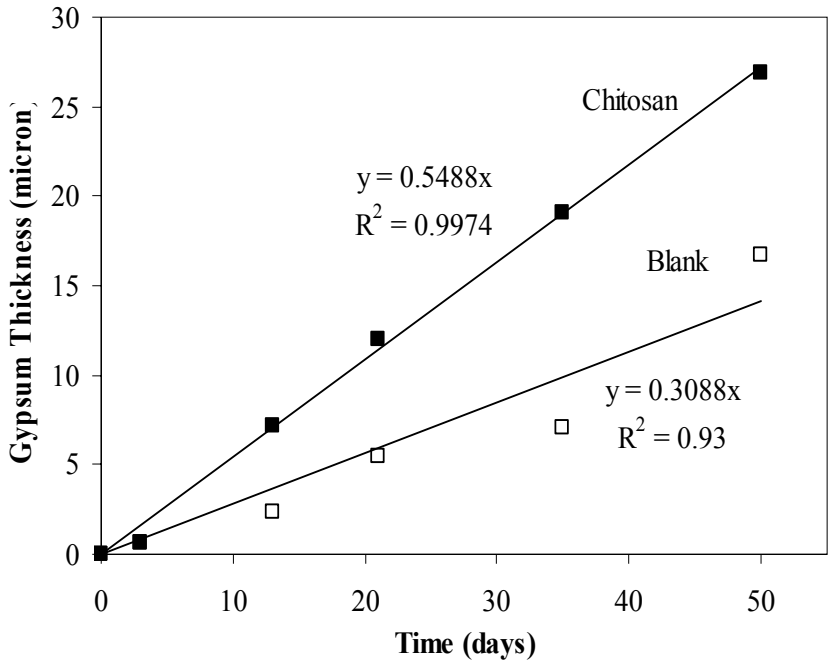

Figure 5.3. Gypsum Crust Thicknesses of Uncoated and Chitosan Coated Marbles.

The average deposition velocity and the crust thicknesses of the chitosan coated and uncoated marble slabs were given in Table 5.3. Its average deposition velocity was defined higher than control marble such as zein and plasticized zein and these values showed that gas barrier biopolymer chitosan was unsuitable for protection.

Table 5.3. The Average Deposition Velocity of the Chitosan Coated and Uncoated Marbles on 50th Day.

Sample	Crust thickness (μm)	Average deposition velocity (cm/sec.)
Chitosan	26.91	0.0249
Uncoated	16.70	0.0140

The second half of the experiment included the biopolymer with showing good water vapor barrier properties. Polyhydroxybutyrate (PHB) and low molecular weight polylactic acid (LPLA) coated and uncoated marble slabs were exposured 3, 13, 21, 35, 50 and 85th days at 8.1 ppm SO_2 concentration in the reactor. In the Figure 5.4 and Figure 5.5 the crust thicknesses of LPLA and PHB coated marble slabs were given.

There was decrease in the formation of the gypsum crust. LPLA and PHB polymer coatings were decreased sulphation products due to their high water vapor barrier and hydrophobic behavior (Weber 2000 and Iwata et al. 1999).

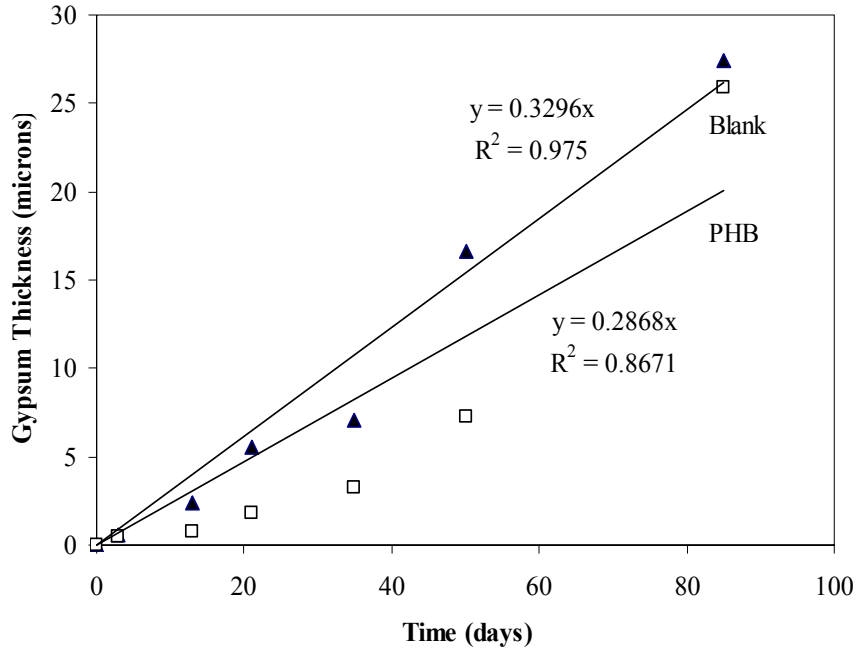

Figure 5.4 Gypsum Crust Thicknesses of Uncoated and PHB Coated Marbles.

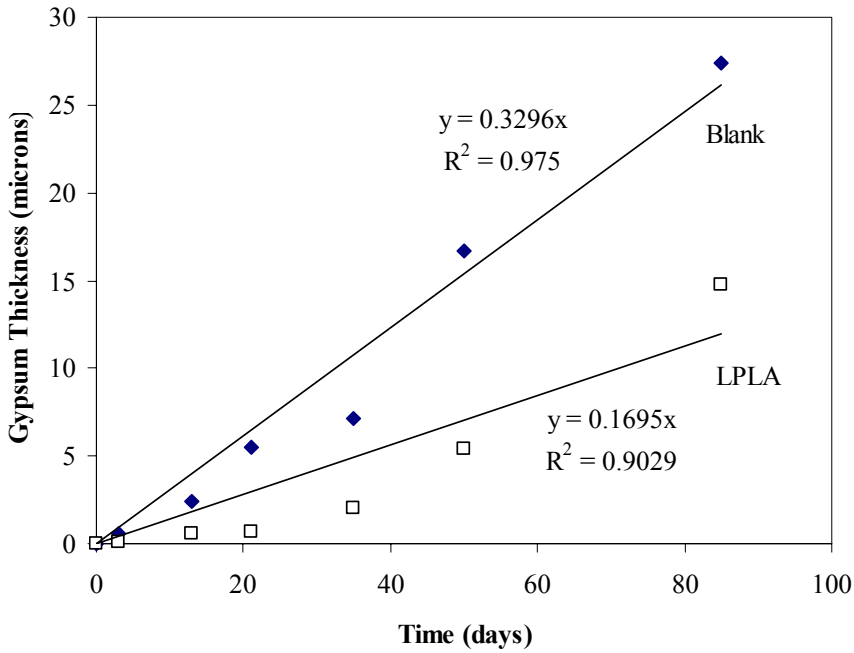

Figure 5.5. Gypsum Crust Thicknesses of Uncoated and LPLA Coated Marbles.

The average deposition velocities of the PHB and LPLA coated marble slabs were slower than control uncoated marble slabs (Table 5.4). Both biopolymers coated the marble slabs showed less crust formation compared to control samples. The LPLA coated surface deposition velocity was a lot lower than PHB coated surface. When these two polymers were compared the difference with the uncoated was quite higher for LPLA.

Table 5.4. The Average Deposition Velocity of the PHB and LPLA Coated and Uncoated Marbles on 85th Day.

Sample	Crust thickness (μm)	Average deposition velocity (cm/sec.)
Uncoated	54.7	0.028
PHB	51.8	0.025
LPLA	29.6	0.015

Due to having a good result for the decrease in the formation of gypsum with low molecular weight PLA, the high molecular weight polylactic acid (HPLA) was experimented for the marble surface protection. This time HPLA coated and uncoated marble slabs were exposured 7, 21, 35, 65 and 90th days in the reactor, and the results were given in Figure 5.6. HPLA showed excellent inhibition of gypsum formation (Figure 5.6). The lowest gypsum crust thickness was obtained with the use of HPLA. Gypsum formation differences between HPLA and LPLA might be resulted in differences of the free volume and glass temperature of polymer. Since, HPLA had less free volume and high glass temperature which caused to slower diffusion of water vapor and SO_2 gas.

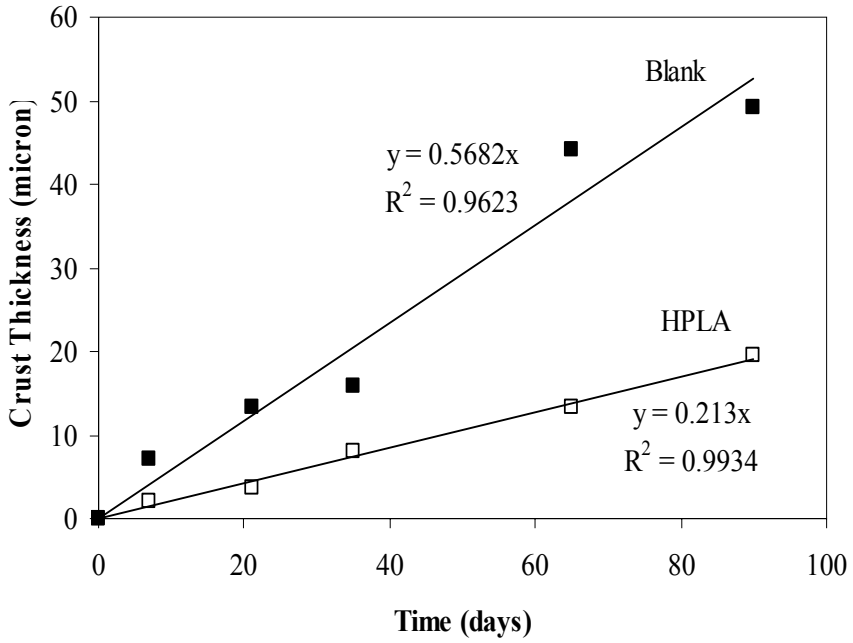

Figure 5.6. Gypsum Crust Thickness of Uncoated and HPLA Coated Marbles.

The inhibition effect was observed in the average deposition velocity. Similarly lowest average deposition velocity was calculated for HPLA. It is concluded that HPLA was found as the most suitable biopolymer for the protection of the marble surfaces due to significant inhibition of SO_2-calcite reaction.

Table 5.5. The Average Deposition Velocity of the HPLA Coated and Uncoated Marbles on 90th Day.

Sample	Crust thickness (μm)	Average deposition velocity (cm/sec.)
HPLA	19.54	0.0097
Uncoated	49.31	0.0258

5.2. Quantities of Calcium Sulphite Hemihydrate and Gypsum

The quantities of the calcium sulphite hemihydrate ($CaSO_3.½H_2O$), and gypsum ($CaSO_4.2H_2O$) of the polymers coated and uncoated marbles were determined by the FTIR spectroscopy technique throughout the experimental study. Polymer coated and

uncoated marble surfaces were shaved with knife carefully. Shaved sulphation products were analyzed with FTIR spectroscopy and quantities of calcium sulphite hemihydrate and gypsum were determined by using peak areas on the IR figures. IR figures of all each polymer coated and uncoated marble are represented in Appendix C. Total sulphate amounts were determined by ion chromatography and compared with quantities of $CaSO_3.½H_2O$ and $CaSO_4.2H_2O$.

In this part, quantities of the $CaSO_3.½H_2O$ and $CaSO_4.2H_2O$ which obtained from IR spectra of the biopolymer coated and uncoated marble slabs and their total sulphate amount will be given.

Formations of $CaSO_3.½H_2O$ and $CaSO_4.2H_2O$ on the plasticized zein coated and uncoated marble slab surfaces were monitored at the determined time intervals. The peaks of $CaSO_3.½H_2O$ and $CaSO_4.2H_2O$ were observed on IR spectra after 35 day. The quantities of the calcium sulphite hemihydrate and gypsum of plasticized zein coated marble was found higher than the uncoated marble (Table 5.6). The acceleration effect on SO_2-calcite reaction with plasticized zein coated marble was also supported with this result. On the other hand, there was a decrease in the oxidation of calcium sulphate hemihydrate to gypsum due to gas barrier property of the film. Similar effect was reported previous study which used the some surfactants as coating agent (Böke et al. 2002). The either zein or glycerol behaved as an inhibitor to cut down oxidation of the calcium sulphate hemihydrate to gypsum.

Table 5.6. The Quantities of the $CaSO_3.½H_2O$ and $CaSO_4.2H_2O$ and Total Sulphate on 35^{th} Days.

Sample	A_{CaSO3}	A_{CaSO4}	$CaSO_4.2H_2O$ (mg)	$CaSO_3.½H_2O$ (mg)	Total SO_4 (mg)
Plasticized zein	0.21	0.08	5.99	11.17	11.65
Uncoated	0.33	0.72	13.75	4.54	11.04

The calculated quantities of the calcium sulphite hemihydrate and gypsum and measured total SO_4 amount on pure zein coated and uncoated marble after 35 days exposure were given in Table 5.7. Pure zein accelerated the SO_2-calcite reaction. While it reduced the oxidation of calcium sulphate hemihydrate to gypsum like plasticized zein. This event point out that pure zein behaved as an inhibitor in some component to

the oxidation of the calcium sulphite hemihydrate to gypsum (Dean 1978, Altwicker 1982).

Table 5.7. The Quantities of the $CaSO_3.½H_2O$ and $CaSO_4.2H_2O$ and Total Sulphate on 35^{th} Days.

Sample	A_{CaSO3}	A_{CaSO4}	$CaSO_4.2H_2O$ (mg)	$CaSO_3.½H_2O$ (mg)	Total SO_4 (mg)
Zein	0.1	0.01	0.6805	4.8268	3.9675
Uncoated	0.02	0.6	5.2935	0.1532	3.0655

Chitosan coated marble surfaces oxidation of calcium sulphite hemihydrate to gypsum was determined higher than uncoated marble proved the acceleration in the gypsum thickness (Table 5.8). The acceleration effect on the gypsum crust thickness was supported with the quantities of the $CaSO_3.½H_2O$ and $CaSO_4.2H_2O$. The highest of the total SO_4 was determined for the chitosan coated marble. Chitosan polymer also found unsuitable for inhibition of the marble from SO_2-calcite reaction as a protection agent.

Table 5.8. The Quantities of the $CaSO_3.½H_2O$ and $CaSO_4.2H_2O$ and Total Sulphate on 50^{th} Days.

Sample	A_{CaSO3}	A_{CaSO4}	$CaSO_4.2H_2O$ (mg)	$CaSO_3.½H_2O$ (mg)	Total SO_4 (mg)
Chitosan	0.32	0.03	3.6463	27.5845	22.538
Uncoated	0.11	0.01	1.8782	14.652	11.9388

The good water vapor barrier biopolymers were gave better results. The peaks of $CaSO_3.½H_2O$ and $CaSO_4.2H_2O$ observed on the LPLA and PHB coated surfaces after 85 days exposure. The quantities of $CaSO_3.½H_2O$ and $CaSO_4.2H_2O$ for LPLA and PHB coated and uncoated marble slabs are given in Table 5.8. LPLA decreased the formation of calcium sulphite hemihydrate and gypsum under high relative humidity and SO_2 concentration. While total SO_4, quantities of $CaSO_3.½H_2O$ and $CaSO_4.2H_2O$ of the

PHB and uncoated marble were very close to each other after 85 days exposure. This proved that PHB started to lose its protection effect on the marble.

Table 5.9. The Quantities of the $CaSO_3.½H_2O$ and $CaSO_4.2H_2O$ and Total Sulphate on 85^{th} Days.

Sample	A_{CaSO3}	A_{CaSO4}	$CaSO_4.2H_2O$ (mg)	$CaSO_3.½H_2O$ (mg)	Total SO_4 (mg)
Uncoated	0.36	0.11	9.5	22.09	21.70
PHB	0.14	0.04	8.95	22.27	21.55
LPLA	0.10	0.03	5.09	12.05	11.80

Quantities of $CaSO_3.½H_2O$ and $CaSO_4.2H_2O$ on the HPLA coated and uncoated marble surfaces are given in Table 5.10. Total SO_4 amount were detected with ion chromatography. While no peaks of products were detected in FT-IR analysis on the HPLA coated marble slabs. This result implied the products of sulphation reaction were occurred under the film. The detection limit was not enough to determine products peaks in FTIR analysis. When the total SO_4 of HPLA compared with its uncoated marble, HPLA had lowest SO_4 amount in the other biopolymers. This proved that HPLA was the most protective coating agent in all biopolymers used in this study.

Table 5.10. The Quantities of the $CaSO_3.½H_2O$ and $CaSO_4.2H_2O$ and Total Sulphate on 90^{th} Day

Sample	A_{CaSO4}	A_{CaSO3}	$CaSO_4.2H_2O$ (mg)	$CaSO_3.½H_2O$ (mg)	Total SO_4(mg)
HPLA	--	--	--	--	16.68
Uncoated	1.153	0.047	67.83	2.32	39.55

5.3. Marble Surface Morphologies

In this part, biopolymer coated and uncoated marble slabs scanning electron microscope (SEM) analysis have been carried out;

to determine the surface morphologies

to determine the sulphation products confirmations

to observe the degradation of the biopolymer coatings

Before exposure to SO_2 gas and humidity, the surface morphologies of the marble slabs were used to observe the film homogeneity. The SEM images showed that the surface covered with film homogeneously for the plasticized zein coated film (Figure 5.7a). Calcite crystals were observed on the uncoated marble surface (Figure 5.7b).

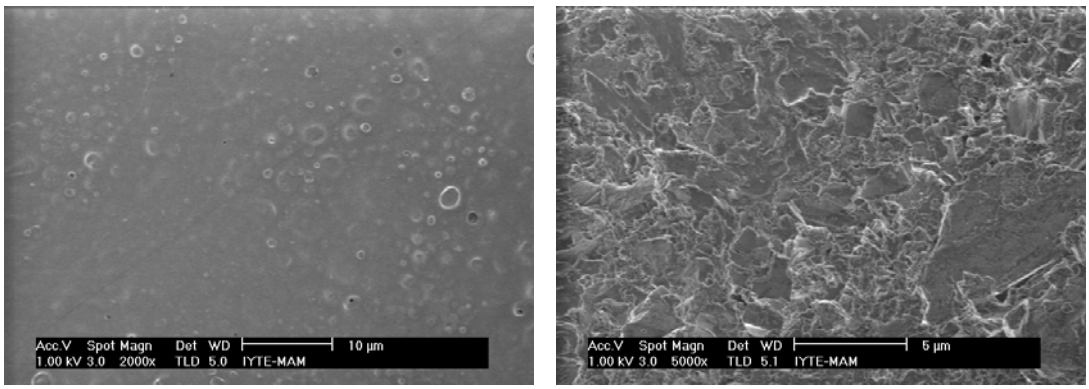

(a) **(b)**

Figure 5.7. SEM Images of the Plasticized Zein Coated (a) Marble Samples Before SO_2-Calcite Reaction.

On the 7th day, the first image taken from marble surfaces showed some cavities on the plasticized zein film, while no sulphation products were determined (Figure 5.8a-b). The sulphate ions analysis resulted detectable amount of sulphation products. This proved that these sulphation products formed under polymer film layer as a result it could not be imaged by SEM analysis.

The sulphation products were also observed with SEM images on the 14th day uncoated surface. The formation of calcium sulphite hemihydrate crystals in stellate bunches (Figure 5.9a-b) and gypsum in prismatic crystals (Figure 5.9c-d) were observed on uncoated marble surfaces. Heterogeneity of these formations showed that calcite crystals did not have uniform microstructure on the marble surface. In previous studies similar properties and sulphation products also have similar crystal structures (Gauri 1999).

After 14 days SO_2 reaction of zein coated marble samples, degradation of polymer accelerated and formation of the sulphation products was observed on the polymer layer (Figure 5.10a-d). According to the SEM images, it is possible to conclude that the gypsum started to form under the plasticized zein film, increased in the size of crystal was appeared on the polymer film. This confirms that plasticized zein coating allowed SO_2 gas and water vapor diffusion through the polymer-marble interface. Then these components reacted with calcite crystals. By the time, non-uniformly formed gypsum growth was seen on the film layer. The total sulphate concentration was high in the polymer coated marble. Faster reaction occurred on the polymer-marble interface with absorption of SO_2 (Figure 5.11a-b).

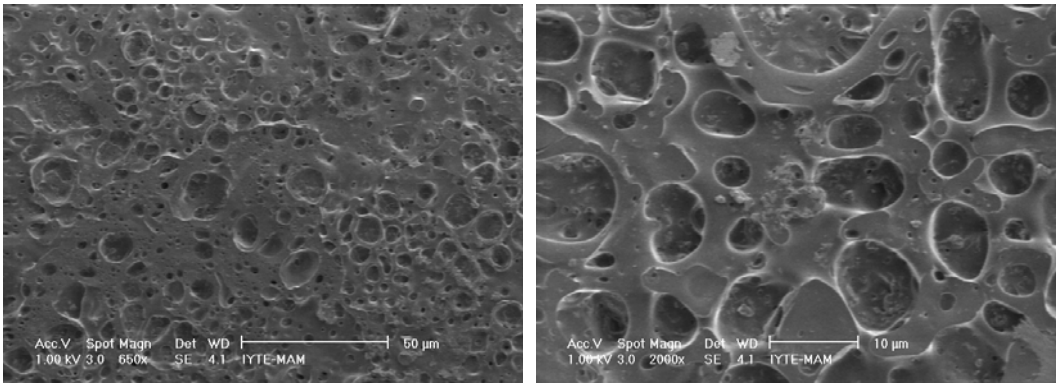

(a) **(b)**

Figure 5.8. SEM Images of the Cavity Formations Which Observed on Plasticized Zein Coated Surfaces After 7 days.

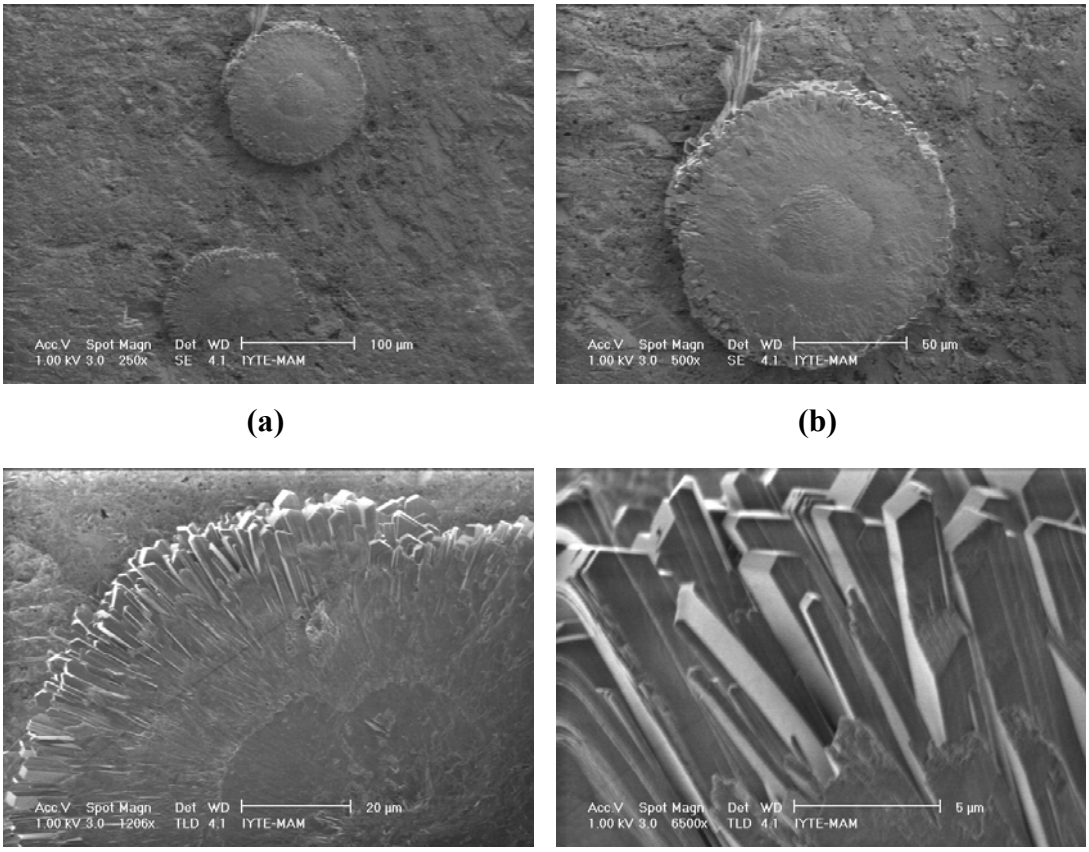

Figure 5.9. SEM Images of the Stellate Bunches (a, b) and Prismatic Crystals (c, d) Which Formed on the Uncoated Marble Surfaces after 7 Days.

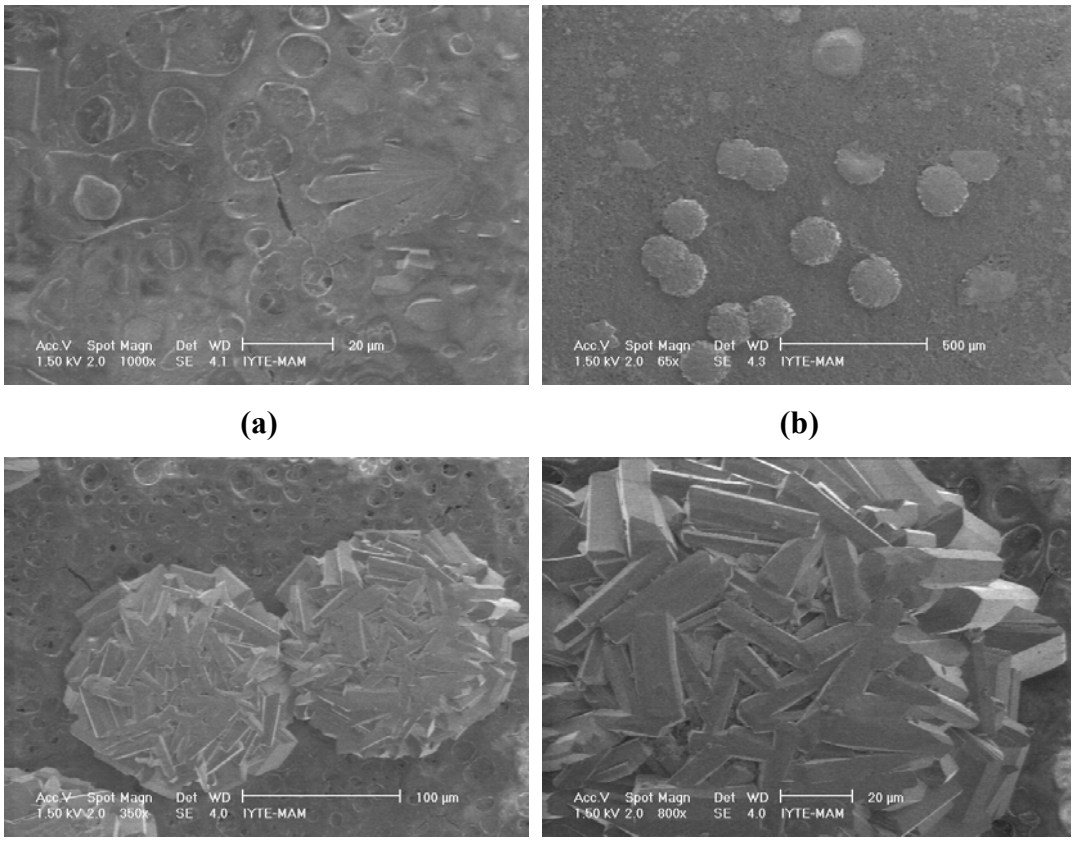

Figure 5.10. SEM Images of the Prismatic Gypsum Crystals Which Formed Under (a) and Upper (b-d) Sides of the Plasticized Zein Polymer After 14 Days.

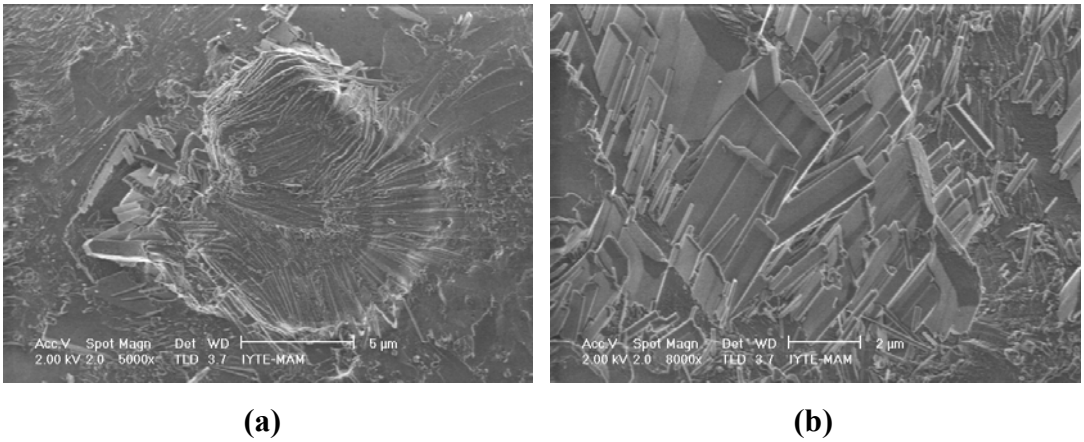

Figure 5.11. SEM Images of the Prismatic Gypsum Crystals Which Formed on Uncoated Marble Samples After 14 Days.

After 21 and 35 days of SO_2 reaction significant amount of sulphation products formed on large portion of the surface and degradation in polymer increased in zein coated marble samples (Figure 5.12a-f). SEM images were the good indicator of the formation of gypsum and the degradation of plasticized zein polymer as well.

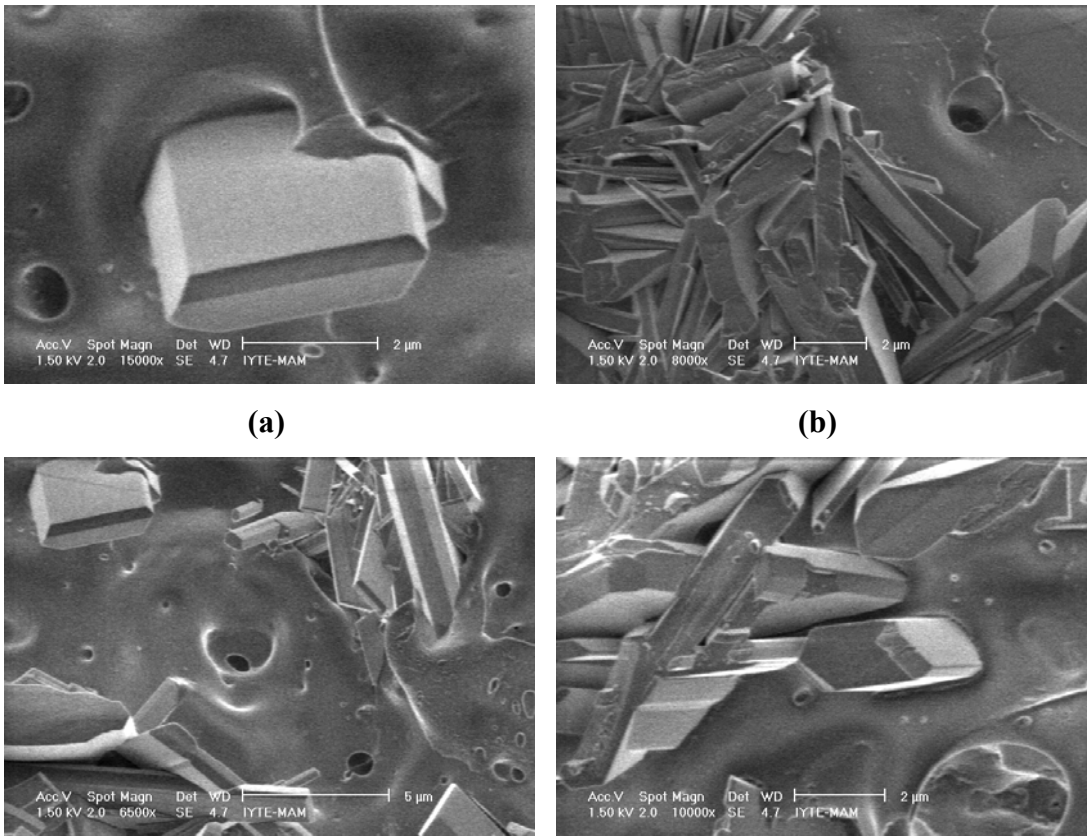

Figure 5.12. SEM Images of the Prismatic Gypsum Crystals Which Formed on Plasticized Zein Polymer Coated Surfaces After 35 Days.

The marble samples uncoated with zein after 21 and 35 days of SO_2 reaction, almost all of the surface sulphation products were seen homogeneously. It is possible to say that sulphation products formed much more comparing to the first week reaction period (Figure 5.13).

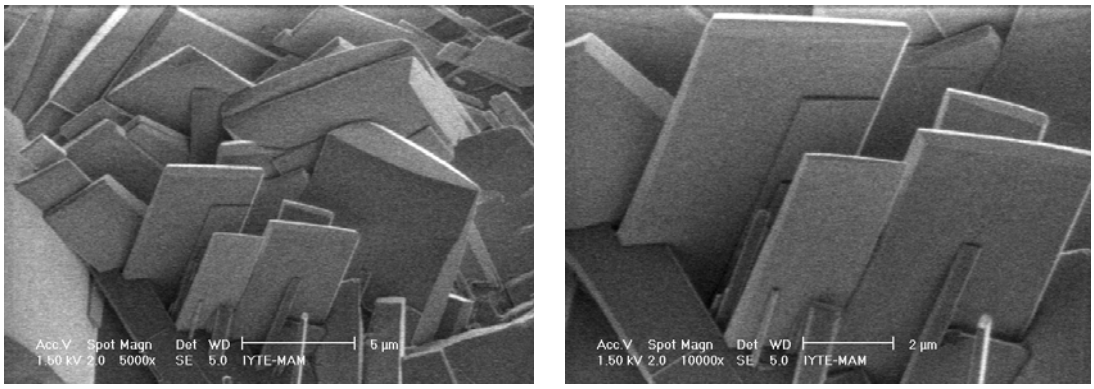

Figure 5.13. SEM Images of the Prismatic Gypsum Crystals Which Formed on Uncoated Surfaces after 35 Days.

Pure zein polymer coated surfaces were also analyzed by SEM analysis. SEM images of the pure zein coated marble samples surfaces were represented in Figure 5.14 before reaction. Bubbles and some holes were determined on the polymer coated surface (Figure 5.14a). Also, some cracks were observed on the edge of the pure coated coated marble surface due to brittle structure of the zein (Figure 5.15b).

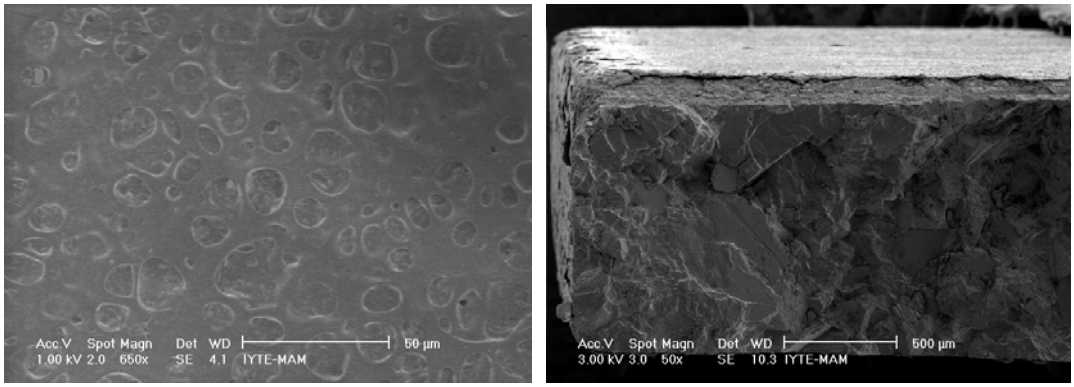

(a) **(b)**

Figure 5.14. SEM Images of the Pure Zein Coated (a) and Uncoated (b) Marble Samples Before SO_2-Calcite Reaction.

When the pure zein coating used for experiment, the results showed the usage of pure zein as a coating material was not effective for the protection (Figure 5.15a-c). Since formations of calcium sulphite hemihydrate and gypsum were determined on the coated marble surfaces, polymer film begun to deteriorate even at the first days of the

reaction. SEM images showed that, zein film was broken into pieces by the effect of SO_2-calcite reaction and high relative humidity. Figure (5.15d) represent that, $CaSO_3.0.5H_2O$ and $CaSO_4.2H_2O$ were occurred homogeneously on the uncoated marble surface.

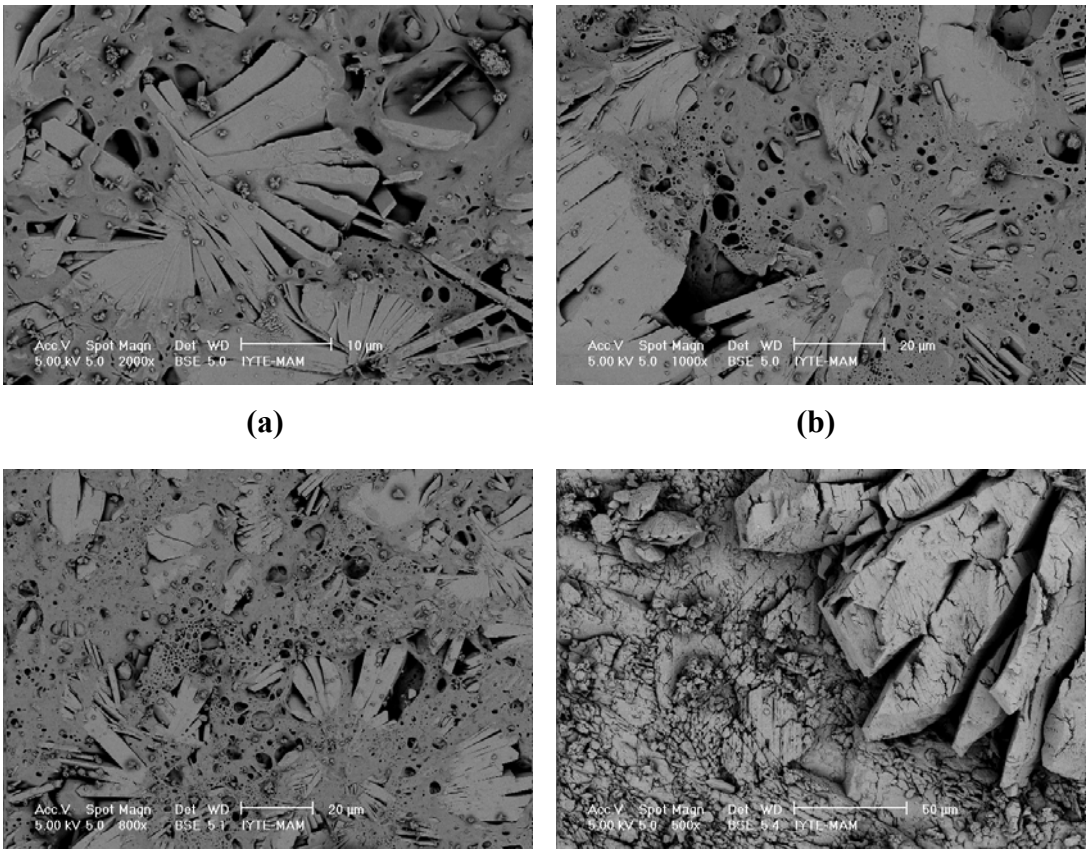

Figure 5.15. SEM Images of the Pure Zein Coated (a-c) and Uncoated (d) Marble Samples After 35 Days.

Chitosan coating resulted in homogeneous marble surfaces represented in Figure 5.16a. After 50 days reaction, sulphation products of SO_2-calcite reaction which obtained from chitosan coated marble surfaces were seen by SEM images in Figure 5.17a-c. As mentioned previously, chitosan has low water vapor barrier property and it is also hydrophilic so its gas permeability may increase manifold when humidity increases. These properties could cause the absorption of SO_2 and water vapor on the polymer film and sulphation products could be easily observed on the chitosan coated marble surfaces (Figure 5.17).

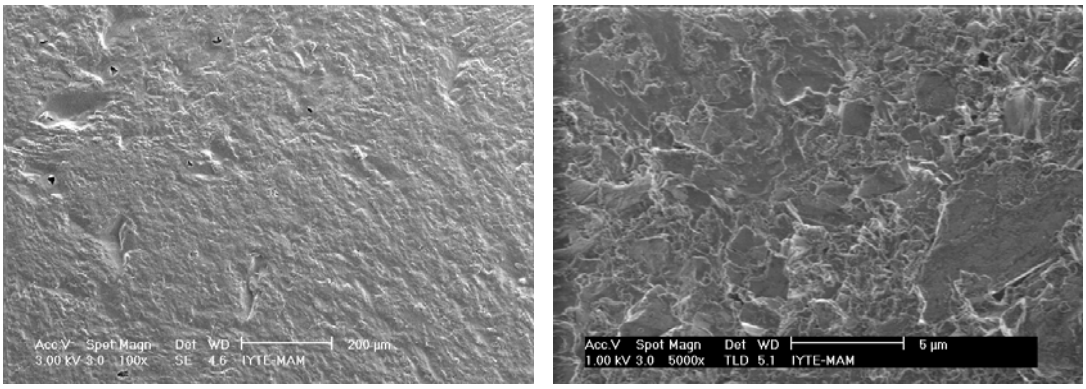

(a) **(b)**

Figure 5.16. SEM Images of the Chitosan Coated (a) and Uncoated (b) Marble Samples Before SO_2-Calcite Reaction.

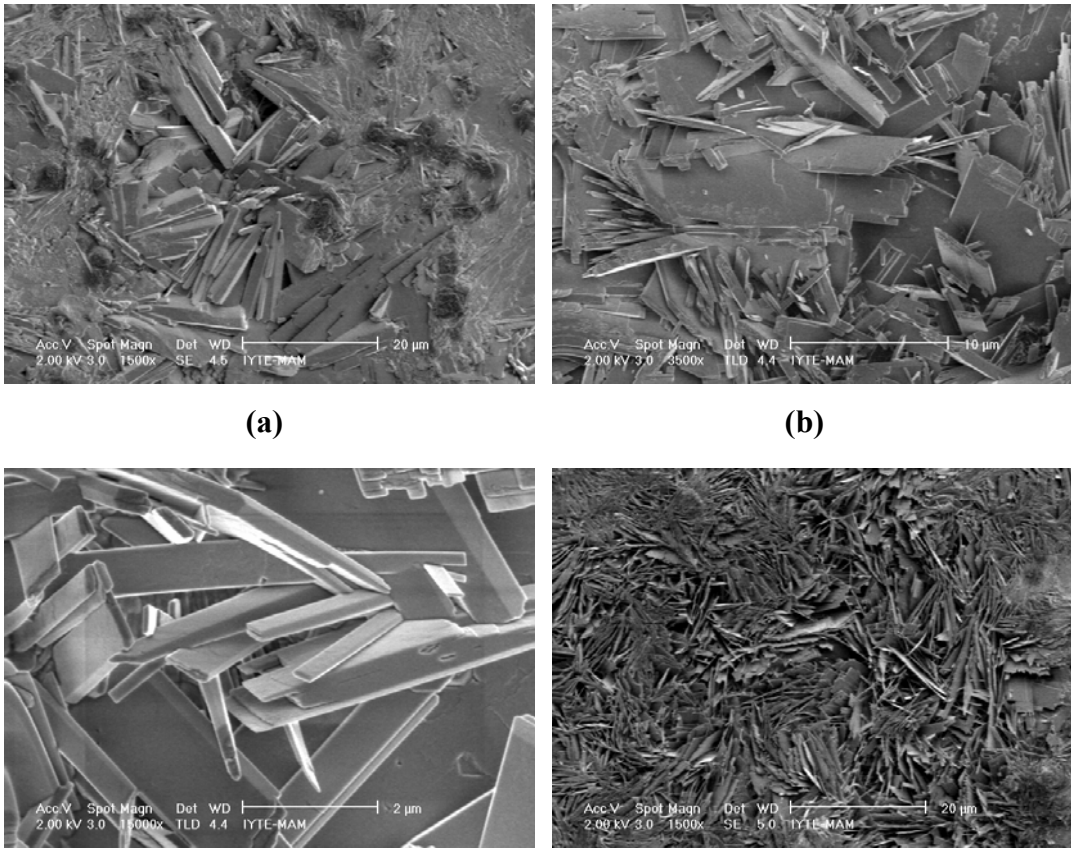

(a) **(b)**

(c) **(d)**

Figure 5.17. SEM Images of the Chitosan Coated (a-c) and Uncoated (d) Marble Samples After 50 Days.

Sulphation products degradation and formation of the other group of polymers coated and uncoated marble samples surfaces were determined by SEM analysis. In this group LPLA, HPLA and PHB were used in the experiment.

Figure 5.18 represented that marble surfaces were coated with LPLA and PHB polymers. Eventhough homogeneous coverage achieved, some bubbles were also observed on the polymer surface. However, these bubbles did not reach as far as marble surfaces and film coverage around the marble was in good condition.

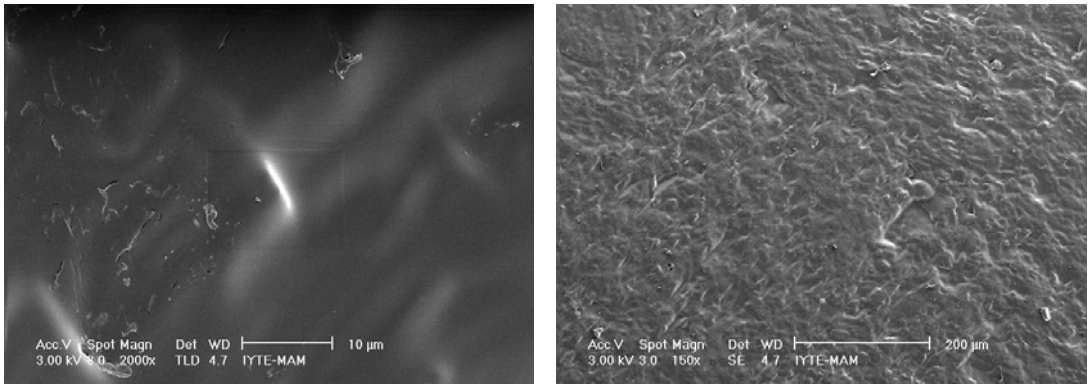

(a) **(b)**

Figure 5.18. SEM Images of the PLA Coated (a) and PHB (b) Marble Samples Before SO_2-Calcite Reaction.

After 3 days in the reaction chamber, there were not any sulphation products observed on the LPLA, PHB coated and uncoated surfaces. However the detection of low total sulphate amount of coated marbles explained that the formation of the sulphation products was started under the film layer slowly. At the same time the formations were observed on the uncoated marble surfaces as shown in Figure 5.19.

LPLA coated marble surface was designated less decomposed than PHB coated marble surfaces after 13 days SO_2 reaction in Figure 5.20. In spite of the sulphate amount, the formations of sulphation products were observed on the coated marble surfaces. This results that $CaSO_4.2H_2O$ and $CaSO_3.½H_2O$ were formed under the polymer coatings similar to 3 days SEM images.

After 21 days, some holes and evidence of the degradation effect were observed on the PHB coated marble surface (Figure 5.21b). In the LPLA coated surface, any presence of sulphation products and degradation was not seen (Figure 5.21a). However

the total sulphate concentrations were measured which showed that the sulphation products started to form under the film layer. Similarly, the sulphation products formation on the uncoated marble surfaces was observed in Figure 21c.

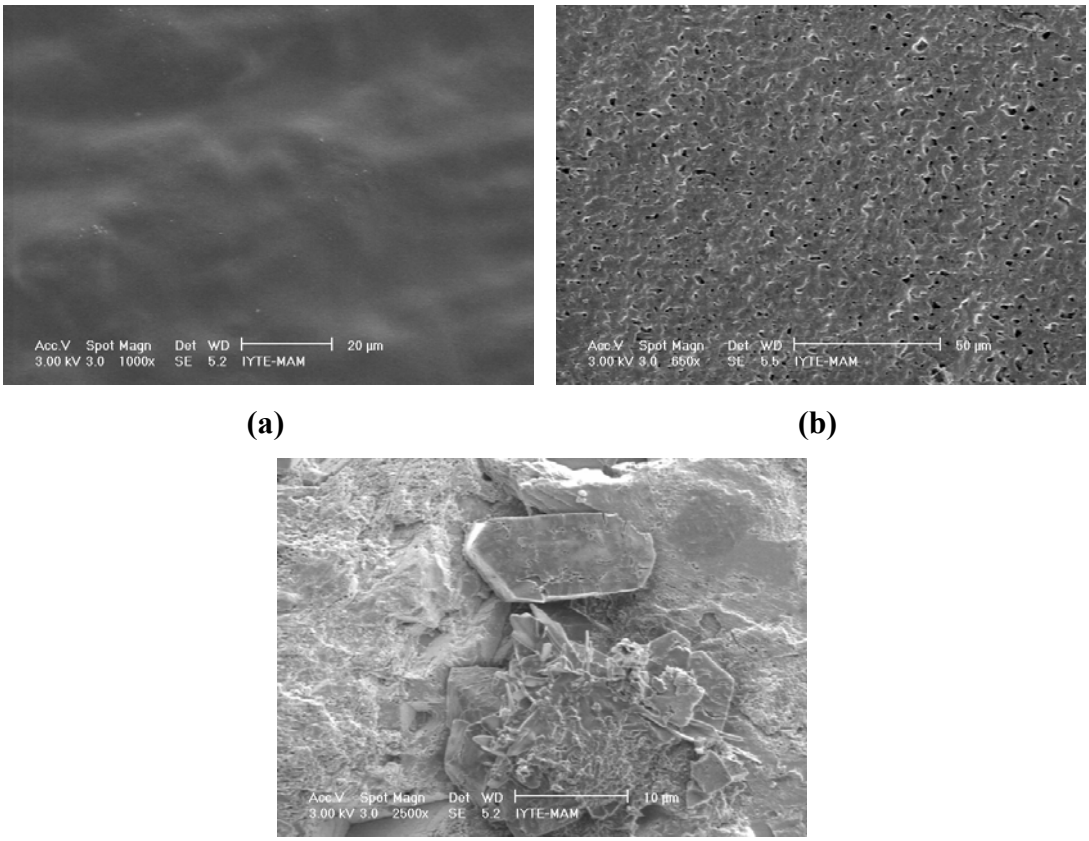

Figure 5.19. SEM Images of the Cavity Formations Which Observed on LPLA (a), PHB (b) Coated and Uncoated (c) Surfaces After 3 Days.

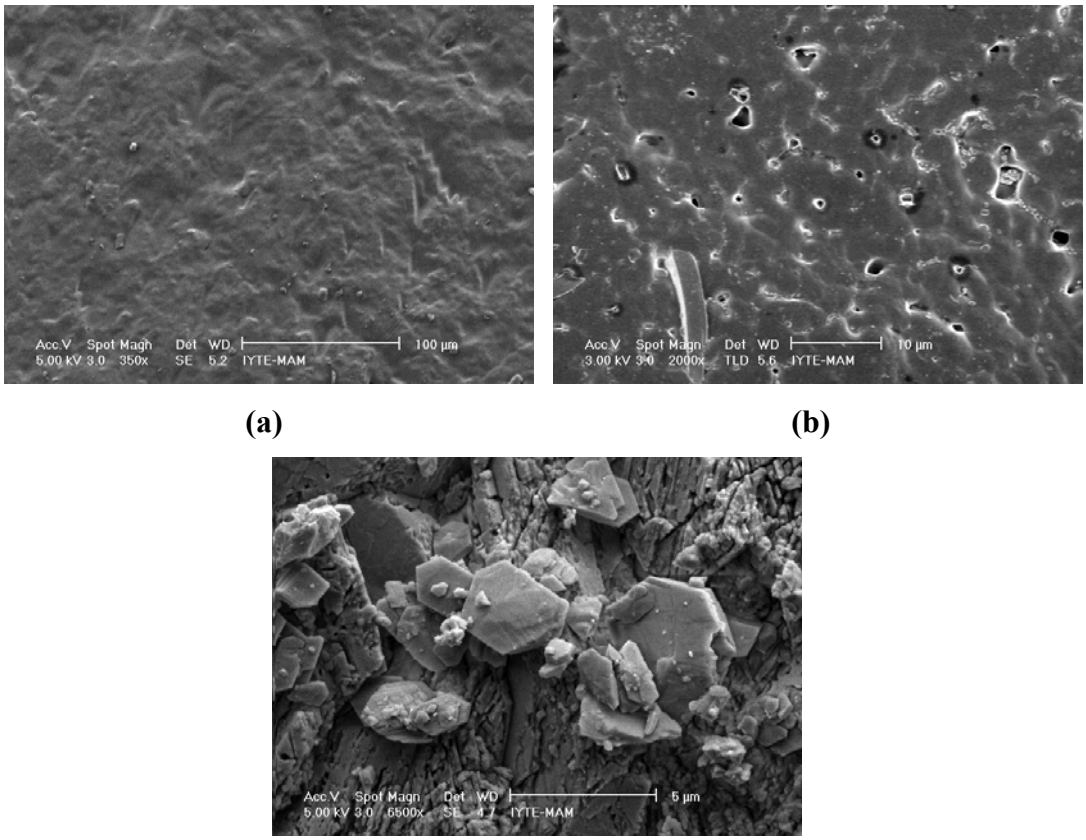

Figure 5.20. SEM Images of the Cavity Formations Which Observed on LPLA (a), PHB (b) Coated and Uncoated (c) Surfaces After 13 Days.

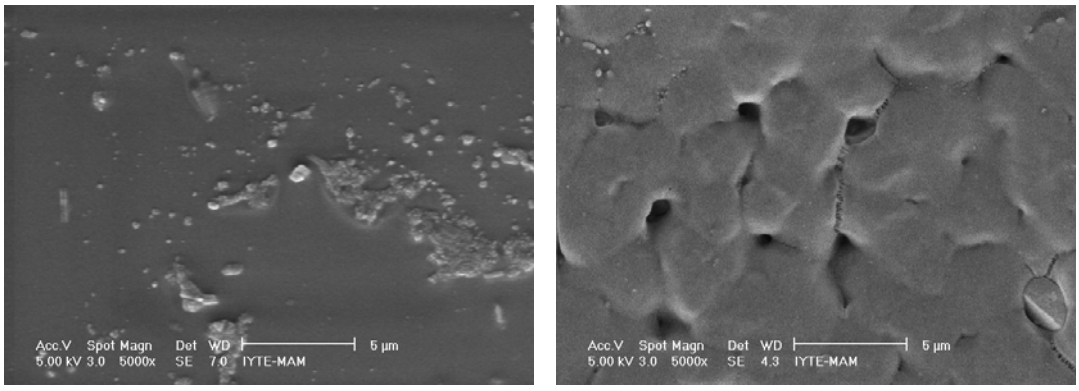

(a) **(b)**

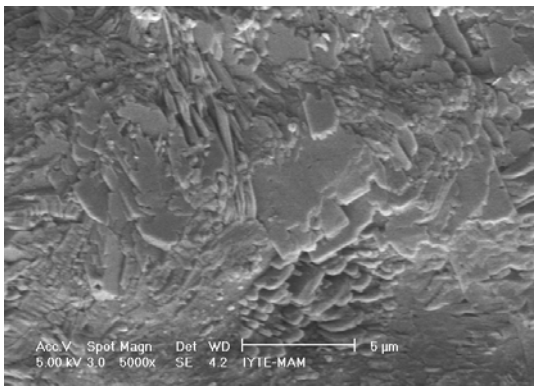

(c)

Figure 5.21. SEM Images of the LPLA (a), PHB (b) Coated and Uncoated (c) Surfaces After 21 Days.

After 35 day of the reaction, LPLA coating still did not show any degradation (Figure 5.22a). However, some deformation was observed on the PHB coated surfaces (Figure 5.22b). Sulphation products were determined on the significant part of the uncoated marble sample surfaces clearly.

Deformation evidences were determined on the LPLA coated surfaces, but the formation of sulphation products not determined in SEM images after 50 days SO_2-calcite reaction (Figure 5.23a). The deformation signs and formation of sulphation products were seen occasionally on the PHB coated marble surfaces. In addition $CaSO_4.2H_2O$ and $CaSO_3.2H_2O$ crystals started to tear the PHB films. Thus, the sulphation products were formed under the film in the first stage and sulphation products improved and tore the film layer in second stage (Figure 5.23b). The uncoated

marble surface was fully covered by calcium sulphite hemihydrate and gypsum (Figure 5.23c).

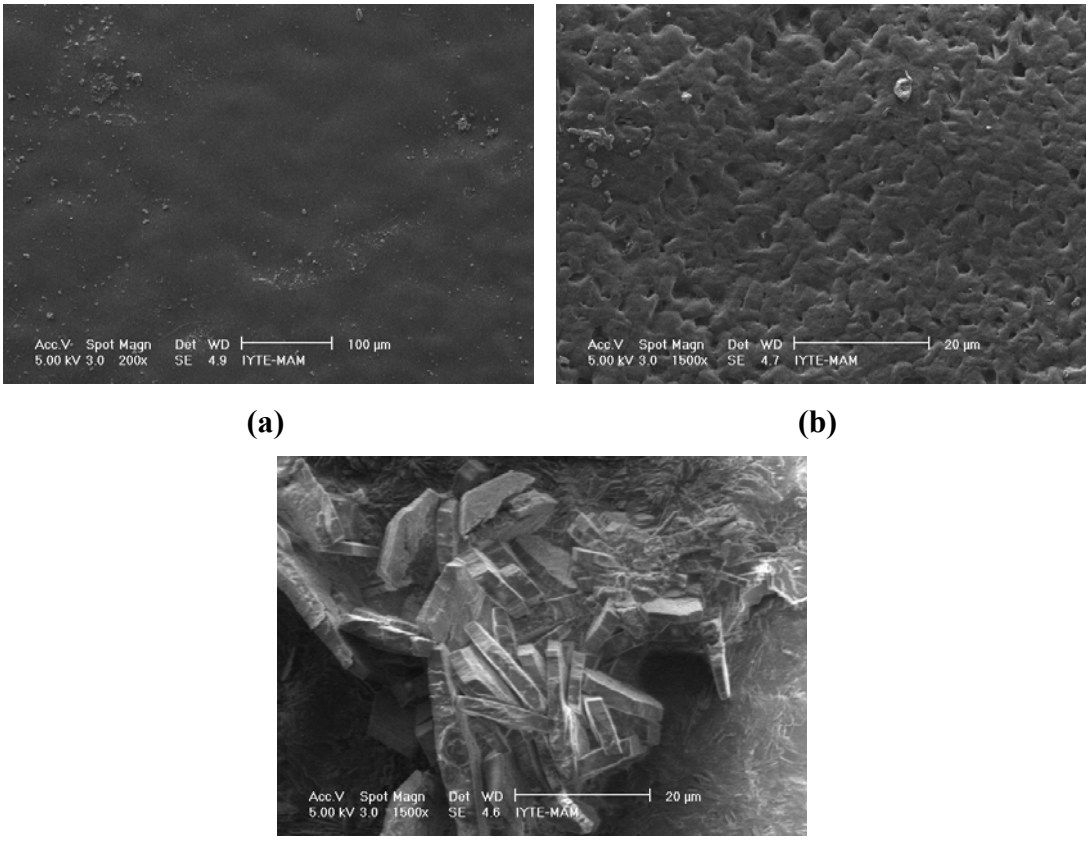

Figure 5.22. SEM Images of the LPLA (a), PHB (b) Coated and Uncoated (c) Surfaces After 35 Days.

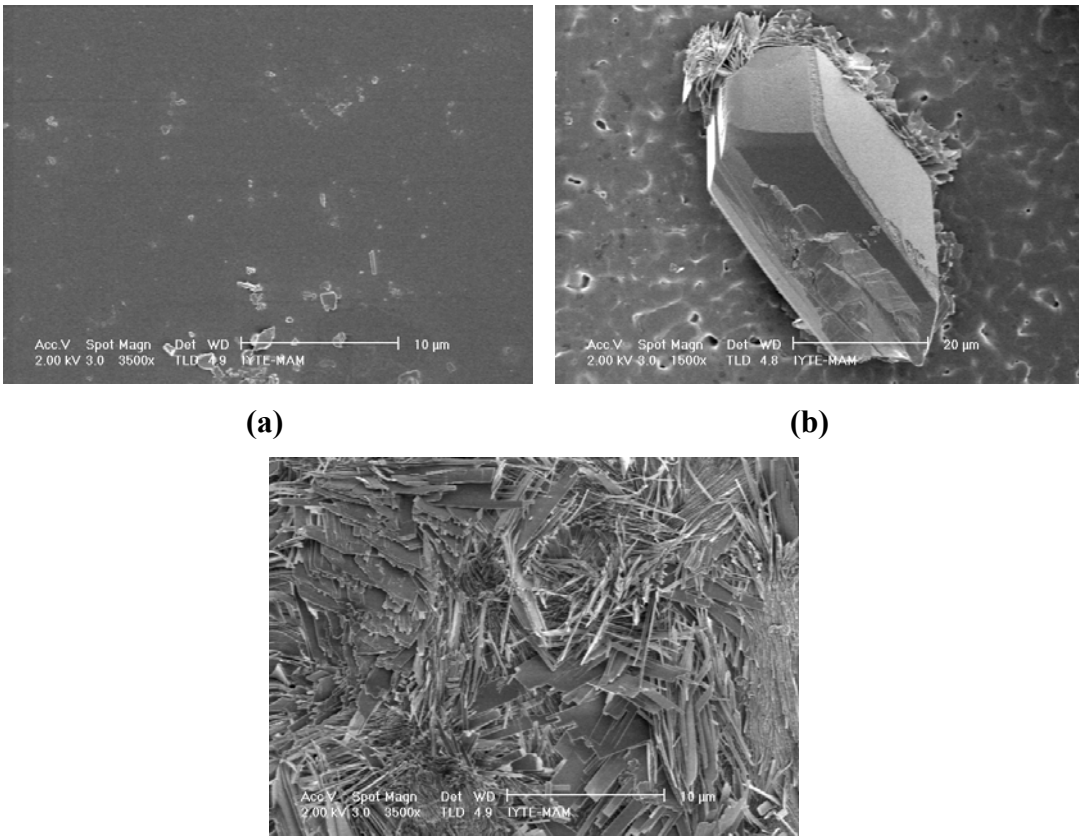

(a) **(b)**

(c)

Figure 5.23. SEM Images of the LPLA (a), PHB (b) Coated and Uncoated (c) Surfaces After 50 Days.

The crystals of sulphation products were observed on the LPLA and PHB coated marble surfaces on 85th day (Figure 5.24a-b). Deformation of PHB film was observed on a large scale and while homogeneous calcium sulphite hemihydrate and gypsum formation were determined on the PHB film surfaces (Figure 5.24b). The sulphation products images on the LPLA coated marble surfaces pictured in patches (Figure 5.24a). Uncoated marble surfaces were entirely covered by calcium sulphite hemihydrate and gypsum (Figure 5.24c). All in all, PHB and LPLA polymers retarded the SO_2-calcite reaction, yet they lost their protective properties in the course of time.

Figure 5.25 showed that the marble surfaces were coated with HPLA polymer homogeneously .

After 21 days, eventhough some pores determined on the polymer the sulphation products were not observed on the polymer surfaces (Figure 5.26a-b). However, the sulphation products were started to form on the uncoated marble surfaces. These

determinations observed on HPLA coated and uncoated marble samples in Figure 5.27 and 5.28 after 35 and 65 days SO_2-calcite reactions.

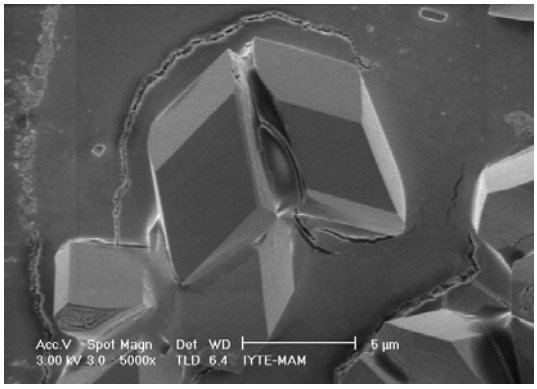

(a)

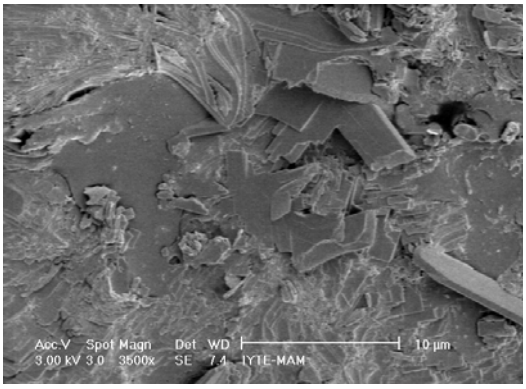

(b)

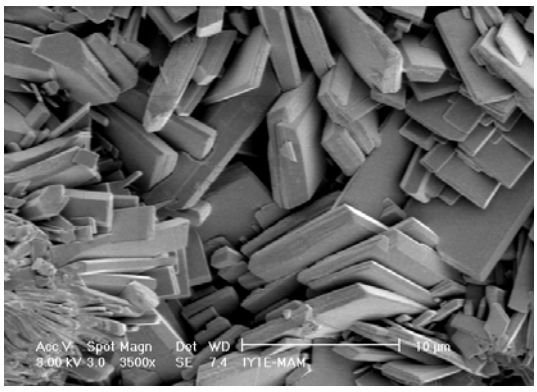

(c)

Figure 5.24. SEM Images of the LPLA (a), PHB (b) Coated and Uncoated (c) Surfaces After 85 Days.

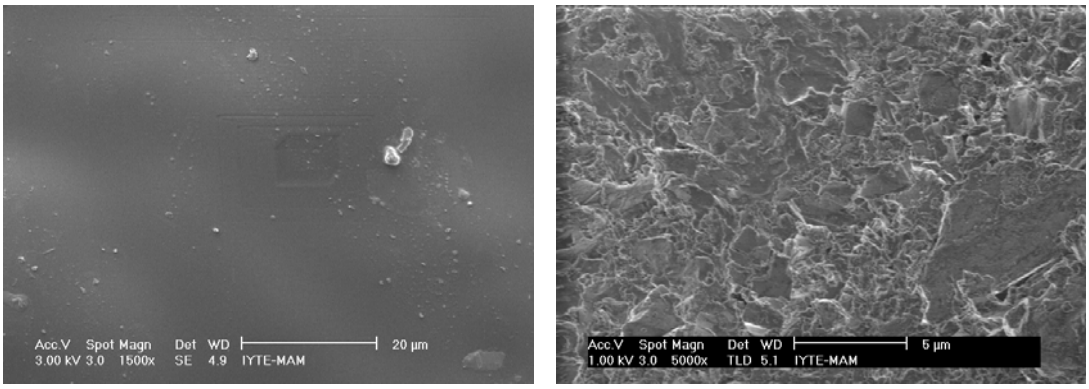

(a) **(b)**

Figure 5.25. SEM Images of the HPLA Coated (a) and Uncoated (b) Marble Samples Before SO_2-Calcite Reaction.

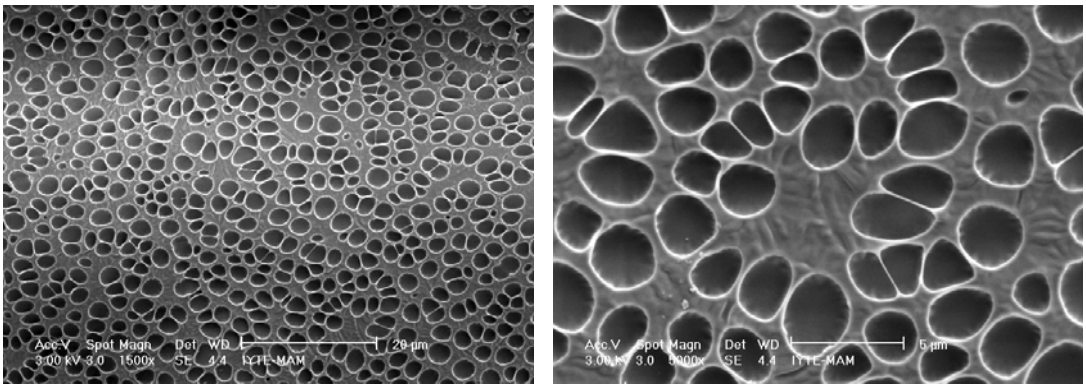

(a) **(b)**

Figure 5.26. SEM Images of the HPLA Coated (a, b) Marble Samples

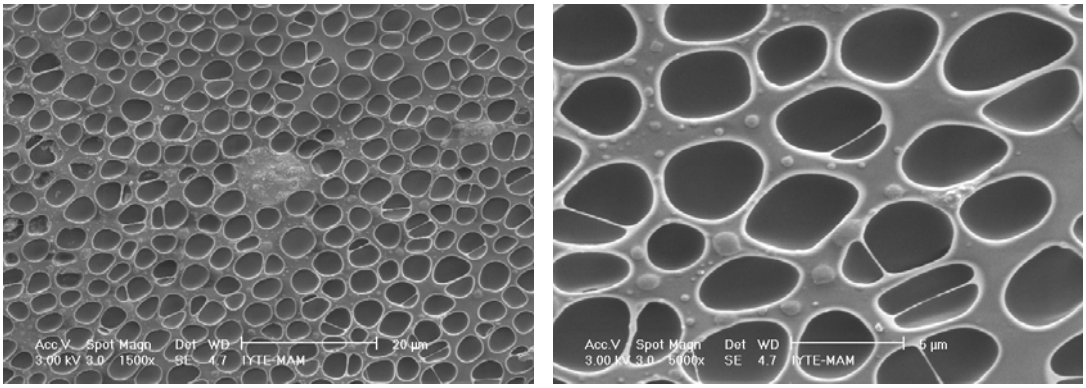

(a) **(b)**

Figure 5.27. SEM Images of the HPLA Coated (a, b) Marble Samples after 35 Days.

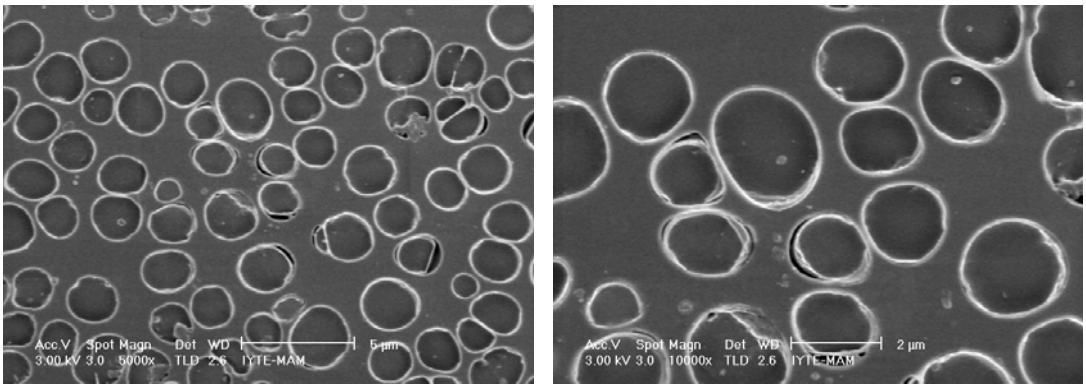

(a) **(b)**

Figure 5.28. SEM Images of the HPLA Coated (a, b) Marble Samples after 65 Days.

Protection effects and sulphation product formation of the HPLA were also monitored by semi-coated marble surfaces. In the first sets of uncoated and coated marbles SEM images pointed out that formation of sulphation products were not formed on the HPLA coated surfaces. At the end of the 65^{th} and 90^{th} days SO_2-calcite reaction, semi-coated surface SEM images were analyzed with SEM and images were given in the Figure 5.29 and Figure 5.30. In the images, it can be clearly seen that how the sulphation products formed on the protected and unprotected surface. On the HPLA coated surface there was no formed products. While huge sulphation products crystals were formed anywhere of the uncoated surface (Figure 5.29). Figure 5.31 showed that, some small cracks and tears were started to form on the PLA coated surfaces.

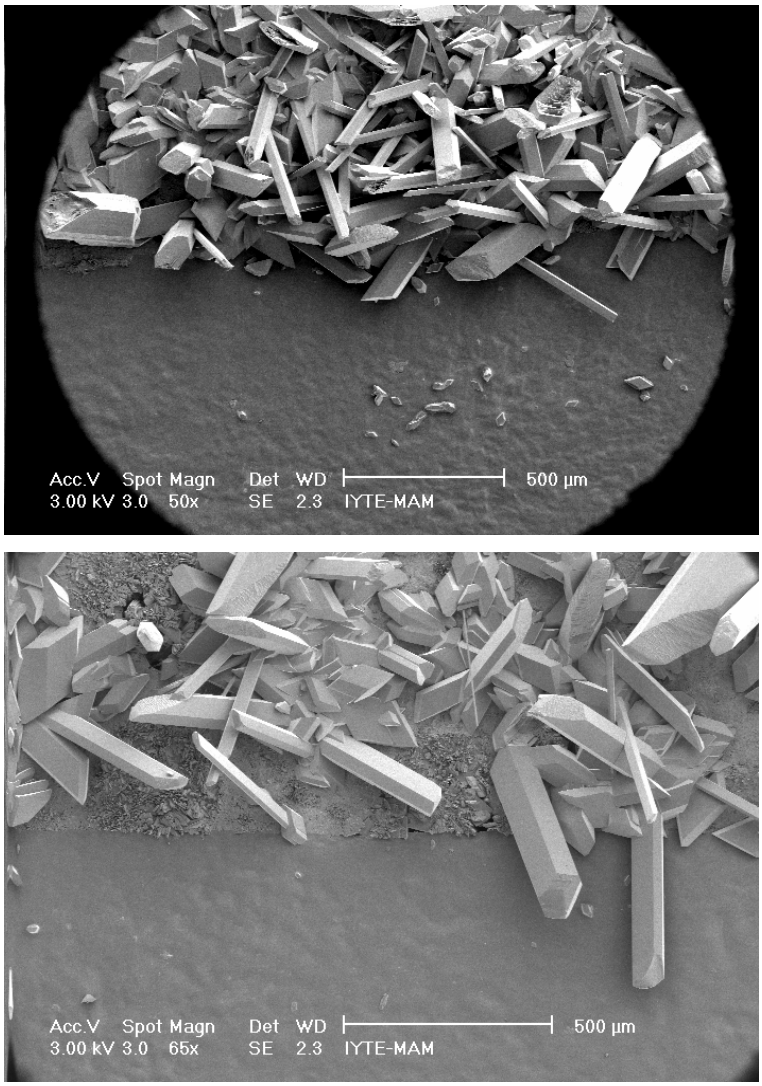

⟶ Uncoated part

⟶ PLA coated part

⟶ Uncoated part

⟶ PLA coated part

Figure 5.29. SEM Images of the Gypsum Formation on Semi-coated Surfaces after 65 Days.

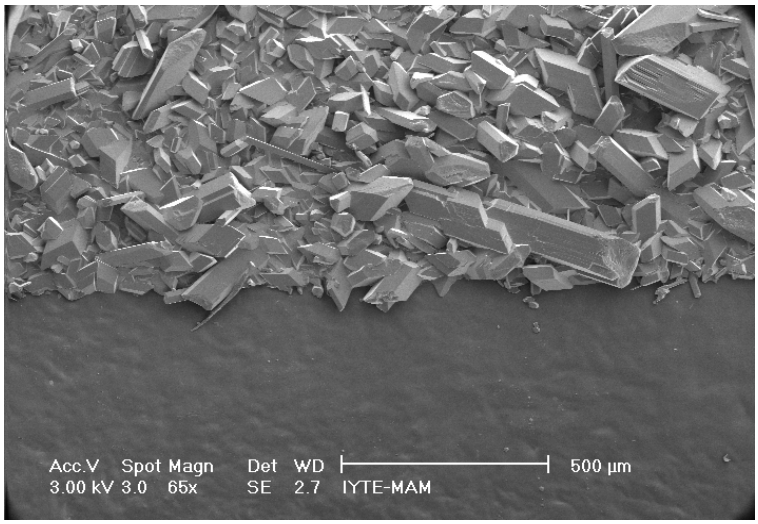

→ Uncoated part

→ PLA coated part

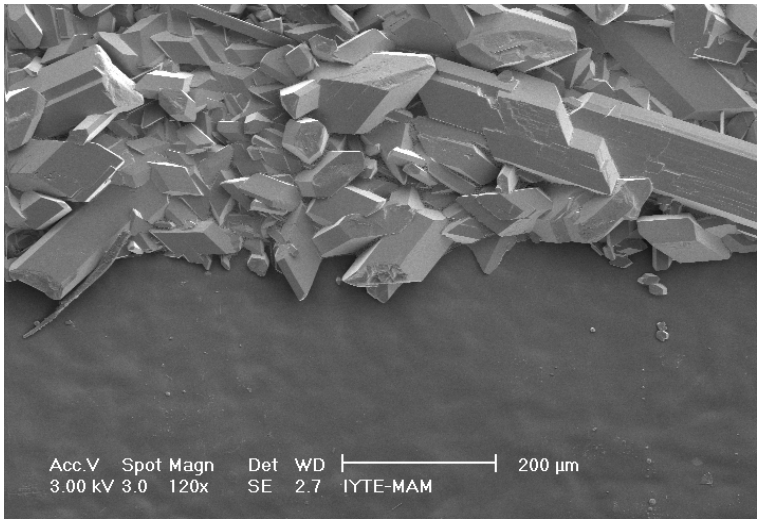

→ Uncoated part

→ PLA coated part

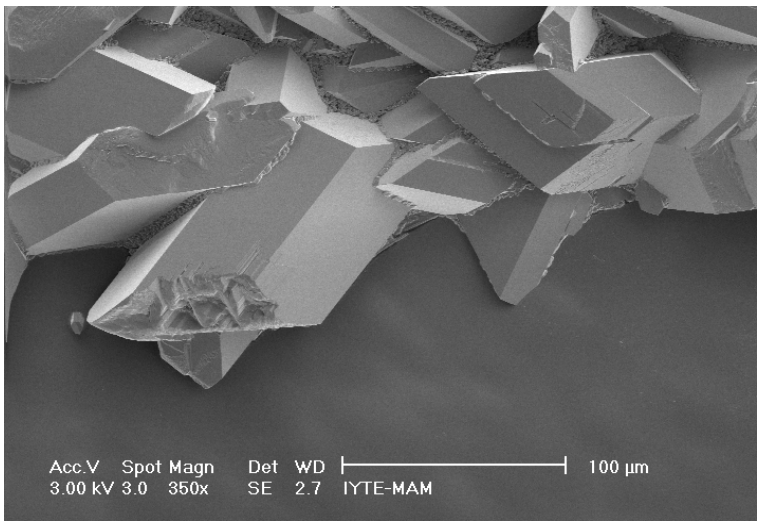

→ Uncoated part

→ PLA coated part

Figure 5.30. SEM Images of the Gypsum Formation on Semi-coated Surfaces after 90 Days.

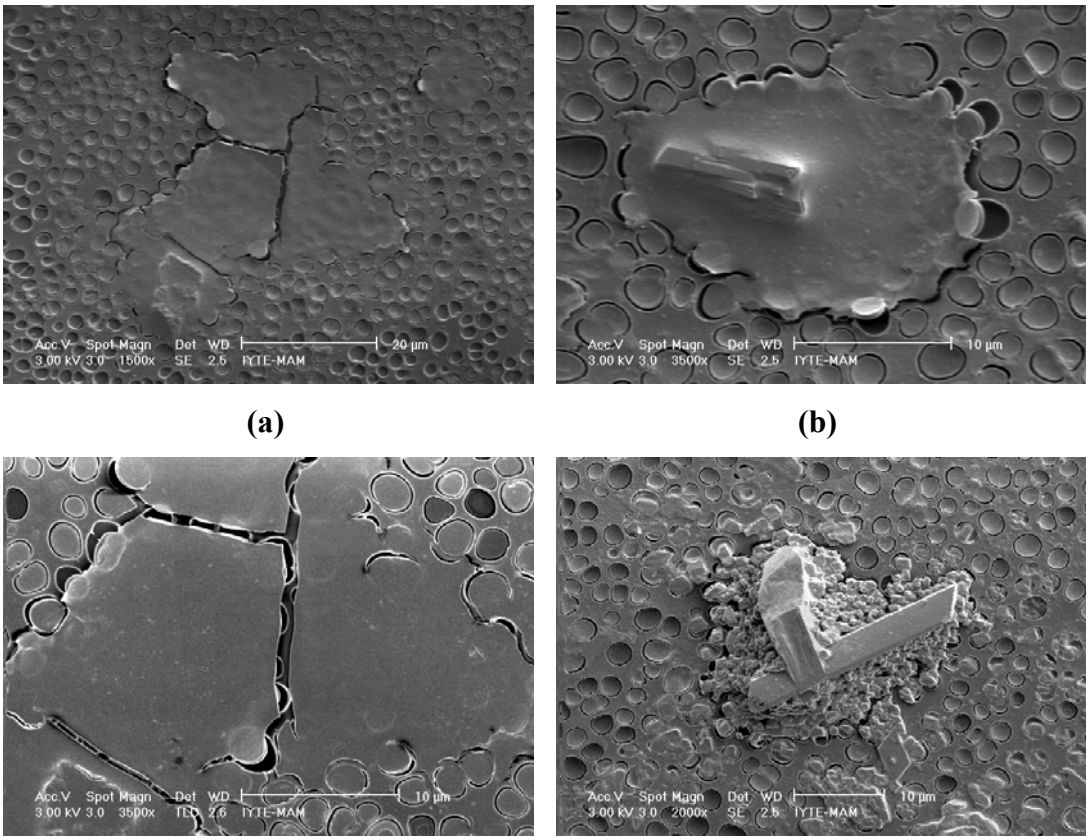

Figure 5.31. SEM Images of the Some Cracks and Tears (a-c) and Gypsum Formation (d) on the HPLA Coated Surfaces after 90 days.

5.4. Determination of Polymers Percentage Protection Factor

Polymer percentage protection factor percentage of the gas and water vapor barrier biopolymers were determined by comparing gypsum crust thickness of biopolymer coated and uncoated marbles. As mentioned previously, gypsum crust thicknesses in the good gas barrier biopolymers (pure zein, plasticized zein and chitosan) coated marbles were significantly higher than uncoated control marbles.

Protection factor calculated from gypsum crust thicknesses revealed from experimental results by using equation (4.7). Especially high water vapor barrier biopolymers (HPLA and PHB) decreased the sulphation products (Figure 5.32). At the end of the 35 days exposure, low molecular weight PLA showed approximately 70 % and PHB showed % 50 protection when they compared with their uncoated control marbles. These polymers indicated excellent protection properties compared to the

polymers have good gas barrier properties. The protection duration extended till 85 days. After 85 days reaction, LPLA protection factor started to decrease (45 %) while it was 5 % for PHB comparatively with their uncoated marble slabs.

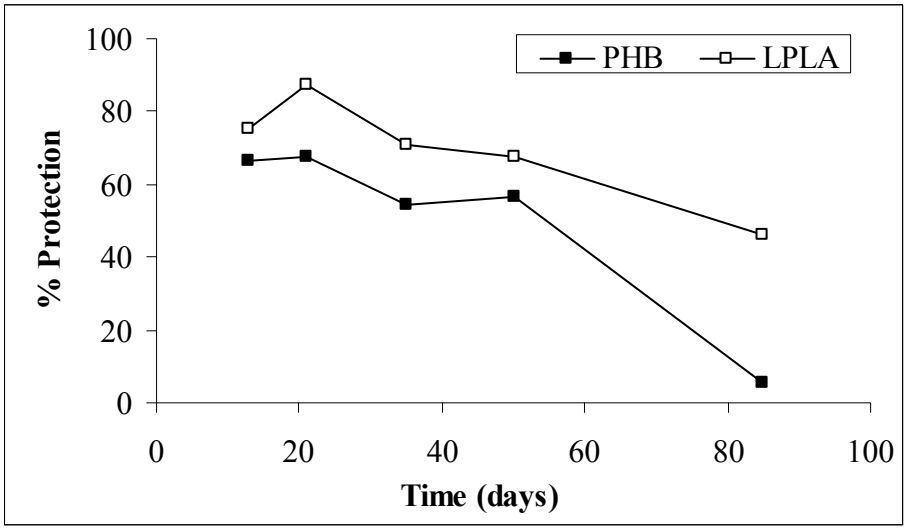

Figure 5.32. Protection Factor Percentage of the PHB and Low Molecular Weight PLA.

HPLA showed more consistent protection till 90th day (Figure 5.33). At the end of 90 days, its % protection factor was found approximately % 60 when it compared with its uncoated control marble.

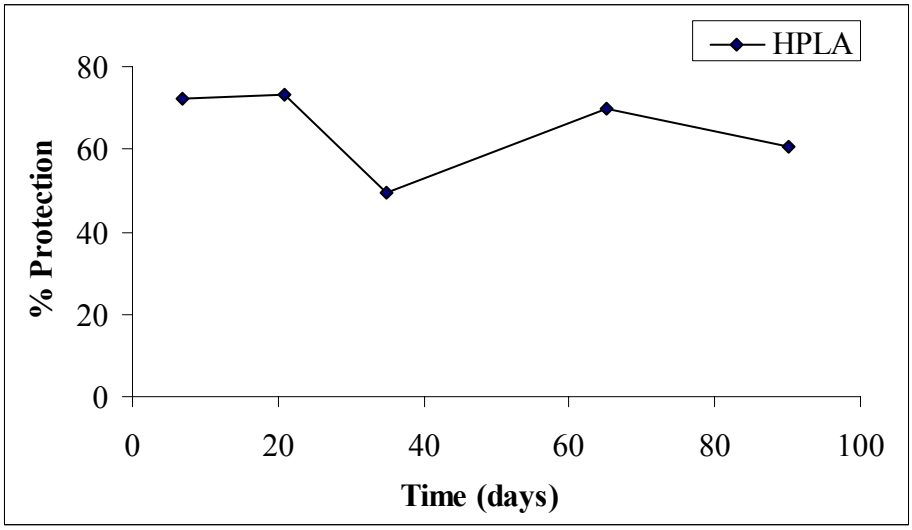

Figure 5.33. Protection Factor Percentage of the High Molecular Weight PLA.

Overall protection for all type of biopolymers can be given in the order of best to worst; HPLA > LPLA > PHB > plasticized zein > pure zein > chitosan. PLA and PHB are known hydrophobic behavior, therefore known as a good water vapor barrier property. PLA and PHB were found more protective among the biopolymers used in this study.

CHAPTER 6

CONCLUSION

In this study pure zein, plasticized zein, chitosan, polyhydroxybutyrate, low molecular weight Polylactic acid and high molecular weight polylactic acid were investigated as a surface protector of the marble in the laboratory conditions. Gypsum crust thickness order for all type of biopolymers can be given in; chitosan > pure zein > plasticized zein > PHB > LPLA >HPLA.

High gypsum formation was observed in the pure zein, plasticized zein and chitosan coated marble samples, when they compared with their uncoated control samples. Mostly the biopolymers with a good gas barrier property showed bad results in protection. They accelerated the sulphation reaction and enhanced the formation of sulphation products due to their low water vapor barrier property. Also, zein and chitosan gas barrier permeability might have been increased due to high relative humidity.

Inhibition of sulphation products was observed on the marble surfaces which were coated with PHB, LPLA and HPLA. These polymers have good water vapor barrier property. Water vapor barrier property was found most effective in the protective surface layer. HPLA was the most effective one among the all tried biopolymers. The structural differences in the polymer affected the protection potential. PLA and PHB polymers can be used for protection of the historical marble surfaces in the polluted air to decrease SO_2-calcite reaction due to the fact that reversibility and reapplicability properties which allow new application on the marble surfaces.

This experimental study was realized into artificial atmosphere and short term effects were investigated. However, this laboratory investigation should be further repeated in polluted city atmosphere and long term effect of biodegradable polymer should be determined.

REFERENCES

Aas, W., Shao, M., Jin, L., Larssen, T., Zhao, D., Xiang, R., Zhang, J.,Xiao, J., Duan, L. 2007. "Air Concentrations and Wet Deposition of Major Inorganic Ions at Five Non-Urban Sites in Chine, 2001-2003", *Atmospheric Environment*. Vol. 41, pp. 1706-1716.

Atlas, R. M., Chowdhury, A.N., Gauri, K. L. 1988. "Microbial Calcification of Gypsum-Rock and Sulfated Marble", *Studies in Conservation. Vol.* 33, pp. 149-153.

Ausset, P., Crovisier, J.L, Monte, M.D., Furlan, V., Girardet, F., Hammecker, C., Jeannette, D.L. 1996. "Experimental Study of Limestone and Sandstone Sulphation in Polluted Realistic Conditions: The Lausanne Atmospheric Simulation Chamber (LASC)", *Atmospheric Environment*. Vol. 30, pp. 3197-3207.

Barrie, L. A., Georgy, H. W. 1976. "An Experimental Investigation of Absorption of Sulphur Dioxide by Water Drops Containing Heavy Metal Ions", *Atmospheric Environment.* Vol. 10, pp. 743-749.

Bernal, J. L. P. and Bello, M. A. 2003. "Modeling Sulfur Dioxide Deposition on Calcium Carbonate", *American Chemical Society*. Vol. 42, pp. 1028-1034.

Böke, H, Göktürk, H., Caner – Salt, E.N., Demerit, Ş. 1999. "Effect of Airborne Particles on SO_2 – Calcite Reaction", *Applied Surface Science*. Vol. 140, pp. 70-82.

Böke, H., Gauri, K.L. 2003. "Reducing Marble-SO_2 Reaction Rate by the Application of Certain Surfactants", *Water Air and Soil Pollution*. Vol. 142, pp. 59-70.

Böke, H., Göktürk, H., Caner – Saltık, E.N. 2002. "Effect of Some Surfactants on SO_2-Marble Reaction", *Materials Letters*. Vol. 57, pp. 935-939.

Böke, H. and Gauri K.L. 2003. "Reducing Marble-SO_2 Reaction Rate by the Application of Certain Surfactants", *Water, Air and Soil Pollution*, Vol. 142, pp. 59-70.

Böke, H., Göktürk, H., Caner – Saltık E.N., Demirci S. 1999. "Effect of Airborne Particles on SO_2 – Calcite Reaction", *Applied Surface Science*. Vol. 140, pp.70-82.

Cheng, J.R., Hwu, R., Kim, J.T., Leu, S.M. 1987. "Deterioration of Marble Structures", *Analytical Chemistry*. Vol. 59, pp.104-106.

Chang, C. S. and Rochelle, G. T. 1981. "SO_2 Absorption into Aqueous Solutions", *AlChE Journal*. Vol. 27, No. 2, pp. 292-298.

Coburn, W.G., Gauri, K.L., Tambe, S., Li, S. and Saltık, E. 1993. "Laboratory Measurement of Sulphur Dioxide Deposition Velocity on Marble and Dolomite Stone Surfaces", *Atmospheric Environment*. Vol. 27 B, No.2, p. 193-201.

Dean, A.H., Hobbs, P.V. 1978. "Oxidation of Sulfur Dioxide in Aqueous Systems with Particular Reference to the Atmosphere", *Atmospheric Environment*. Vol. 12, pp. 241-253.

Elfving, P., Johannson, L.G., Lindquist 1994. "A Study of the Sulphation of Silane-Treated Sandstone, *Studies in Conservation*. Vol. 39, pp. 199-209.

Elfving, P., Panas, I., Lindqvist, O. 1994. "Model Study of the First Steps in the Deterioration of Calcareous Stone I. Initial Surface Sulphite Formation on Calcite", *Applied Surface Science*. Vol. 74, pp. 91-98.

Fassina, V. 1986. "Environmental Pollution in Relation to Stone Decay, Paper Presented at the Symposium "Air Pollution and Conservation-Safeguarding Our Architectural Heritage" Rome, Italy, (October 15-17, 1986), pp. 317-357.

Garland, J.A., 1978. "Dry and Wet Removal of Sulphur from the Atmosphere", *Atmospheric Environment*. Vol. 9, pp. 661-672.

Gauri, K.L., Bandyopadhyay J.K. 1999. *Carbonate Stone, Chemical Behavior, Durability and Conservation*, (JohnWiley & Sons, New York), pp.125-157, 212-237.

Gauri, K.L., Kulshreshtha, N.P., Punuru, A.R., Chowdhury A. 1989. "Rate of Decay of Marble in Laboratory and Outdoor Exposure", *Journal of Materials in Civil Engineering.* Vol. 1, pp. 73-83.

Gauri, K.L., Doderer, G.C., Limscomp, N.T., Sarma, A.C., 1973. "Reactivity of Treated and Untreated Marble Specimens in an SO_2 Atmosphere", *Studies in Conservation*. Vol. 18, pp. 25-35.

Gauri, K.L, Popli, R., Sarma, A.C. 1982. "Effect of Relative Humidity and Grain Size on the Reaction Rates of Marble at High Concentration of SO_2", *Durability of Building Materials*. Vol. 1, pp. 209-216.

Gauri, K.L., Kulshreshtha, N.P., Punuru, A.R., Chowdhury, A. 1989. "Rate of Decay of Marble in Laboratory and Outdoor Exposure", *Journal of Materials in Civil Engineering*. Vol. 1, pp. 73-83.

Gauri, K.L., Doderer, G.C., Limscomp, N.T., Sarma, A.C. 1973. "Reactivity of Treated and Untreated Marble Specimens in SO_2 Atmosphere", *Studies in Conservation*. Vol. 18, pp.25-35.

Gauri, K.L. and Gwinn, J.A. 1982; 1983. "Deterioration of Marble in Air Containing 5-10 ppm SO_2 and NO_2", *Durability of Building Materials*. Vol. 1, pp.217-223.

Grossi, C.M. and Murray M. 1999. “Characteristic of Carbonate Building Stones That Influence the Dry Deposition of Acidic Gases”, *Construction and Building Materials*. Vol. 13, pp. 101-108.

Hales, J. M. and Sutter, S. L. 1973. “Solubility of SO_2 in Water at Low Concentrations”, *Atmospheric Environment*. Vol. 7, pp. 997-1001.

Haugaard, V.K., Udsen, A.M., Hoegh, L.,Petersen, K., Mohan, F. 2001. “Potential Food Applications of Biobased Materials. An Eu-concerted Action Project”, *Starch.* Vol. 53, pp. 189-200.

Hikita, H., Sataru, A. and Nose, H. 1978. “Absorption of SO_2 into Water”, *AIChE Journal*. Vol. 24, No.1, pp. 147-149.

Howards, G. M. 1982. “Sulphur Dioxide/ Water Equilibria between 0^oC and 50^oC”. *In an Examination of Data at Low Concentrations, Heterogeneous Atmospheric Chemistry*, edited by David R. Schryer, (Geophysical Monograph, Washington D.C)., pp. 187-195.

Innocentini-Mei L.H., bartoli J.R., Baltieri R.C. 2003. “Mechanical and Thermal Properties of Poly-3-Hydroxybutyrate Blends with Starch and Starch Derivatives”, *Macromol Symp.* Vol. 197, pp. 77-87.

Iwata, T., Doi, Y., Nakayama, S., Sasatsuki, H. Teramachi, S. 1999. ” Structure and Enzymatic Degradation of Poly(3-hydroxybutyrate) Copolymer Single Crystals with an Extra Cellular PHB Depolymerase from *Alcaligenes faecalis* T1”. *International Journal of Biological Macromolecules.* Vol. 25, pp. 169-176.

Johansson, L.G., Lindquist, O. and Mangio, R.E. 1988. “Corrosion of Calcareous Stones in Humid Air Containing SO_2 and NO_2”. *Durability of Building Materials*. Vol. 5, pp. 439-449.

Kim, S., Maeda, Y., Tsujino, Y. 2004. “Assessment of the Effect of Air Pollution on Material Damages in Northeast Asia”, *Atmospheric Environment*. Vol. 38. pp. 37-48.

Koziol, A. and Mackowiac J. 1993. “Determination of Equilibrium Data for Sulphur Dioxide-Water Systems in the Range of Low Concentrations of SO_2”, *International Chemical Engineering*. Vol. 33, No.3, pp. 442-449.

Kulshreshtha, N.P., Punuru, A.R., Gauri, K.L. 1989. “Kinetics of Reaction of SO_2 with Marble”, *Journal materials in Civil Engineering*. Vol. 1, pp. 60-72.

Larson, T. V., Horike, N. R. and Harrison, H. 1978. “Oxidation of SO_2 by O_2 and O_3 in Aqueous Solution: a Kinetic Study with Significance to Atmospheric Rate Process”. *Atmospheric Environment*. Vol. 12, pp. 1597-1611.

Lawton, J.W. 2002. “Zein: a History of Processing and Use”, *Cereal Chem*. Vol. 79, No 1, pp. 1-18.

Lawton, J.W. 2004. “Plasticized for Zein: Their Effects on Tensile Properties and Water Absorption of Zein Films”. *Cereal Chem.* Vol. 81, No. 1, pp. 1-5.

Martin, M.A., Childers, J.W., Palmer, R.A. 1987. “Fourier Transform Infrared Photoacoustic Spectroscopy Characterization of Sulfur-Oxygen Species Resulting From The Reaction Of SO_2 with CaO and $CaCO_3$”, *Applied Spectroscopy*. Vol. 41, pp. 120-125.

McKay, H. A. C. 1971. “The Atmospheric Oxidation of SO_2 in Water Droplets in Presence of ammonia1”, *Atmospheric Environment*. Vol. 5, pp. 7-14.

Nord, A.G., and Holenyi, K. 1999. “Sulphur Deposition and Damage on Limestone and Sandstone in Stockholm City Buildings”, *Water, air and soil pollution*. Vol. 109, pp.147-162.

Penkett, S. A., Jones, B. M. R., Brice, K. A. and Eggleton, A. E. J. 1979. “The Importance of Atmospheric O_3 and H_2O_2 in Oxidizing SO_2 in Cloud and Rainwater”, *Atmospheric Environment*. Vol. 13, pp. 123-137.

Pinotti, A., Garcia M.A, Martino M.N., Zaritzky N.E. 2007. “Study on Microstructure and Physical Properties of Composite Films Based on Chitosan and Methylcellulose”, *Food Hydrocolloids*. Vol. 21, pp. 66-72.

Pope, G.A., Meierding, T.C., Paradise, T.R. 2002. “Geomorphology’s Role in the Study of Weathering of Cultural Stone”, *Geomorphology.* Vol. 47, pp. 211-225.

Reddy, C.S.K., Ghai R., Rashmi, Kalia V.C. 2003. “Polyhydroxyalkanoates: an overview, Bioresource Technology”, Bioresearch *Technology*. Vol. 87, pp. 137-146.

Sevilla, J. M. R., Fe, G. L. D. L. and Gonzalez, F. D. 1993. “Absorption of SO_2 Determination of Mass Transfer Coefficients in a Continuous Stirred- tank Reactor”, *International Chemical Engineering*. Vol. 33, No.1, pp. 85-92.

Shukla, R.,Cheryan M. 2001. “Zein: The Industrial Protein from Corn, Industrial Crops and Products, *Industrial Crops and Products*. Vol. 13, 171-192.

Skoulikidis, T.N., Beloyannis, N. 1984. “Inversion of Marble Sulfation – Reconversion of Gypsum Films into Calcite on the Surfaces of Monuments and Statues”, *Studies in Conservation*. Vol. 29, pp. 1733-1743.

Skoulikidis, T.N., Beloyannis, N. 1984. “Inversion of Marble Sulfation – Reconversion of Gypsum Films into Calcite on the Surfaces of Monuments and Statues”, *Studies in Conservation*. Vol. 29, pp. 1733-1743.

Södengard, A, Stolt M. 2002. “Properties of Lactic Acid Based Polymers and Their Correlation with Composition”, *Progress in Polymer Science*. Vol. 27, pp. 1123-1163.

Spiker, E.C., Hosker, R.P., Comer, V.J., White, J.R., Werre, R.W., Harmon, F.L., Gandy, G.D. and Sherwood, S.I. 1992. "Environmental Chamber for Study of the Deposition Flux of Gaseous Pollutants to Material Surfaces". *Atmospheric Environment*. Vol. 26 A, No.16, pp. 2885-2892.

Srinivasa, P.C., Ravi R., Tharanathan R.N. 2007. "Effect of Storage Conditions on the Tensile Properties of Eco-Friendly Chitosan Films by Response Surface Methodology", *Journal of Food Engineering*. Vol. 80, pp. 184-189.

Stern, D.I. 2005. "Global Sulfur Emissions from 1850 to 2000", *Chemosphere*. Vol. 58, pp. 163-175.

Striegel, M.F. Guin, E.B., Hallett, K., Sandoval, D., Swingle, R., Knox, K., Best, F., Fornea, S. 2003. "Coatings, and Cultural Resources", *Progress in Organic Coatings*. Vol. 48, pp. 281-288.

Ta, W., Wei, C., Chen, F. 2005. "Long-term Measurements of SO_2 Dry Deposition over Gansu Province, Chine", *Atmospheric Environment*. Vol. 39, pp. 7095-7105.

Tapia-Blácido, D., Sobral, P. J., Menegalli, F. C. 2005. "Effects of Drying Temperature and Relative Humidity on the Mechanical Properties of Amaranth Flour Films Plasticized with Glycerol", *Brazilian Journal of Chemical Engineering.* Vol. 22, No. 2, pp. 249-256.

Tharanathan, R.N. 2003. "Biodegradable Films and Composite Coatings: Past, Present and Future", *Trends in Food Science and Technology*. Vol. 14, pp. 71-78.

Thompson, M., Shelley, J., Compton, R.G., Viles, H.A. 2003. "Polymer Coatings to Passivate Calcite from Acid Attack: Polyacrylic Acid and Polyacrylonitrile", Jounal *of Colloidal Interface Science*. Vol. 260, pp. 204-210.

Thompson, M., Wilkins, S.J., Compton, R.G., Viles, H.A. 2002. "Polymer Coatings To Passivate Calcite From Acid Attack: Polyacrylic Acid and Polyacrylonitrile", *Journal of Colloid and Interface Science*. Vol. 260, pp. 204-210.

Torfs, K. and Grieken, R.V. 1997. "Chemical Relations between Atmospheric Aerosols, Deposition and Stone Decay Layers on Historic Buildings at the Mediterranen Coast", *Atmospheric Environment.* Vol. 31, No. 15, pp. 2179-2192.

Weber, C.J., Haugaard V., Festersen R.,Bertelsen G. 2002. Production and Applications of Biobased Packaging Materials for the Food Industry". *Food Additives and Contaminants*. Vol. 19, pp. 172-177.

Weber, J.C. 2000. "Biobased Packaging Materials for the Food Industry: Status and Prospectives", (KVL). pp. 1-136.

WEB_1, 2007. www.ace.mmu.ac.uk. Web site, (15/05/2007) http://www.ace.mmu.ac.uk/eae/Air_Quality/Older/Air_Pollutants.html

WEB_2, 2007. DIE Web site, (15/06/2007).
http://www.tuik.gov.tr/yillik/yillik_2004.pdf

WEB_3, 2007. Wikipedia Web site, (15/07/2007)
http://en.wikipedia.org/wiki/Image:Pla_synthesis.png

Xie, S., Qi, L., Zhou, D. 2004. "Investigation of the Effects of Acid rain on the Deterioration of Cement Concrete Using Accelerated Tests Established in Laboratory", *Atmospheric Environment*. Vol. 38, pp. 4457-4466.

APPENDIX A

Table A.1. Weight Loss Which Depend on Time of SO_2 Permeation Tube at 30 C Temperatures

Time (Day)	Weight loss (gr)
0	0
3	0.0369
7	0.061
11	0.0917
14	0.1116
18	0.1381
28	0.1942
39	0.271
52	0.3583
63	0.4304

Table A.2. Gypsum Crust Thicknesses of the Plasticized Zein Coated and Uncoated Marble Slabs.

Sample Name	Exposure (Days)	Area (cm^2)	Total SO_4 (ppm)	Gypsum (gr)x10^{-4}	Thickness (µm)
Uncoated	3	11.60	3.23	1.45	0.09
Uncoated	7	10.51	29.74	13.33	0.94
Uncoated	14	11.74	122.62	54.94	3.47
Uncoated	21	11.83	180.87	81.05	5.08
Uncoated	35	10.60	441.58	197.87	13.84
Zein+Gly. Coated	3	11.39	10.79	4.84	0.32
Zein+Gly. Coated	7	12.11	31.29	14.02	0.86
Zein+Gly. Coated	14	9.97	158.70	71.11	5.29
Zein+Gly. Coated	21	10.52	267.76	119.98	8.45
Zein+Gly. Coated	35	10.20	465.92	208.77	15.18

Table A.3. Gypsum Crust Thicknesses of the Zein Coated and Uncoated Marble Slabs

Sample Name	Exposure (Days)	Area (cm^2)	Total SO_4 (ppm)	Gypsum (gr)x10^{-4}	Thickness (μm)
Uncoated	10	7.76	26.23	11.76	1.12
Uncounted	25	9.69	83.35	37.35	2.86
Uncoated	35	9.93	122.621	54.94	4.10
Zein Coated	10	10.06	37.7936	16.93	1.25
Zein Coated	25	9.77	114.359	51.24	3.89
Zein Coated	35	9.12	158.699	71.11	5.78

Table A.4. Gypsum Crust Thicknesses of the Chitosan Coated and Uncoated Marble Slabs

Sample Name	Exposure (Days)	Area (cm^2)	Total SO_4 (ppm)	Gypsum (gr)x10^{-4}	Thickness (μm)
Uncoated	3	11.06	19.38	8.68	0.58
Uncoated	13	11.22	80.57	35.85	2.37
Uncoated	21	10.63	175.77	78.76	5.50
Uncoated	35	9.44	202.23	90.62	7.1
Uncoated	50	9.53	477.55	213.98	16.7
Chitosan Coated	3	10.40	19.38	8.68	0.62
Chitosan Coated	13	10.22	221.42	99.21	7.20
Chitosan Coated	21	10.51	379.11	169.88	11.98
Chitosan Coated	35	10.77	618.036	276.93	19.07
Chitosan Coated	50	11.13	901.52	403.96	26.91

Table A.5. Gypsum Crust Thicknesses of the PHB and Low Molecular Weight PLA Coated and Uncoated Marble Slabs

Sample Name	Exposure (Days)	Area (cm^2)	Total SO_4 (ppm)	Gypsum (gr) $x10^{-4}$	Thickness (μm)
Uncoated	3	11.06	19.38	8.68	0.58
Uncoated	13	11.22	80.57	35.85	2.37
Uncoated	21	10.63	175.77	78.76	5.50
Uncoated	35	9.44	202.23	90.62	7.1
Uncoated	50	9.53	477.55	213.98	16.7
Uncoated	85	10.55	434.43	778.64	54.7
PHB Coated	3	10.13	13.61	6.1	0.45
PHB Coated	13	11.36	26.94	12.07	0.79
PHB Coated	21	9.71	51.92	23.27	1.78
PHB Coated	35	10.47	102.03	45.72	3.24
PHB Coated	50	10.44	244.55	109.58	7.27
PHB Coated	85	11.05	861.88	386.20	25.92
LPLA Coated	3	10.09	2.76	1.24	0.09
LPLA Coated	13	10.78	19.09	8.55	0.59
LPLA Coated	21	11.05	23.13	10.36	0.70
LPLA Coated	35	10.80	66.62	29.85	2.05
LPLA Coated	50	10.44	169.87	76.12	5.41
LPLA Coated	85	10.60	471.96	211.48	14.79

Table A.6. Gypsum Crust Thicknesses of High Molecular Weight PLA Coated and Uncoated Marble Slabs.

Sample Name	Exposure (Days)	Area (cm^2)	Total SO_4 (ppm)	Gypsum (gr)x10^{-4}	Thickness (μm)
Uncoated	7	9.84	210.33	94.25	7.11
Uncoated	21	11.26	455.75	204.22	13.45
Uncoated	35	10.99	527.26	236.26	15.93
Uncoated	65	11.01	1464.70	656.31	44.18
Uncoated	90	10.66	1581.90	708.83	49.31
HPLA coated	7	9.84	59.06	26.47	1.99
HPLA coated	21	9.53	103.91	46.56	3.62
HPLA coated	35	10.48	254.16	113.88	8.06
HPLA coated	65	10.25	408.36	182.98	13.24
HPLA coated	90	11.35	667.32	299.02	19.54

APPENDIX B

B.1. Sample Calculation of the Thickness of Gypsum Crust on Marble Surface

Sample calculations for uncoated 35 days (Glycerol added zein experiment);
Dimensions of the 35 days SO_2 exposured marble slab = 2.835 x 1.505 x 0.238 cm.
Area of the marble slab = 10.59919 cm^2
Sulphate which was determined with IC (in the 25 ml. ultra pure water) at the end of 35 days = 441.58 ppm

W_A = 0.025 (l) x 441.58 ppm = 11.0395 mg sulphate

$$W_p = \frac{172.17(M_p)}{96.056(M_a)}.11.0395(W_A) = 19.787mg = 0.019787g$$

$$\delta_p = \frac{0.019787(W_p)}{10.59919(A)\times 2.71(\rho_c)} \times \frac{172.17(M_p)\times 2.71(\rho_c)}{100.09(M_c)\times 2.32(\rho_c)} = 1.38\times 10^{-3}\,cm$$

$_p$ = 1.38x10^{-3}x 10000 = 13.8 micrometer (μm)

B.2. Sample Calculation of average deposition velocity

Average deposition velocity;

C_s = concentration of SO_2 = 8.1 ppm = 3.43 x 10^{-10} mol/cm^3

$$1.632\times 10^{-6}\,cm = \frac{172.17(M_p)}{2.32(\rho_p)} \times V_d \times 3.43\times 10^{-10} \times (60\times 60\,\mathrm{sec}\,ond)$$

V_d = 0.0178 cm/second

B.3. Sample Calculation of the Quantity of Calcium Sulphite Hemihydrate and Gypsum

For uncoated marble after 35 days SO_2- calcite reaction;

$W_{Total\ (SO4)} = W_{SO3\ \ SO4} + W_{SO4}$

$W_{Total\ (SO4\ )} = 0.025$ (l) x 441.58 ppm (from IC) = 11.0395 mg

$$mmol_{Total\ (SO_4)} = \frac{W_{Total\ (SO_4)}}{MW_{(SO_4)}}$$

$$mmol_{Total\ (SO_4)} = \frac{11.0395}{96} = 0.115$$

$mmol_{Total\ (SO4\ )} = mmol_{(SO3\ \ SO4)} + mmol_{(SO4\ )} = 0.115$

$mmol_{(SO3\ \ SO4)} = 0.115 - mmol_{(SO4\ )}$

Absorption quantities of the SO_3 and SO_4 from the IR analysis

$A_{(SO3)} = 0.33$ $A_{(SO4)} = 0.72$

$$\frac{A_{SO_3}}{A_{SO_4}} = \frac{0.33}{0.72} = 0.458$$

These values were replaced into the equation which obtained from the FTIR figures.

$$\frac{A_{SO_3}}{A_{SO_4}} = 1.0584 \times \frac{mmol_{(SO_3)}}{mmol_{(SO_4)}} - 0.0075 \qquad \text{(Figure 4.5)}$$

$$\frac{A_{SO_3}}{A_{SO_4}} = 0.458 = 1.0584 \times \frac{0.115 - mmol_{(SO_4)}}{mmol_{(SO_4)}} - 0.0075$$

$mmol_{(SO4\ )} = 0.07986$

$mmol_{(SO3)} = 0.115 - mmol_{(SO4\ )} = 0.03514$

$mmol_{(SO4\ )} = mmol\ _{(CaSO4.2H2O\ )}$

$mmol_{(SO3)} = mmol\ _{(CaSO3.0.5H2O\ )}$

$CaSO_4.2H_2O$ (mg) = mmol $_{(CaSO4.2H2O\ )}$ x M.W **(**$CaSO_4.2H_2O$)

$CaSO_4.2H_2O$ (mg) = 0.07986 x 172.168

$CaSO_4.2H_2O$ = 13.75 mg

$CaSO_3.0.5\ H_2O$ (mg) = mmol $_{(CaSO3.0.5\ H2O\ )}$ x M.W ($CaSO_3.0.5H_2O$)

$CaSO_3.0.5H_2O$ (mg) = 0.03514 x 129.1458

$CaSO_3.0.5H_2O$ = 4.54 m

B.4. Sample calculaton of Polymers Protection Factor Percentage

After 35 days SO_2-calcite reaction, following experimental results were determined for glycerol added zein coated and uncoated marble slabs.

Gypsum crust thickness which formed on the uncoated marble surface: 13.84 micron
Gypsum crust thickness which formed on the glycerol added zein coated marble surface: 15.18 micron.

$$\text{Polymer Protection Factor Percentage} = 100 - \frac{(15.18)\cdot 100}{(13.84)}$$

Polymer Protection Factor Percentage = - 9.7

APPENDIX C

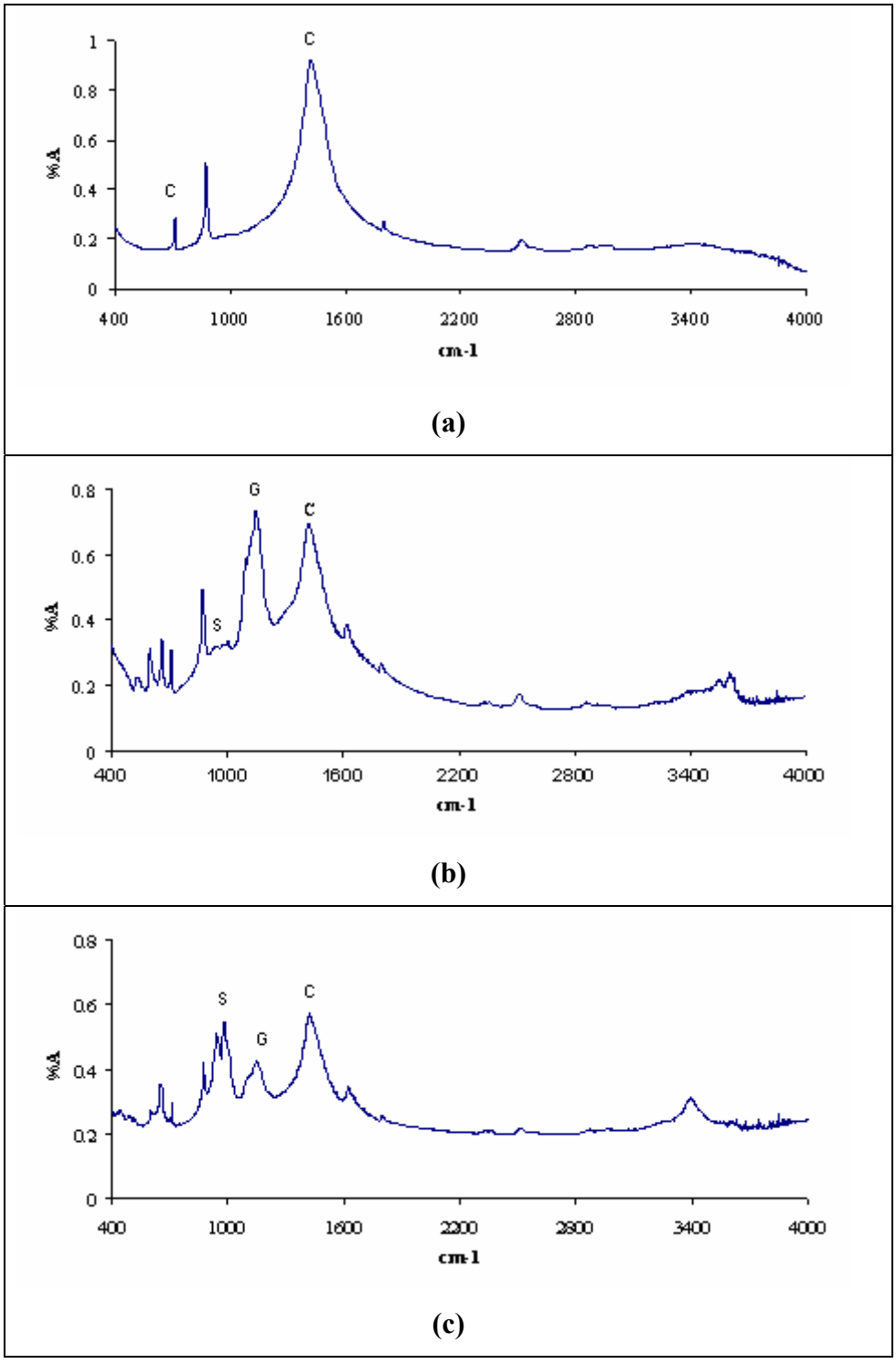

Figure C.1. FTIR Spectrum of the Unexposed (A), Plasticized Zein Coated (B) And Uncoated (C) Marble after 35 Days Exposure (C: Calcite; G: Gypsum; S: Calcium Sulphite Hemihydrate)

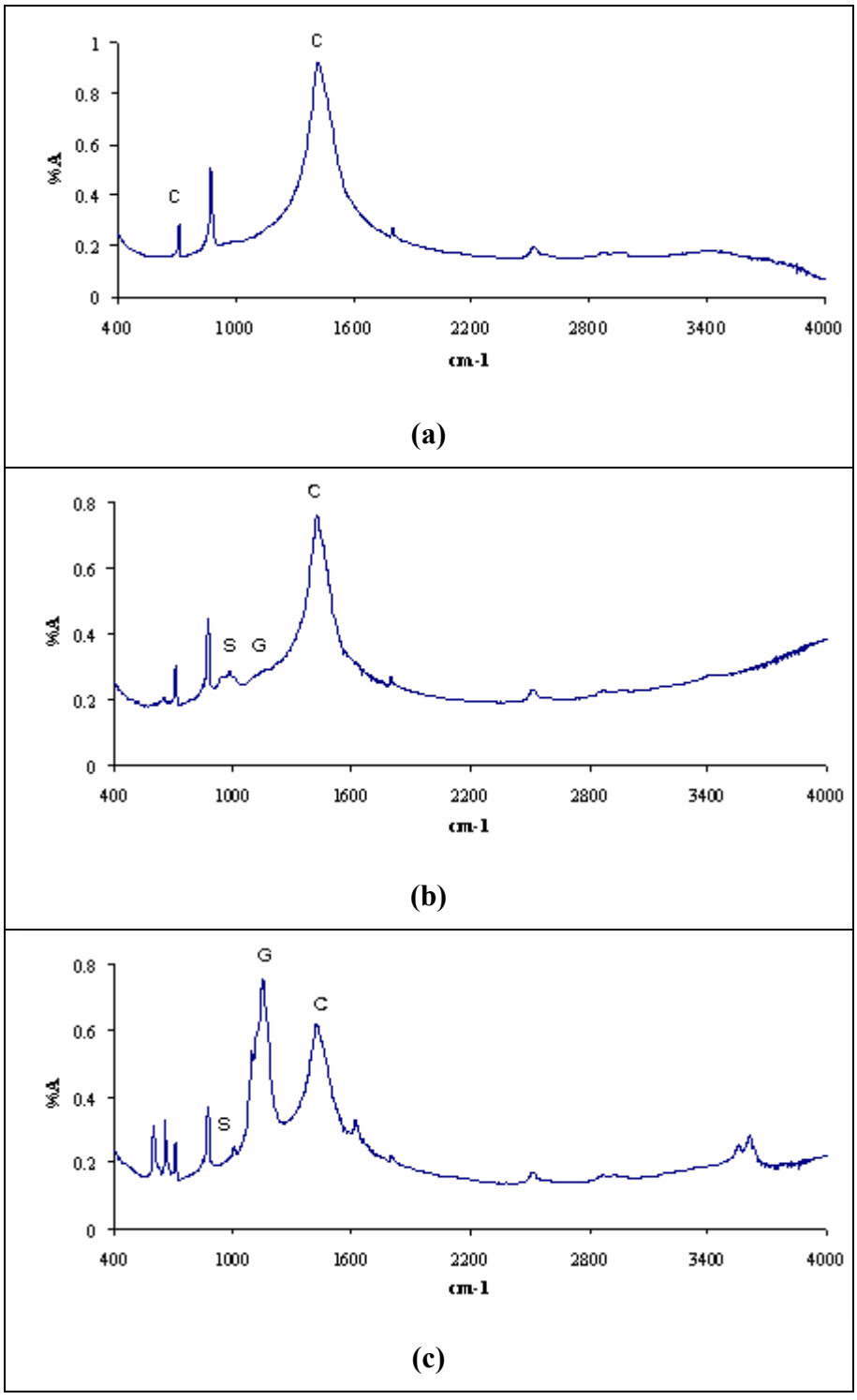

Figure C.2. FTIR Spectrums of the Unexposed (a) Zein Coated (b) and Uncoated Marble after 35 Days Exposure (C: Calcite; G: Gypsum; S: Calcium Sulphite Hemihydrate)

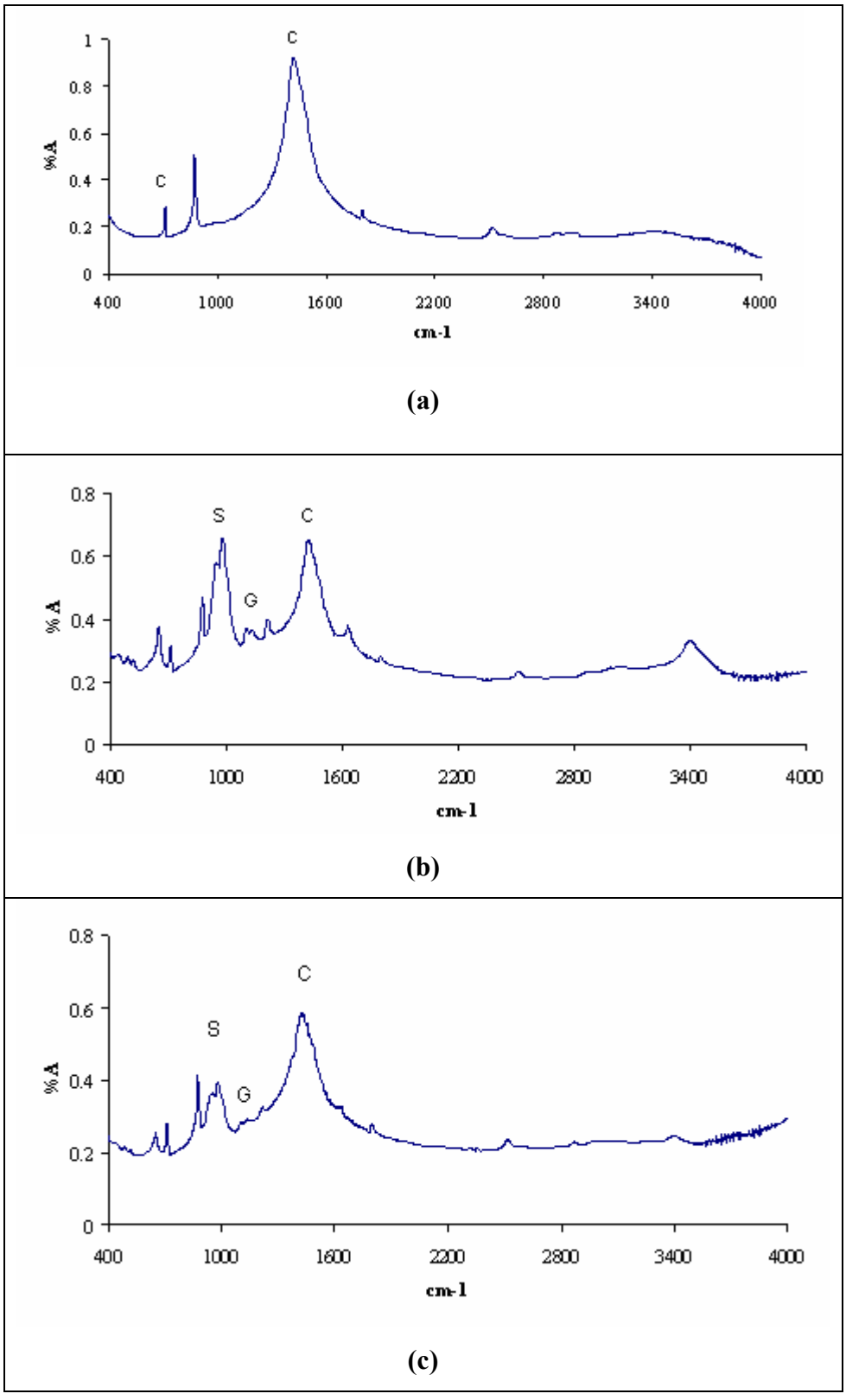

Figure C.3. FTIR Spectrums of the Unexposed (a) Chitosan Coated (b) and Uncoated (c) Marble after 50 Days Exposure (C: Calcite; G: Gypsum; S: Calcium Sulphite Hemihydrate)

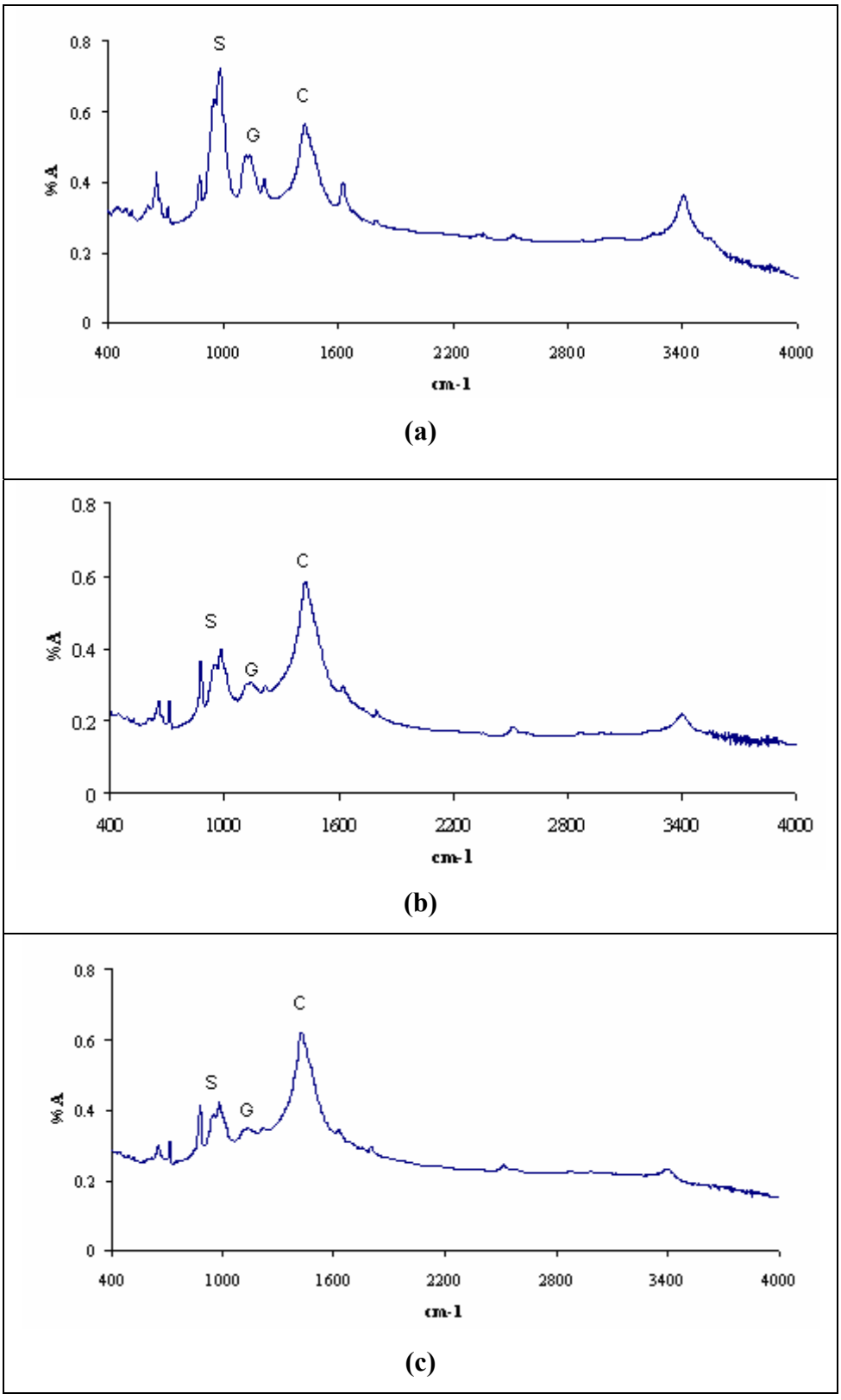

Figure C.4. FTIR Spectrums of Uncoated (a), PHB Coated (b) and LPLA Coated (c) Marble After 85 Days Exposure (C: Calcite; G: Gypsum; S: Calcium Sulphite Hemihydrate)

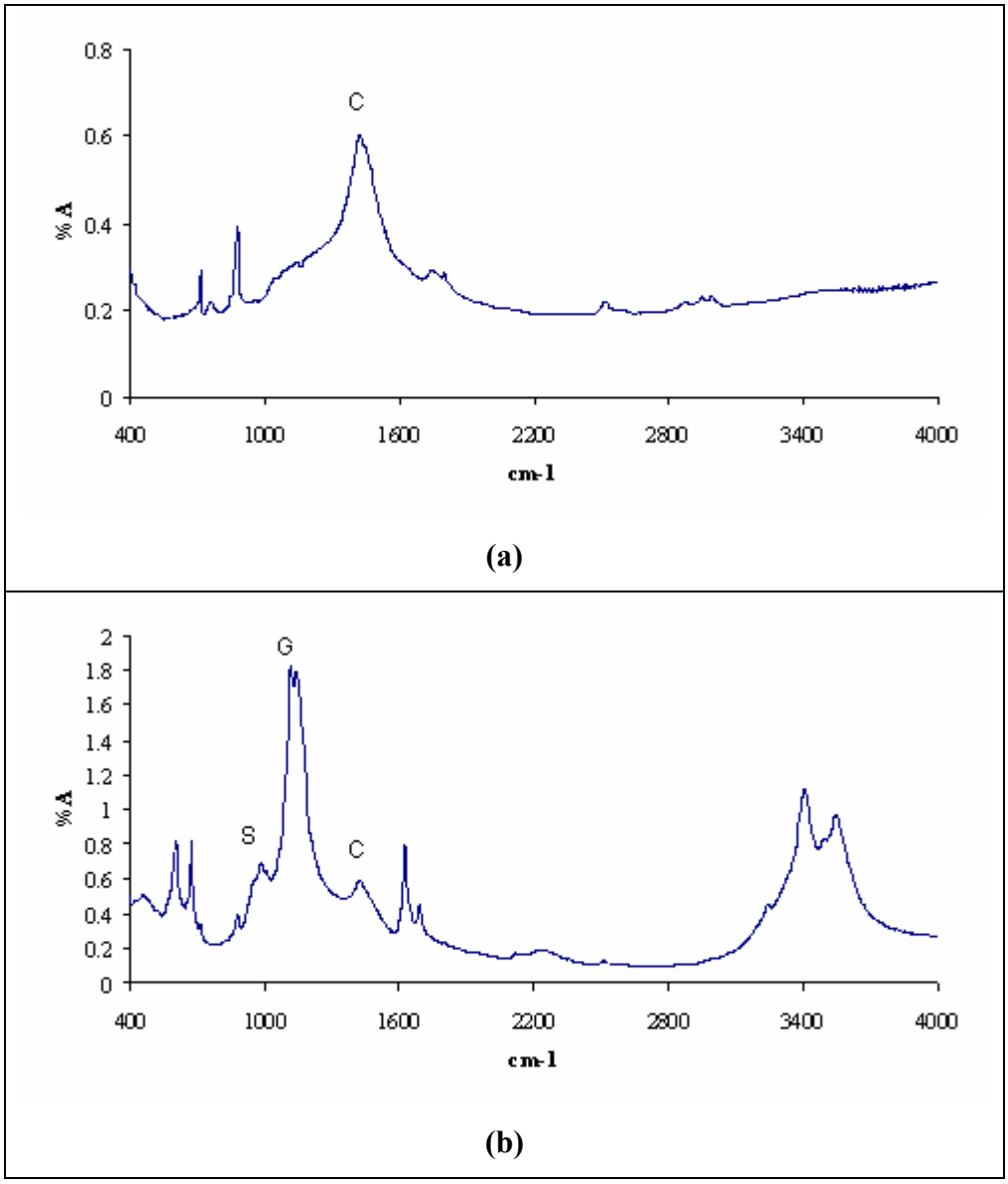

Figure C.5. FTIR Spectrums of HPLA Coated (a) and Uncoated (b) Marble After 90 Days Exposure (C: Calcite; G: Gypsum; S: Calcium Sulphite Hemihydrate).